ABSTRACT

Title of Thesis:	LINKING TRANSIENT CHANGES IN DISSOLVED ORGANIC CHEMISTRY TO WETLAND CARBON EMISSIONS
	Isabelle Van Benschoten, Masters of Science 2025
Thesis Directed By:	Assistant Professor, Jared Lee Wilmoth, Environmental Science & Technology

Wetlands form a massive reservoir of soil carbon (C) that is disproportionately impacted by climate change and displays extreme variability in C cycling over different spatiotemporal scales. The biogeochemical pathways underpinning this variability remain a critical knowledge gap due in part to the oversimplification of soil organic matter (SOM) transformations in the wetland rhizosphere. Tidal marshes bordered by forest are of unique concern due to natural gradients in SOM chemistry along the wetland-to-forest transect. In addition to sea level rise, SOM chemistry is regulated by transient shifts in vegetation growth, organic molecular characteristics, and redox conditions. To better understand how these factors influence the correspondence between wetland C emissions and SOM transformations, we incubated soils collected from a tidal marsh dominated by the plant Phragmites australis. This plant is globally distributed and is recognized as a driver of soil C cycling and soil redox perturbations. We measured CO_2 and CH_4 emissions and characterized SOM transformations with high-resolution mass spectrometry to assess the effects of seasonality (relevant to plant growth in the field), local

soil characteristics (based on transect position, relevant to sea level), and soil redox perturbation (analogous to plant radial oxygen loss) on C emissions. Our results suggest that redox modulation by Phragmites, as well as other wetland plants, has the potential to increase C emissions in the field (depending on transect location and seasonality) by stimulating the degradation of high-molecular-weight compounds in SOM. We find that the molecular mass and nominal oxidation state of C (NOSC) in the dissolved fraction are key metrics for understanding general trends in C chemistry and emissions, but variability in CH_4 uniquely corresponds to transient changes in carboxylic-rich alicyclic molecules (CRAM). Considering that sea level rise will likely extend Phragmites into new soil zones, our work allows for predictions of how it could affect C cycling in newly invaded soils. This provides deeper mechanistic insight into the C cycle of wetland soils and underscores a need for further investigations of the wetland-to-forest ecotone to help improve landscape and global C models while informing new climate mitigation policies.

LINKING TRANSIENT CHANGES IN DISSOLVED ORGANIC CHEMISTRY TO WETLAND CARBON EMISSIONS

by

Isabelle Eileen Van Benschoten

Thesis submitted to the Faculty of the Graduate School of the
University of Maryland, College Park, in partial fulfillment
of the requirements for the degree of
Master of Science
2025

Advised by:
Jared Lee Wilmoth, Chair
Stephanie A Yarwood
Matthew Fischel

© Copyright by

Isabelle Van Benschoten

2025

ACKNOWLEDGEMENTS

I would like to express my deepest gratitude to my advisor and mentor, Dr. Jared Wilmoth, for all of your guidance and support during my academic career. You have played an instrumental role in shaping not only my development as a scientist, but also as a person. Thank you for your kindness, patience, and enthusiasm to answer my many questions, dive down philosophical rabbit holes, and, of course, navigate the many ups and downs this project took. I will forever be grateful for the opportunity I have had to learn from your expertise and your trust in me to help lay the groundwork of your lab. I am incredibly honored to be a part of your beginnings in Maryland and to have seen both your family and career grow.

I would also like to extend my sincere thanks to Dr. Stephanie Yarwood for your advice and support throughout the project. Both you and Dr. Nora Hamovit have been an inspiration to me as women in the field. In these unprecedented times, I would also like to thank Dr. Andy Baldwin for his uplifting spirit while still staying grounded in our reality as scientists. Thank you to Dr. Matt Fischel for stepping in and providing crucial support in unforeseen circumstances.

I would also like to thank the Smithsonian Environmental Research Center for providing access to the Global Change Research Wetlands, and a special thanks to the COSMIC lab at Old Dominion University, especially Dr. Alex Goranov, whose expertise has been invaluable.

This work would not have been possible without the contributions of my lab mates and colleagues; I am incredibly grateful for Nathaniel Spicer, Caroline Melton, Colin Simmons, Grace Hartnett, and Hannah Moore for their late nights and early mornings hovered over the GC and getting dirty in the marsh. I am incredibly proud and thankful to be a part of the W-SCI lab in HJP, and I extend my thanks to Jason, Ruifang, Griffin, Aileen, Grace, and Daniel.

I would also like to thank the many students who have given me the opportunity to teach and mentor throughout my time as a grad student. I have taken much inspiration from early teachers, including Mrs. Glancey, Mr. Manzo, Dr. Panzer, and Dr. Yarwood, in both their views of our natural world and their dedication to communicating it. My goal has never been to make more soil scientists, but at the minimum, encourage curiosity and critical thought about the world around us, and hopefully, acknowledge at least some of what is happening below our feet.

Lastly, and arguably most importantly, I would like to thank my friends and family for their support throughout this project. Navigating the aforementioned ups and downs would not have been possible without AJ, Cam, Caroline, Chloe, Colin, Courtney, Helena, Izzy, Nate, my parents, and grandparents —their late-night phone calls, proofreading support, and serving as sounding boards, among much more.

I am incredibly grateful to all of you. Thank you.

Table of Contents

INTRODUCTION

"Biogeochemistry is a nightmare to a traditional laboratory chemist: the reactants are impure, the concentrations are low, and the temperature is variable" - Bernhardt & Schlesinger 2013

Wetlands account for 20-30% of Earth's soil carbon (C) pool while occupying only 5- 8% of the land surface(Craft, 2016; Mitsch, 2007; Nahlik & Fennessy, 2016). Wetlands are increasingly vulnerable to accelerated biogeochemical transformations under climate change, which could further destabilize soil C and increase greenhouse gas emissions (Canadell, 2021; Stagg et al., 2017). Predicting C transformations more accurately requires a detailed characterization of soil C chemistry in the wetland rhizosphere. This remains a critically overlooked area of soil C research, where a major knowledge gap lies within the transient nature of dissolved organic C (DOC) chemistry (Noyce et al., 2023).

Transient environmental perturbations can exert a strong influence on C cycling, as well as the cycling of nitrogen (N), iron (Fe), phosphorus (P), and sulfur (S) (Noyce & Megonigal, 2021; Zhang et al., 2019). For example, the intermittent or variable presence/concentration of oxygen (O_2) in soil tightly regulates these cycles (Wilmoth et al., 2021). Oxygenation has long been considered to inhibit methane (CH_4) production, consistent with the observation of CH_4 generation in relatively deep, anoxic sediments (Sowers, 2019). However, the potential for periodic oxygenation of anoxic soils to *prime* organic C toward elevated CH_4 is becoming more widely recognized (i.e., the soil "methane paradox") (Wilmoth, 2021). To date, no conclusive chemical evidence based on broader SOM transformations has ever been shown to verify such a priming mechanism in surface soils like those of the wetland rhizosphere. In the case of CO_2

production, which has been shown to be stimulated in redox-oscillating soils, some tropical forests (e.g., Luquillo Critical Zone Observatory, Puerto Rico) rich in Fe^{III} minerals and large organic inputs from overlying tree canopy (e.g., fallen leaves) have been shown to release more CO_2 under anaerobic vs aerobic conditions (Wilmoth et al., 2018).

Many environmental drivers influence the presence of O_2 in soils; in particular, wetland plants transfer O_2 to the rhizosphere. Radial oxygen loss (ROL) is a well-known mechanism whereby O_2, initially directed by the plant for root respiration, is lost to the rhizosphere soil in contact with the roots and rhizomes. In such cases, any spatiotemporal variation (e.g., gradient, transition, oscillation) in rhizosphere oxygenation could influence CH_4 and CO_2 production via broad transformations in organic C, potentially increasing the vulnerability of wetland C stocks and fueling greenhouse gas emissions. The mechanistic details of how transient O_2 exposure stimulates C emissions from redox-oscillating soils in general require further investigation using a multifaceted analytical approach (Lacroix et al., 2023; Wilmoth et al., 2018).

For the present study, the correlation between changes in broad-spectrum SOM chemistry and transient oxygenation in soil collected from the wetland rhizosphere of a tidal marsh dominated by *Phragmites* was investigated using Fourier transform ion cyclotron resonance mass spectrometry (FTICR-MS). We measured corresponding CH_4 and CO_2 emissions to understand how diverse SOM chemical transformations might help inform our current conceptual frameworks on C cycling in redox-dynamic soils. We hypothesized that transient oxygen *priming* of different SOM fractions would positively correlate with increasing C speciation and mineralization (e.g., nominal oxidation state of C (NOSC) with C emissions). Our overall goal is to provide researchers and stakeholders with better mechanistic and

practical/applied understanding, including the advancement of numerical and conceptual frameworks of wetland C emissions in coastal regions relevant to earth system models.

WORKS CITED

Canadell, J. G., P.M.S. Monteiro, M.H. Costa, L. Cotrim da Cunha, P.M. Cox, A.V. Eliseev, S. Henson, M. Ishii, S. Jaccard, C. Koven, A. Lohila, P.K. Patra, S. Piao, J. Rogelj, S. Syampungani, S. Zaehle, and K. Zickfeld. (2021). Global Carbon and other Biogeochemical Cycles and Feedbacks. *Sixth Assessment Report of the Intergovernmental Panel on Climate Change*(Climate Change 2021: The Physical Science Basis).

Craft, M. J. V. a. C. B. (2016). *Wetland Soils: Genesis, Hydrology, Landscapes, and Classification* (Second Edition ed.). CRC Press.

Lacroix, E. M., Aeppli, M., Boye, K., Brodie, E., Fendorf, S., Keiluweit, M., Naughton, H. R., Noël, V., & Sihi, D. (2023). Consider the Anoxic Microsite: Acknowledging and Appreciating Spatiotemporal Redox Heterogeneity in Soils and Sediments. *Acs Earth and Space Chemistry*, *7*(9), 1592-1609. https://doi.org/10.1021/acsearthspacechem.3c00032

Mitsch, W. J. a. G. J. G. (2007). *Wetlands* (Fourth Edition ed.). John Wiley & Sons, Inc.

Nahlik, A. M., & Fennessy, M. S. (2016). Carbon storage in US wetlands. *Nature Communications*, *7*, Article 13835. https://doi.org/10.1038/ncomms13835

Noyce, G. L., & Megonigal, J. P. (2021). Biogeochemical and plant trait mechanisms drive enhanced methane emissions in response to whole-ecosystem warming. *Biogeosciences*, *18*(8), 2449-2463. https://doi.org/10.5194/bg-18-2449-2021

Noyce, G. L., Smith, A. J., Kirwan, M. L., Rich, R. L., & Megonigal, J. P. (2023). Oxygen priming induced by elevated CO₂ reduces carbon accumulation and methane emissions in coastal wetlands. *Nature Geoscience*, *16*(1), 63-+. https://doi.org/10.1038/s41561-022-01070-6

Sowers, K. R. (2019). Methanogenesis. In *Encyclopedia of Microbiology, 4th Ediition - Reference Module in Biomedical Sciences*. Ellsevier Inc. https://doi.org/10.1016/b978-0-12-801238-3.02447-8

Stagg, C. L., Schoolmaster, D. R., Krauss, K. W., Cormier, N., & Conner, W. H. (2017). Causal mechanisms of soil organic matter decomposition: deconstructing salinity and flooding impacts in coastal wetlands. *Ecology*, *98*(8), 2003-2018. https://doi.org/10.1002/ecy.1890

Wilmoth, J. L. (2021). Redox Heterogeneity Entangles Soil and Climate Interactions [Article]. *Sustainability*, *13*(18), 14, Article 10084. https://doi.org/10.3390/su131810084

Wilmoth, J. L., Moran, M. A., & Thompson, A. (2018). Transient O₂ pulses direct Fe crystallinity and Fe(III)-reducer gene expression within a soil microbiome. *Microbiome*, *6*, Article 189. https://doi.org/10.1186/s40168-018-0574-5

Wilmoth, J. L., Schaefer, J. K., Schlesinger, D. R., Roth, S. W., Hatcher, P. G., Shoemaker, J. K., & Zhang, X. N. (2021). The role of oxygen in stimulating methane production in wetlands. *Global Change Biology*, *27*(22), 5831-5847. https://doi.org/10.1111/gcb.15831

Zhang, L. H., Shao, H. B., Wang, B. C., Zhang, L. W., & Qin, X. C. (2019). Effects of nitrogen and phosphorus on the production of carbon dioxide and nitrous oxide in salt-affected soils under different vegetation communities. *Atmospheric Environment*, *204*, 78-88. https://doi.org/10.1016/j.atmosenv.2019.02.024

CHAPTER I

The Interfaces of Marshes: Visualizing and Contextualizing Ecosystem Drivers of Carbon Dynamics Across Space and Time

ABSTRACT

At the interface of land and water, coastal wetlands store massive reservoirs of soil carbon (C) that are being impacted by sea level rise. As we seek the development of more accurate models to predict changes in wetland C cycling, there remain critical knowledge gaps due to the oversimplification of numerous C transformations in the wetland rhizosphere. A major challenge in measuring these transformations is that they occur over short spatiotemporal scales in a heterogeneous environment, which also undergoes diurnal and tidal oscillations. A multifaceted analytical approach is needed to better understand how the global C cycle is regulated by these fine-scale dynamics. To understand the role of plant-mediated oxygenation on these C transformations, we investigated the anatomy and physiology of *Phragmites australis*; shedding light on their gas transport mechanisms and influence on the soil and surrounding microbial communities. These communities, their biochemical pathways, and the potential trophic cascade of substrates were also explored in order to hypothesize potential concurrent influences these variables could induce at these incredibly dynamic soil interfaces. Our emerging conceptual framework is that short spatiotemporal dynamics in the wetland rhizosphere drive large-scale variability in wetland C storage and emissions. Further studies could provide a deeper

mechanistic understanding of the wetland C cycle and have the potential to inform greenhouse gas modeling and subsequent effective climate mitigation policies.

INTRODUCTION

Wetlands account for 20-30% of Earth's soil carbon (C) pool while occupying only 5- 8% of the land surface (Craft, 2016; Mitsch, 2007; Nahlik & Fennessy, 2016). Under climate change conditions, wetlands are increasingly vulnerable to accelerated biogeochemical transformations, which could further destabilize soil C and increase greenhouse gas emissions (Canadell, 2021; Stagg et al., 2017). IN order to predict C transformations more accurately the soil C chemistry of the wetland rhizosphere requires a detailed characterization given the variability and lack of reproducibility of surface emission results. This remains a critically overlooked area of soil C research, where a significant knowledge gap lies within the transient nature of dissolved organic C (DOC) chemistry (Noyce et al., 2023).

Transient environmental perturbations can exert a strong influence on C cycling, as well as the cycling of nitrogen (N), iron (Fe), phosphorus (P), and sulfur (S) (Noyce et al., 2023; Zhang et al., 2019). For example, soil's intermittent or variable presence/concentration of oxygen (O_2) tightly regulates these cycles (Wilmoth, 2021). Oxygenation has long been considered to inhibit methane (CH_4) production, consistent with the observation of CH_4 generation in anoxic sediments (Sowers, 2019). However, it is becoming more widely recognized that periodic oxygenation of otherwise anoxic soils can be important for priming organic C toward elevated CH_4 production (i.e., the soil "methane paradox") (Wilmoth, 2021). Similarly, CO_2 production

can also be stimulated in redox-oscillating soils, where some tropical soils rich in Fe^{III} minerals have been shown to release more CO_2 under anaerobic conditions (Wilmoth et al., 2018).

The mechanistic details of how periodic O_2 exposure stimulates C emissions from redox-oscillating soils remain poorly understood (Lacroix et al., 2023). Many environmental drivers influence the presence of O_2 in soils; in particular, wetland plants transfer O_2 to the rhizosphere. Radial oxygen loss (ROL) is a well-known mechanism whereby O_2, initially directed by the plant for root respiration, is lost (i.e., leaks out) to the rhizosphere soil in contact with the roots and rhizomes. In such cases, any spatiotemporal variation (e.g., gradient, transition, oscillation) in rhizosphere oxygenation could influence CH_4 and CO_2 production via broad transformations in organic C, potentially increasing the vulnerability of wetland C stocks and fueling greenhouse gas emissions.

CARBON CYCLING & MODELING

Upwards of 30% of global CH_4 emissions can be attributed to natural wetlands (Bastviken, 2009; Jackson et al., 2020; Saunois et al., 2020). CH_4 undergoes a plethora of chemical reactions in the atmosphere, including oxidation to water vapor and methyl radicals, formaldehyde, and carbon monoxide, and eventually fully oxidized to CO_2 (Myhre et al., 2007). Though CH_4 concentrations are 200 times lower than that of CO_2, CH_4 is much more potent, being able to absorb 28 times more energy over 100 years and 84 times more energy over 20 years (Dean et al., 2018; Kirschke et al., 2013; Myhre et al., 2007). Other than anthropogenic activity, CH_4 can be naturally released from the digestive systems of ruminant animals and

termites, incomplete combustion of biomass and soil C during forest fires, saturated soils like wetlands, as well as vented from terrestrial and marine seeps, and mud volcanos (Cicerone & Oremland, 1988; Kirschke et al., 2013).

As organic C breaks down in wetlands, it can be converted to CH_4 by methanogens, depending on specific environmental conditions. CH_4 can then be reoxidized to CO_2 (its fully oxidized form) or biomass by methanotrophic microorganisms. CO_2 can then be fixed within the terrestrial or marine biospheres through photosynthesis (Dean et al., 2018). The CH_4 that escapes oxidation can be released into the atmosphere by one of three physical mechanisms: ebullition, diffusion, or plant-mediated transport (Vroom et al., 2022). Most studies emphasize ebullition and diffusive CH_4 fluxes leaving plant-mediated emissions to be included at varying degrees, even though it has been estimated that up to 22% of annual CH_4 flux to the atmosphere may be from vegetation (Carmichael et al., 2014; Johnson et al., 2021). Some studies estimate plant-mediated CH_4 emissions separately from wetlands regardless of their contribution to not only emissions but CH_4 oxidation (Saunois et al., 2020).

Seasonal and spatial variations in plant shoot density, the ratios of alive vs. dead shoot cover, rooting depth, root length, root branching patterns, redox potential, and volumetric rates of soil O_2 demand also need to be understood in order to estimate plant-mediated contributions to CH_4 budgets, regardless of scale (Sorrell & Brix, 2013). However, with limited data and high variability, plant-mediated emissions are often omitted (Hayman et al., 2014; Kirschke et al., 2013), ultimately leading to questions regarding the validity of large-scale global reports, including the IPCC and Global Carbon Project (Canadell, 2021; Saunois et al., 2020). Beyond physical release mechanisms, ecosystem conditions such as temperature and moisture seasonal

changes, diurnal variability, freeze-thaw dynamics, and overall climatic zones must also be considered (Johnson et al., 2021).

Surface-level CH_4 emissions have been recorded over numerous spatiotemporal scales, with limited explanation and reproducibility of results (Vroom et al., 2022). This is because of the enigmatic below-ground mechanisms at play, yielding the discrepancies seen in the above-ground emissions. C species undergo numerous biotic and abiotic transformations below ground, interacting with plants and microbes, as well as atmospheric, geologic, and hydrologic parameters. Calculating global C budgets is difficult given the current lack of mechanistic understanding of C transformations in soil linked to CH_4 and CO_2 production. Models typically either take a "top-down" or "bottom-up" approach, looking at emissions and deducing the pathways, or looking at the pathways and inductively coming to estimates, respectively (Saunois et al., 2020). To estimate C emissions from natural wetlands, bottom-up, process-based models are preferred, but wetlands are generally oversimplified in earth system models.

PHRAGMITES OXYGENATION

Wetland plants act as conduits for gas exchange between soils and the atmosphere. In particular, *Phragmites australis*, an invasive aquatic/subaquatic perennial grass in many environments, can make these gas exchanges at higher rates compared to other wetland plants (Srivastava et al., 2014). Aerenchyma tissues are porous, hollow, tube-like structures that actively transport gas downward to oxygenate and ensure the survival of subaqueous portions of the plant (Armstrong et al., 1996). Its porosity decreases the O_2 demand given the smaller

amount of living, respiring cells, in addition to facilitating gas transport throughout the plant (Justin & Armstrong, 1987). The subaqueous portions of the plant include a dense network of roots and rhizomes, characterized as underground, horizontal extensions of the stem with the propensity to create new lateral shoots and roots (Engloner, 2009). The rhizomes of *Phragmites* are mostly hollow but also comprised of aerenchyma tissue, allowing for O_2 transport to prevent root rot in more saturated environments. The O_2 does not stay within the plant structures but is radially leaked into the rhizosphere (i.e., ROL), ultimately influencing the otherwise anaerobic and saturated surrounding soils (Justin & Armstrong, 1987).

Aerenchyma tissues primarily transport O_2 but can also transport other gases like CH_4 and CO_2 from the soil. The directions of this transport are not limited to downward movement into the rhizosphere but also upward into the atmosphere, depending on environmental conditions (Vroom et al., 2022). Aerenchyma tissues in *Phragmites* transport gasses either via diffusion or pressurized gas flow. Diffusion is the most common gas transport mechanism in vascular plants, where gasses travel from high to low concentrations along a gradient (Sorrell & Brix, 2013). In the case of most wetlands, O_2 would be transported from the atmosphere to the roots, used for respiration, or lost to the rhizosphere. CH_4, on the other hand, would be transported in the opposite direction (Vroom et al., 2022). Pressurized gas flow is responsible for 5 times greater O_2 input into the soil than diffusive gas flow (Brix et al., 2001).

Pressurized gas flow is either humidity-, wind-, or temperature-induced, all entirely physical processes in the leaf sheaths around living stems (Vroom et al., 2022). Humidity-induced transport occurs when the gases inside the plant, aerenchyma, have higher humidity than the surrounding atmosphere. Although the gas composition is similar both in and out of the plant,

the water vapor pressure is much higher inside the aerenchyma. This is because water evaporates continuously from the surrounding cells, keeping the air inside close to saturated with water. With the high amount of water vapor inside, the gasses in the aerenchyma become diluted, allowing for gas diffusion inward from the atmosphere (Armstrong et al., 1992; J. Armstrong et al., 1996; Sorrell & Brix, 2013). Temperature-induced pressurized flow is caused by solar heating of the leaves and stems, resulting in comparatively lower temperatures in the atmosphere and subsequent gas flux into the plant (W. Armstrong et al., 1996; Grosse et al., 1996). Wind can also facilitate pressurized gas flow through venturi-induced convection currents in *Phragmites*. As wind blows through a stand of *Phragmites*, the lower broken stems capture less wind than fully grown stems, causing a decrease in pressure and airflow from the rhizomes to the atmosphere (Armstrong et al., 1992). These mechanisms do not have to occur independently, with potential synergistic or antagonistic effects. Both humidity and thermal transpiration-induced pressurized transport can increase the overall flow rate. However, if temperatures are lower inside the plant, due to evaporative cooling and transpiration, the effects can counteract (Vroom et al., 2022). In addition to the transport mechanisms at play, physical plant structure and environmental conditions also impact the rate and direction of gas transport. *Phragmites'* anatomy and structure directly influence its function, not only as an individual species or stand, but also its influence on its environment and its role in driving soil C chemistry.

PHRAGMITES IN THE SYSTEM

Phragmites is one of the most ubiquitous invasive species globally, being present on nearly every continent (Srivastava et al., 2014). Its dense network of roots and rhizomes are just one adaptation that has impacted its incredible hardiness and ability to thrive in unfavorable conditions. Because of the high concentration of potassium (K^+) ions in their leaves, the K^+/Na^+ ratio allows *Phragmites* to withstand varying levels of salinity (Srivastava et al., 2014). *Phragmites* also has two survival strategies. When temperatures are less than 22 ℃ and in aqueous conditions, *Phragmites* utilize the C3 pathway, having less mycorrhization, and in turn, accumulating less underground biomass. The opposite holds true in dry conditions where temperatures are greater than 22 ºC, as the plant instead utilizes the C4 pathway. Switching pathways from C3 to C4 increases its ability to trap atmospheric CO_2 and accordingly increases efficiency in transporting carbohydrates to the rhizomes. Possessing both pathways enables them to adjust to changing environmental conditions and protects them from severe conditions throughout the year (Srivastava et al., 2014).

The *phragmites* growing season begins in mid to late spring as temperatures start to rise. New green/purple shoots will pop up near remnants of old stems. They continue to grow tall with a thin immature head throughout the spring and summer alongside old shoots of previous years. Old shoots provide structure for tall growth, and the diffusive and convective aeration currents toward the rhizosphere support the new shoot growth. In the late summer, they will translocate sugars and other photosynthetic products to storage in the roots for the winter as their now-mature heads begin to flower. They will then enter dormancy in the late fall and remain this way

throughout the winter as the aboveground tissue and eventually remaining plant die until the growing season returns and the process can begin again.

Throughout the year, *Phragmites'* rhizosphere below-ground exudate input changes. Exudates are both primary and secondary plant metabolites that assist plants in acquiring nutrients through either acidifying the surrounding soil to change the redox conditions or directly chelating with the nutrient. *Phragmites* exudates help maintain high below-ground C content with excretions of phenols, short-chained organic acids, sugars, and amino acids (Srivastava et al., 2014). These inputs, coupled with high concentrations of O_2 to the rhizosphere, typically favor eutrophic, high-nutrient-requiring bacterial communities compared to oligotrophic ones (Hu et al., 2021). Community composition and function are heterogeneous over short spatial scales. While comparing direct rhizosphere soil to bulk soil, differences in populations that involved salinity stress minimization (Pseudomonas, Ramlibacter, Trichococcus, Arthrobacter), plant growth hormone release, phosphate solubilization, and nitrogen fixation (some strains of Gammaproteobacteria) were observed (Hu et al., 2021). *Phragmites* below ground inputs, whether nutrients or gases, directly influence the communities that take hold there.

With temperature, light, and wind changing from day to night, diel patterns of gas transport occur, whereas diffusion transport processes are steadier (Vroom et al., 2022). Not only do these conditions change on a 12-hour cycle but also seasonally, making venturi-induced flow much more relevant in winter compared to humidity or temperature-induced flow (Vroom et al., 2022). With pressurized gas flow being an active process, shorter 6-hour tidal-induced saturating changes also impact the degree of transport. Pressurized gas flow is largely dependent on stomatal conductance and aperture. The small diameter of stomatal gas spaces allows for higher

resistance to the pressurized flow than diffusion, therefore, the diffusion of gas into the aerenchyma increases the pressure. If the stomatal aperture or pore size is too large, there would not be enough resistance for pressure to build up, if too small, diffusion rates would be too slow. However, if the stomatal aperture is appropriate, the lower pressure in the rhizomes forces gasses to diffuse from the higher-pressure zones in the aerenchyma downward, either being vented out or lost radially within the rhizosphere (J. Armstrong et al., 1996; Brix et al., 1992).

Plant physiology and environmental conditions are not independent, as the system impacts the plant and vice versa. Stomatal conductance, aperture, and leaf sheath area are directly affected by the irradiance experienced by the plant (Afreen et al., 2007; Armstrong & Armstrong, 1990). Regarding below-ground plant structure, root anatomy must be accounted for when trying to predict and understand all transport pathways. ROL was found to be the highest in emerging main roots, followed by the main root tip, and the emerging lateral roots, most likely due to the hardening of the roots creating a barrier. Continuous O_2 release from the lateral roots can also cause iron oxidation and subsequent ferric iron plaque formation, blocking gas transport. This process,, though, can aid in nutrient immobilization since phosphorus tends to sorb to these plaques (Li et al., 2022). With a consortium of factors impacting flow rates, *Phragmites* still manage to have optimal physiological traits to support these processes. *Phragmites* has a pore size of 0.2 micrometers and a large pith cavity, efficiently connecting the atmosphere and rhizosphere and allowing it to thrive in saturated conditions (Armstrong et al., 2000; Brix et al., 1992).

MICROBIAL BIOGEOCHEMICAL TRANSFORMATIONS

Microbial metabolic pathways in soil are highly diverse. Chemoorganotrophy has a range of energy efficacies, the highest being respiration. Here, organic C is oxidized to CO_2; NADH is the electron donor, and O_2 is reduced as the terminal electron acceptor. Large complex C molecules can be used for this process because of the large amount of energy gained since the $NADH/NAD^+$ electron couple can be recycled in the electron transport chain and four different cytochromes transporting the electrons. In anaerobic environments, microorganisms have much slower metabolic rates since the pathways yield far less energy, which is part of why wetland degradation occurs at such a slow speed. Anaerobic fermentation processes can drive energy production through substrate-level phosphorylation and an internal flow of electrons. This happens through the Entner Doudrof pathway or glycolysis; in either case, glucose is converted to pyruvate that can then go through many different pathways yielding a variety of organic alcohols and acids. Fermentation is the most common anaerobic pathway, often carried out by facultative aerobes in wetland environments, they are predominantly inundated systems but have periods of oxic conditions. Anaerobic respiration is also common in wetland systems, being at the crossroads of many biogeochemical cycles in which C is still the electron donor, but the terminal electron acceptor shifts as O_2 availability does creating redox couples.

The reduction of terminal electron acceptors is common in wetland environments, as the system creates saturated soils and the necessary conditions. The reduction of terminal electron acceptors can be predicted based on thermodynamics, as processes producing the most energy will occur first, and the subsequent reduction process will only occur once energetically favorable (Sapkota et al., 2022). This concept, referred to as the redox ladder, predicts nitrate

reduction will be followed by the reduction of iron (Fe), manganese (Mn), sulfate (SO_4), and finally the reduction of CO_2, or the production of CH_4. As you move down the 'ladder', less energy is gained, insinuating that these processes happen in a stepwise fashion. However, the anaerobic degradation of complex organics involves a number of cooccurring steps performed by interacting organisms (Nozhevnikova et al., 2020).

Denitrifying microorganisms follow a similar electron transport pathway as aerobic respiring microorganisms, veering course after the third cytochrome complex where ubiquinone is the electron donor and nitrate is the terminal acceptor. The dissimilatory nitrate reduction reaction is due to nitrite reductase (nirK and nirS), intermediately producing nitrite, nitric oxide, nitrous oxide, and finally N^2. Denitrification produces about 75% of the energy as aerobic respiration since the electron chain skips cytochrome complex III (Bleam & Bleam, 2017). Fe^{III} dissimilatory reduction utilizes Fe^{III} or Mn^{IV} as the terminal electron acceptor through the ferric reductase enzyme. The mtr operon encodes the mtrC/omcA cytochromes, allowing the electron transport chain to cross the inner and outer membranes so that the microorganism can come in direct contact with the insoluble Fe oxides (DiChristina et al., 2002; Lovley, 2006). Studies by Lovely have found that some organisms can secrete soluble electron shuttles to elongate contact points among the communities (Lovley, 2017). Energy is only generated from Complex I; complex IV is skipped, and the electrochemical gradient created by complex III is lost as the mtrC/omcA cytochromes is an extracellular transport process (Lovley, 2006). SO_4 dissimilatory reduction can only use the first cytochrome complex; however, the energy gain is far less than that of Fe. Initially, energy must be invested to transform SO_4 to hydrogen sulfite (SO3), the first of four intermediates, using adenosine 5'-phosphosulfate. However, the remaining reactions of

the pathway are energetically favorable, resulting in the production of hydrogen sulfide (Bleam & Bleam, 2017; Bradley et al., 2011).

C reduction is not technically classified as a redox reaction unlike the reduction pathways. Methanogenesis, the methane-generating pathway, is a series of disproportionation reactions utilizing small chain or single C molecules and H. There are three classes of methanogenesis: acetoclastic, methylotrophic, and hydrogenotrophic (Kurth et al., 2020); each utilizes different substrates: acetate, single C compounds, H^+, and CO_2, respectively. Hydrogenotrophic methanogenesis involves the enzymes: Fwd, Ftr, Mch, Mtd, and Mer. Acetoclastic methanogenesis utilizes Acs and Cdh. Lastly, C1 methanogenesis or methylotrophic, requires genes encoding methyltransferase, including Mts, Mra, Mrm, Mtb, and Mtt (Holmes et al., 1995). All methanogenesis pathways conclude with the use of methyl coenzyme M reductase I (MRI), encoded by mcr, a conglomerate of mcrA, mcrB, and mcrG or mrt, encoding methyl coenzyme M reductase II (MRII), isofunctional of MRI (Luo et al., 2002).

The oxidation of CH_4 by microbes is termed methanotrophy. Methanotrophs can operate aerobically, combining O_2 and CH_4 to create many single C intermediates and, eventually CO_2. There are three types of methanotrophs, characterized by their pathways. Type I methanotrophs utilize the RuMP pathway, Type II use the serine pathway, and Type X uses a combination of the two (Kurth et al., 2020). The key enzymes of these bacteria are methane monooxygenases (MMO), a membrane-bound, particulate form with a copper active center (pMMO), and a soluble form with a non-heme iron center (sMMO) (Bowman, 2006; Knief, 2015). Type II and X methanotrophs encode the soluble form, and Type I encodes the membrane-bound form. Among other biogeochemical cycles, methanotrophy is linked to denitrification with MMO's extreme

similarity to AMO (ammonia monooxygenase). Therefore, many CH_4 oxidizers can also perform nitrogen transformations (Zhu et al., 2016).

Some microorganisms are also able to anaerobically oxidize CH_4, coupling with other organisms and other biogeochemical cycles. Initially coupled to sulfate reduction in marine sediments, anaerobic oxidation of CH_4 was observed as sulfate reducers utilized the protons generated from the "reverse methanogenesis" (Barnes & Goldberg, 1976). Denitrifiers are also able to link with anaerobic CH_4 oxidizers to generate overall energetically favorable reactions. There is also coupling with the nitrogen cycle, using nitrite and nitrate as the alternative electron acceptor, mediated by NC10 and ANME-2 bacteria (Wei et al., 2022). Ettwig and his team also found that this can also be true when utilizing soluble Fe^{III} and Mn^{IV}, though the pathways are still unclear (Ettwig et al., 2016). Both methanogens and anaerobic CH4 oxidizers share the aforementioned enzyme complex, methyl coenzyme M (CoM) reductase, which produces or oxidizes CH_4 (Thauer, 2019).

Given the numerous processes and species of microbial life within soils, it would be assumed that the energy potentials and substrate availability would be the sole determinant of competition and microbial populations in systems. However, many factors impact the community composition and their collective impact on the larger system.

CARBON TRANSFORMATIONS AT O_2-DYNAMIC INTERFACES

With the heterogeneous nature of soils, many microenvironments can house microbial populations that are mediating numerous processes simultaneously within close proximity to one another. Substrate availability has been found to be the main driver of C transformations, however, the origin and concentration of these substrates can be from a variety of different sources, including other microorganisms, plant exudates, and preexisting soil characteristics (Sun et al., 2012). In addition to substrate availability; salinity, O_2 availability, and pH are just some of the 'master variables' that impact the biochemical pathways the electrons take and the resulting communities that take shape. Community composition, though, is a transient metric as many organisms have multiple pathways to utilize and uptake energy, impacting the substrates consumed and produced; therefore, composition is as important as activity. The communities themselves are connected and syntrophic.

Microbial communities' substrate use and production facilitate a trophic flow of electrons, energy, and C transformations. Heterotrophic aerobes hydrolytically break down large, complex organics into fermentable, smaller C chains. Fermentation processes create byproducts of organic acids, alcohols, aromatics, and other single-C compounds. This includes CO_2, acetate, and H^+ ions that can then be used for methanogenesis and CH_4 generation (Sowers, 2019). The CH_4 can be oxidized to CO_2, which can work its way through the soil profile through ebullition, diffusion, or plant-mediated transport. Once on the surface with available sunlight, CO_2 can be fixed by phototrophic microbes. Numerous C transformation processes are possible, however, many of them require contrasting conditions to undergo said pathways.

This contradictory phenomenon could potentially be caused by interspecies elemental and electron transfer processes and spatiotemporal O_2 concentration differences. Interspecies electron transfer processes involve electron shuttling via conductive pili, electron transport proteins, electrically conductive materials such as quinone or cystine, or direct use of substrates like H_2 (Lovley, 2017). Functioning not as a donor but as an electron shuttle for methanogens, Cystine has been shown to increase CH_4 production in rice paddy soils (Zhuang et al., 2017).

Beyond syntrophic relationships, spatiotemporal condition changes, whether over space within microsites or time from diel plant-mediated ROL or tidal water table patterns could also explain the differing growth conditions required by one community. Within anoxic microsites of aerated soils, CH_4 generation has been observed. Conventionally, it was thought that this wasn't possible and if so, aerobic CH_4 oxidation would predominate, reducing overall CH_4 emissions. However, there is little evidence to support that CH_4 oxidation rates would increase due to the increased CH_4 generation in these microsites, which would lead to increased CH_4 emissions (Yang et al., 2017). Diel, plant-mediated ROL could provide the necessary O_2 concentrations for these trophic processes to take place. If O_2 can be consumed by aerobic species fast enough, not inhibiting reduction processes, the minute pulses of O_2 from aerenchymatic plants could 'prime' the soil and stimulate CH_4 generation. CH_4 generation is just one of the many transformations that C undergoes within the rhizosphere. Because of the spatiotemporal condition changes brought on by tides, plant inputs, and subsequent microsite changes, a consortium of bacteria with different metabolic potentials coexist.

CONCLUSION

With the need for understanding our global carbon cycle ever more important, it is equally important that we begin to take into account the unknown mechanisms at play below our surface. There is a rising concern of sea level rise, especially in areas like the Eastern Shore of the Chesapeake Bay, at a subduction plate boundary. In turn, understanding the entangled effects of spatiotemporal variation of inundation, salt concentrations, and oxygenation is ever more crucial considering plant-mediated gas transport processes are typically excluded from global change C models.

WORKS CITED

Armstrong, J., Armstrong, W., Beckett, P. M., Halder, J. E., Lythe, S., Holt, R., & Sinclair, A. (1996). Pathways of aeration and the mechanisms and beneficial effects of humidity- and Venturi-induced convections in Phragmites australis (Cav) Trin ex Steud. *Aquatic Botany*, *54*(2-3), 177-197. https://doi.org/10.1016/0304-3770(96)01044-3

Bastviken, D. (2009). Methane. In G. Likens (Ed.), *Encyclopedia of Inland Waters* (First Edition ed., pp. Pages 783-805). Oxford: Elsevier.

Canadell, J. G., P.M.S. Monteiro, M.H. Costa, L. Cotrim da Cunha, P.M. Cox, A.V. Eliseev, S. Henson, M. Ishii, S. Jaccard, C. Koven, A. Lohila, P.K. Patra, S. Piao, J. Rogelj, S. Syampungani, S. Zaehle, and K. Zickfeld. (2021). Global Carbon and other Biogeochemical Cycles and Feedbacks. *Sixth Assessment Report of the Intergovernmental Panel on Climate Change*(Climate Change 2021: The Physical Science Basis).

Carmichael, M. J., Bernhardt, E. S., Brauer, S. L., & Smith, W. K. (2014). The role of vegetation in methane flux to the atmosphere: should vegetation be included as a distinct category in the global methane budget? *Biogeochemistry*, *119*(1-3), 1-24. https://doi.org/10.1007/s10533-014-9974-1

Cicerone, R. J., & Oremland, R. S. (1988). BIOGEOCHEMICAL ASPECTS OF ATMOSPHERIC METHANE. *Global Biogeochemical Cycles*, *2*(4), 299-327. https://doi.org/10.1029/GB002i004p00299

Craft, M. J. V. a. C. B. (2016). *Wetland Soils: Genesis, Hydrology, Landscapes, and Classification* (Second Edition ed.). CRC Press.

Dean, J. F., Middelburg, J. J., Rockmann, T., Aerts, R., Blauw, L. G., Egger, M., Jetten, M. S. M., de Jong, A. E. E., Meisel, O. H., Rasigraf, O., Slomp, C. P., in't Zandt, M. H., & Dolman, A. J. (2018). Methane Feedbacks to the Global Climate System in a Warmer World [Review]. *Reviews of Geophysics*, *56*(1), 207-250. https://doi.org/10.1002/2017rg000559

Hayman, G. D., O'Connor, F. M., Dalvi, M., Clark, D. B., Gedney, N., Huntingford, C., Prigent, C., Buchwitz, M., Schneising, O., Burrows, J. P., Wilson, C., Richards, N., & Chipperfield, M. (2014). Comparison of the HadGEM2 climate-chemistry model against in situ and SCIAMACHY atmospheric methane data. *Atmospheric Chemistry and Physics*, *14*(23), 13257-13280. https://doi.org/10.5194/acp-14-13257-2014

Jackson, R. B., Saunois, M., Bousquet, P., Canadell, J. G., Poulter, B., Stavert, A. R., Bergamaschi, P., Niwa, Y., Segers, A., & Tsuruta, A. (2020). Increasing anthropogenic methane emissions arise equally from agricultural and fossil fuel sources. *Environmental Research Letters*, *15*(7), Article 071002. https://doi.org/10.1088/1748-9326/ab9ed2

Johnson, M. S., Matthews, E., Bastviken, D., Deemer, B., Du, J. Y., & Genovese, V. (2021). Spatiotemporal Methane Emission From Global Reservoirs. *Journal of Geophysical Research-Biogeosciences*, *126*(8), Article e2021JG006305. https://doi.org/10.1029/2021jg006305

Justin, S., & Armstrong, W. (1987). THE ANATOMICAL CHARACTERISTICS OF ROOTS AND PLANT-RESPONSE TO SOIL FLOODING. *New Phytologist*, *106*(3), 465-495. https://doi.org/10.1111/j.1469-8137.1987.tb00153.x

Kirschke, S., Bousquet, P., Ciais, P., Saunois, M., Canadell, J. G., Dlugokencky, E. J., Bergamaschi, P., Bergmann, D., Blake, D. R., Bruhwiler, L., Cameron-Smith, P., Castaldi, S., Chevallier, F., Feng, L., Fraser, A., Heimann, M., Hodson, E. L., Houweling, S., Josse, B., . . . Zeng, G. (2013). Three decades of global methane sources and sinks. *Nature Geoscience*, *6*(10), 813-823. https://doi.org/10.1038/ngeo1955

Lacroix, E. M., Aeppli, M., Boye, K., Brodie, E., Fendorf, S., Keiluweit, M., Naughton, H. R., Noël, V., & Sihi, D. (2023). Consider the Anoxic Microsite: Acknowledging and Appreciating

Spatiotemporal Redox Heterogeneity in Soils and Sediments. *Acs Earth and Space Chemistry*, *7*(9), 1592-1609. https://doi.org/10.1021/acsearthspacechem.3c00032
Mitsch, W. J. a. G. J. G. (2007). *Wetlands* (Fourth Edition ed.). John Wiley & Sons, Inc.
Myhre, G., Nilsen, J. S., Gulstad, L., Shine, K. P., Rognerud, B., & Isaksen, I. S. A. (2007). Radiative forcing due to stratospheric water vapour from CH4 oxidation. *Geophysical Research Letters*, *34*(1), Article L01807. https://doi.org/10.1029/2006gl027472
Nahlik, A. M., & Fennessy, M. S. (2016). Carbon storage in US wetlands. *Nature Communications*, *7*, Article 13835. https://doi.org/10.1038/ncomms13835
Noyce, G. L., Smith, A. J., Kirwan, M. L., Rich, R. L., & Megonigal, J. P. (2023). Oxygen priming induced by elevated CO₂ reduces carbon accumulation and methane emissions in coastal wetlands. *Nature Geoscience*, *16*(1), 63-+. https://doi.org/10.1038/s41561-022-01070-6
Saunois, M., Stavert, A. R., Poulter, B., Bousquet, P., Canadell, J. G., Jackson, R. B., Raymond, P. A., Dlugokencky, E. J., Houweling, S., Patra, P. K., Ciais, P., Arora, V. K., Bastviken, D., Bergamaschi, P., Blake, D. R., Brailsford, G., Bruhwiler, L., Carlson, K. M., Carrol, M., . . . Zhuang, Q. L. (2020). The Global Methane Budget 2000-2017. *Earth System Science Data*, *12*(3), 1561-1623. https://doi.org/10.5194/essd-12-1561-2020
Sorrell, B. K., & Brix, H. (2013). *Gas Transport and Exchange through Wetland Plant Aerenchyma* (Vol. 10). Soil Science Society of America.
Sowers, K. R. (2019). Methanogenesis. In *Encyclopedia of Microbiology, 4th Ediition - Reference Module in Biomedical Sciences*. Ellsevier Inc. https://doi.org/10.1016/b978-0-12-801238-3.02447-8
Srivastava, J., Kalra, S. J. S., & Naraian, R. (2014). Environmental perspectives of Phragmites australis (Cav.) Trin. Ex. Steudel. *Applied Water Science*, *4*(3), 193-202. https://doi.org/10.1007/s13201-013-0142-x
Stagg, C. L., Schoolmaster, D. R., Krauss, K. W., Cormier, N., & Conner, W. H. (2017). Causal mechanisms of soil organic matter decomposition: deconstructing salinity and flooding impacts in coastal wetlands. *Ecology*, *98*(8), 2003-2018. https://doi.org/10.1002/ecy.1890
Vroom, R. J. E., van den Berg, M., Pangala, S. R., van der Scheer, O. E., & Sorrell, B. K. (2022). Physiological processes affecting methane transport by wetland vegetation - A review. *Aquatic Botany*, *182*, Article 103547. https://doi.org/10.1016/j.aquabot.2022.103547
Wilmoth, J. L. (2021). Redox Heterogeneity Entangles Soil and Climate Interactions [Article]. *Sustainability*, *13*(18), 14, Article 10084. https://doi.org/10.3390/su131810084
Wilmoth, J. L., Moran, M. A., & Thompson, A. (2018). Transient O₂ pulses direct Fe crystallinity and Fe(III)-reducer gene expression within a soil microbiome. *Microbiome*, *6*, Article 189. https://doi.org/10.1186/s40168-018-0574-5
Zhang, L. H., Shao, H. B., Wang, B. C., Zhang, L. W., & Qin, X. C. (2019). Effects of nitrogen and phosphorus on the production of carbon dioxide and nitrous oxide in salt-affected soils under different vegetation communities. *Atmospheric Environment*, *204*, 78-88. https://doi.org/10.1016/j.atmosenv.2019.02.024

CHAPTER II

Variation in Wetland Carbon Emissions Driven by Growing Season, Transect Position, and Soil Redox Perturbation

ABSTRACT

Wetlands form a massive reservoir of soil carbon (C) that is disproportionately impacted by climate change and displays extreme variability in C cycling over different spatiotemporal scales. The biogeochemical pathways underpinning this variability remain a critical knowledge gap due in part to the oversimplification of soil organic matter (SOM) transformations in the wetland rhizosphere. These transformations occur over short spatiotemporal scales in often heterogeneous environments, influenced by transient shifts in seasonality, organic molecular characteristics, and redox conditions. Tidal marshes bordered by forest are of unique concern due to marked differences in SOM chemistry along the wetland-to-forest transect, some of which are experiencing accelerated sea level rise, furthering their complexities. We incubated soils collected from a wetland transect dominated by *Phragmites australis* to test the effect of differences in seasonality (relevant to plant growth in the field), local SOM profiles (based on transect position, relevant to sea level), and soil redox perturbation (analogous to radial oxygen loss (ROL)) on C emissions. Our results suggest that the redox modulation expected to be carried out by *Phragmites* in the field can potentially increase C emissions depending on transect location and seasonality. Considering that sea level rise will likely extend *Phragmites* into new soil zones, our work allows for predictions of how it could affect C cycling in the newly invaded soils. This provides deeper mechanistic insight into the C cycle of coastal soils and underscores

the need for further investigations of the wetland-to-forest ecotone to help improve landscape and global C models while informing climate mitigation policies under rising seas.

HIGHLIGHTS

- Soil incubations from the wetland interior position collected during the pre-growing season released a CH_4 burst immediately following brief O_2 pulsing.
- O_2 pulses stimulated higher CO_2 emission rates on average using pre-growing season soils compared to those collected during the growing season.
- Soils collected at the wetland-forest boundary during the growing-season displayed unchanged CO_2 production regardless of O_2 pulsing, indicating similarly high levels of SOM degradation under both anoxic and oxic conditions.
- Taken together, plant-mediated oxygenation is expected to prime/stimulate CH_4 and CO_2 emissions in the field, requiring either equivalent or longer time scales relative to our laboratory conditions.

INTRODUCTION

Wetlands account for 20-30% of Earth's soil C pool, the most dynamic pool of global C; therefore, understanding their dynamics is ever more critical (Craft, 2016; Lacroix et al., 2021; Mitsch, 2007; Nahlik & Fennessy, 2016). At the interface of land and water, complex, accelerated biogeochemical transformations are possible under climate change conditions, some of which could further destabilize soil C and increase greenhouse gas emissions (Canadell, 2021;

Stagg et al., 2017). Predicting these transformations requires a detailed characterization of soil organic chemistry in the wetland rhizosphere under short spatiotemporal changes. Process-based models lack the spatial and temporal variability of plant-mediated transport. Most current models are one-dimensional on the depth axis, not accounting for soil salinity, redox potential, root permeability, root length, proportion of root aerenchyma, and nitrogen content (Raivonen et al., 2017; Wania et al., 2010). Variability in senescence and diurnal dynamics influence both atmospheric gas emissions and ROL but are not accounted for in most land-scale and earth system models (Ge et al., 2023; Korrensalo et al., 2022). A critical knowledge gap still remains due to the transient nature of different environmental drivers (e.g., seasonality, local soil chemistry, redox shifts), which influence soil organic C chemistry in coastal wetlands across different spatiotemporal scales (Noyce & Megonigal, 2021; Noyce et al., 2023).

The complexity of C exchange between the atmosphere and wetland soil is furthered by variable redox conditions and organic chemistry controlled by vegetation. The aerenchyma tissue of wetland plants acts as a conduit between the rhizosphere and atmosphere, allowing CH_4 to bypass oxidation and the hydrostatic pressure that slows gas diffusion while soils are inundated (Zhuang et al., 2004). *Phragmites* is known to oxygenate the soil at high levels, even slightly greater than atmospheric conditions (> 20% O_2). It also has an extensive rhizome network and a high tolerance to saturation and salinity levels (Srivastava et al., 2014). Recent planar optode imaging during mesocosm studies has shown tightly coupled diurnal patterns of ROL and concurrent C mineralization within the rhizosphere near plant roots/rhizomes (Lenzewski et al., 2018; Li et al., 2022; van den Berg et al., 2020). Consequently, *Phragmites* could be an overlooked bioindicator of soil redox status due to its ability to oxygenate the otherwise O_2-

limited soil and subsequent wetland C cycling as salinity and water levels transform and wetlands migrate into upland soils (Afreen et al., 2007; Armstrong & Armstrong, 1988; Canadell, 2021; Justin & Armstrong, 1987; Kirwan & Gedan, 2019; Srivastava et al., 2014).

It is well known that oxygenation of wetland soil tightly regulates biogeochemical cycles, including that of nitrogen (N), iron (Fe), phosphorus (P), and sulfur (S) (Noyce et al., 2023; Zhang et al., 2019). This requires a closer examination when considering broader SOM transformations that lead to C emissions (Wilmoth et al., 2021). For example, CH_4 production has generally been considered to be inhibited by O_2, consistent with the observation of CH_4 generation in anoxic sediments (Sowers, 2019). However, it is becoming more widely recognized that periodic oxygenation of otherwise anoxic soils and sediments may play a major role in priming organic C toward elevated CH_4 production (i.e., the soil "methane paradox") (Angle et al., 2017; Wilmoth et al., 2021; Yang et al., 2017).

It has been shown that upward of 90% (or more) of CH_4 emitted from wetlands may originate in the uppermost layers of the soil where O_2 is intermittently present (Angle et al., 2017). Similarly, it has also been observed that CO_2 production can be stimulated in redox-oscillating soils, where some tropical soils rich in Fe^{III} minerals have been shown to release more CO_2 under anaerobic conditions when organic inputs are high (Hu et al., 2021; O'Connell et al., 2018; Wilmoth et al., 2018; Zhao et al., 2019). An analogous observation has been made in Prairie Pothole wetlands, a freshwater wetland system running between Canada and the US Midwest, where SO42- and CH_4 are known to be produced simultaneously without apparent competition due to high levels of DOC (Martins et al., 2017). In *Phragmites* invaded systems,

elevated CH_4 emissions have also been observed, with speculation of the role O_2 played in these soils (Mueller et al., 2016).

The mechanistic details of how periodic O_2 exposure stimulates C emissions from redox-oscillating soils remain poorly understood (Angle et al., 2017; Lacroix et al., 2023; Wilmoth et al., 2021). O_2 can potentially stimulate heterotrophic microbial respiration, reinitiating the production of competing terminal electron acceptors. Theoretically, terminal electron acceptors are used in order of decreasing thermodynamic yield; however, in a dynamic system, these substrates and terminal electron acceptors are simultaneously present and utilized (Megonigal, 2019). Considering organic matter degradation is limited under anaerobic conditions relative to aerobic, we believe that in a predominantly anaerobic system receiving small pulses of O_2, in space (distributed throughout the profile) and time (diurnal and seasonally), C transformations, specifically CH_4 generation, could be stimulated. This is based on the fact that oxidase and dioxygenase enzymes require O_2 to degrade complex aromatic structures like lignin in organic matter (Wang et al., 2018; Xu et al., 2022).

In coastal regions, sea level rise and the resulting migration of wetlands are expected to further complicate C transformations between the wetland interior and adjacent upland soils. Tidal marshes bordered by forest are of unique concern due to marked differences in SOM chemistry along the wetland-to-forest transect. To better understand the variability of C emissions in such a dynamic system, we investigated the behavior of CH_4 and CO_2 emissions corresponding to both anoxic conditions and plant-mediated oxygenation of soil. A modified oxygenation analogous to that of *Phragmites* was initiated after three weeks of anoxic incubation of soils collected before natural oxygenation occurred (in March) as well as soils collected

during the active growing season (in July) to test the effect of diurnal oxygenation. We hypothesized that oxygenation would increase C emissions after brief pulsing of O_2. Our reasoning is that there should be an increase in smaller, more bioavailable C substrates for methanogenesis following oxidation due to the temporary stimulation of SOM degradation. Importantly, if the redox perturbation by O_2 pulsing is transient in an otherwise anoxic/anaerobic system, methanogenesis should not be hindered (i.e., it should be stimulated). We predict that soils collected before the growing season, having not recently experienced the plant-mediated O_2 pulses in the field, will yield a greater generation of CO_2 and CH_4 after the laboratory (analog) pulses compared to those collected during the growing season that had recently experienced the natural oxygenation by plants.

MATERIALS & METHODS

Field Sampling & Site Description

Soil samples were collected within the Smithsonian Environmental Research Center's Global Change Research Wetlands (G-CREW) in Edgewater, Maryland (38.87516782°, –76.54525616°). This oligohaline marsh, previously occupied by the Indigenous Piscataway People, is on the Rhode River, a tributary of the Chesapeake Bay. The transect used runs from the center of Kirkpatrick Marsh, crossing a small land-fed creek, and ends at the forest edge shown in **Figure 1**. *Phragmites australis* dominates the *entire* transect; however, the soil characteristics and inundation levels varied from site to site. It has a salinity of about 8.45 ppt during the growing season, changing slightly with the tides, and has a pH of approximately 6.01.

Using a McCauley Auger, six soil cores were collected perpendicular to the transect at each location from 20 cm below the surface where rhizomes were abundant. Similar profiles were observed at Sites 1 and 2 with a more extensive organic layer from 0 cm to 5 cm followed by a layer of peat, likely from a prior population of *Spartina alterniflora.* We observed that many actively growing rhizomes from standing *Phragmites* did not pass below this dense bottom layer of peat. The third profile from Site 3, closest to the forest, had much more development with more distinct horizonation. First, a much darker silty first layer, followed by a redox feature-rich bottom layer with an apparent increase in sand and clay content. Profile pictures are in **Figure 2**. Pore water was collected from the "Pore Water Collection Site" indicated by the blue marker in **Figure 1**. Two cores were augered to a depth of 20 cm to allow for the collection of porewater via core recharge with Falcon sample tubes. Both soil and water were kept in coolers to maintain their temperature and transferred to the lab for immediate assembly into incubations.

Soil Incubation Setup

Benchtop incubations were carried out to test the effect of transient oxygenation on soil dissolved organic chemistry using our collected soil and porewater from the field site. Soil and water were collected before and during the active growing season of *Phragmites* in early March and mid-July of 2024, respectively, and stored at ambient conditions until their assembly within 24 hours of sampling. Once brought into the lab, the six cores from each transect site were homogenized by hand in ambient conditions, large plant material was picked out by hand, and fine roots were removed with forceps. Porewater from the bulk collection site shown in **Figure 1** was taken back to the lab and spun down at 10 *g* for 15 minutes to remove suspended solids. Soil slurries were established using a soil-to-water ratio of 1:10 in 120 ml amber serum bottles with a

total slurry volume of 60 ml, leaving 60 ml of headspace, then sealed with butyl stoppers and aluminum crimp caps. The headspace was flushed with pure N_2 gas while stirring to maintain/initiate anaerobic conditions. Serum bottles were gently shaken end-over-end at each sample time point and kept in the lab at 22 to 25°C.

Experimental Scheme

In the pre-growing season incubation (March sampling), four triplicated incubations were constructed for each location along the transect. One set of bottles was destructively harvested each week to see liquid and solid phase changes over time. At the beginning of the third week, a pulse of 10 ml of ambient air was injected into the bottles, making the headspace O_2 concentration 3.5%. This was done every 24 hours for 72 hours. At the conclusion of the fourth week, the last set of bottles was destructively harvested, as shown in **Figure 3.** This process was repeated for the growing season incubations, with soil and water collected in mid-July. For this incubation, six sets were constructed for each point along the transect. Sets were destructively harvested after one and three weeks. At the beginning of week three, O_2 was introduced in the same fashion to three of the four remaining sets, which were destructively harvested weekly following the pulse, while the anoxic control set was harvested during the last (6th) week of the incubation, also shown in **Figure 3.**

Carbon Measurements: CO_2 & CH_4

Headspace gas samples were collected, on average, twice weekly. First, 0.5 ml of N_2 was injected to overpressurize the serum bottle headspace and then swirled. Next, 0.5 ml of mixed headspace gas was removed and directly injected into an SRI-8610C Gas Chromatograph Mass

Spectrometer equipped with a flame ionization detector (FID) fitted to measure CH_4 and CO_2 in a single run. The area under the curve was calculated using Peak Simple and compared to the standard curve to extrapolate a concentration in ppm.

All main figures were made with R Studio version 2024.09.1+394, Cranberry Hibiscus, using the tidyverse and ggplot. To assess significance, a two-way repeated measures ANOVA was conducted using the aov() function in R, with treatment and site as fixed effects and replicate as the within-subjects (repeated) factor. This approach allowed for testing interactions between site and treatment phase while accounting for repeated measurements within each replicate. Then accounting for the nested replicate structure, a linear mixed-effects model (LMM) was fitted using the lmer() function from the lme4 package. In the LMM, treatment, site, and their interaction were treated as fixed effects, and replicate was included as a random intercept to account for within-group correlation across repeated measures. In some models, seasonality (March vs. July) was also included as an additional fixed effect. Finally, Type III ANOVA tables with Satterthwaite's approximation for degrees of freedom were generated using the lmerTest package to assess the significance of fixed effects in the mixed-effects models. All statistical analyses were conducted in R (version [insert R version]), with an alpha level of 0.05 used to determine statistical significance.

RESULTS

Site Differences

Pre-growing Season. The CO_2 concentrations increased in all three sites after the O_2 pulse, with the third site being higher throughout the incubation both before and after the pulse (**Fig. 4**). Less CO_2 was observed in Site 1 during the anoxic portion of the experiment, but after oxygenation, there was an increase in CO_2 concentrations (from 0.03-0.1 ugC/kg Soil to 0.16-0.275). However, CH_4 concentrations decreased within the first 3 days, where Sites 2 and 3 quickly surpassed their initial values by the end of week one, with Site 2 being slightly higher. Around day 10 in Sites 2 and 3, CH_4 began to plateau and remain relatively constant even after the oxygenation treatments. Site 1 remained near the detection limit of the instrument for CH_4 that showed a sharp increase following the O_2 pulse **(Fig. 5)**. The linear mixed effects model showed there were significant main effects for site ($F(2, 20) = 50.39$, $p < .001$) and oxygen pulse ($F(1, 20) = 9.37$, $p = .006$), as well as a significant interaction ($F(2, 20) = 11.00$, $p < .001$), indicating that the response to treatment differed across sites. For CO_2, a significant effect of oxygenation, $F(1, 20) = 29.26$, $p < .001$; The main effect of site was not significant, $F(2, 20) = 2.19$, $p = .14$, and there was no significant interaction between location and treatment phase, $F(2, 20) = 2.19$, $p = .40$, indicating the treatment effect was consistent across locations.

Growing Season. CO_2 concentrations, as shown in **Figure 6**, showed Site 3 was the site to have small differences between the anoxic and oxygenation treatment groups compared to Sites 1 and 2. The oxygenated treatment groups show higher CO_2 concentrations in both Sites 1 and 2. However, prior to the O_2 pulse, during the anoxic phase of the incubation, Sites 2 and 3 had a

steady increase in CH_4 concentration until the beginning of the second week when a plateau was observed **(Fig. 7)**. After the O_2 pulse, a larger difference in CH_4 concentration between the control and treatment compared to that of Site 1 was observed. Even though the oxygenated treatment had lower CH_4 concentrations than that of the anoxic control, the rate of CH_4 production in week 6 (steepness of the line) was greater than that of the anoxic control. Site 1 had low concentrations of CH_4 for both groups throughout the entirety of the incubation. Similarly to CH_4 concentrations shown in **Figure 7**, the three sites along the transect from the growing season incubations varied in CO_2 concentrations amongst the sites. The linear mixed effect model revealed significant main effects on CH_4 of Site ($F(2, 20) = 50.39$, $p < .001$)* and oxygen pulse ($F(1, 20) = 9.37$, $p = .006$) as well as a significant interaction ($F(2, 20) = 11.00$, $p < .001$), indicating that the response to treatment varied across locations. The model also revealed there was a significant effect on CO_2 concentrations from location, $F(2, 21) = 60.13$, $p < .001$, as well as a significant main effect of treatment phase, $F(1, 21) = 95.54$, $p < .001$; The interaction between location and treatment phase was significant, $F(2, 21) = 5.83$, $p = .0097$, indicating that the treatment effect on CO_2 varied by location.

Seasonal Comparisons

When comparing the samples collected in March and July, differences in CO_2 concentration were observed amongst sites. Sites 1 and 3 both had higher concentrations of CO_2 in the July sampling time frame compared to March before the O_2 treatment; this relationship became opposite after the oxygenation **(Fig. 8)**. When looking at CO_2 while comparing the three sites seasonally, as shown in **Figure 9**, the anoxic portion of the incubation were pretty variable.

However, all three sites did have higher CH_4 concentrations in the July sampling groups right before the oxygenation events. This changed post oxygenation events, observing that incubations from Pre-growing Season soils collected in March were higher in CH_4 those of the Growing-Season collected in July after oxygenation. The model results indicated a significant effect of site ($F(2, 41) = 5.31$, $p = 0.0089$), oxygen pulse ($F(1, 41) = 48.31$, $p < 0.001$), but not seasonality ($F(1, 41) = 1.86$, $p = 0.18$) on CH_4 concentrations. A significant interaction was found between treatment phase and seasonality ($F(1, 41) = 17.33$, $p < 0.001$), suggesting that the treatment effect varied between the seasons. For CO_2, the model suggested that site ($F(2, 41) = 108.40$, $p < 0.001$) and treatment ($F(1, 41) = 25.51$, $p < 0.001$), indicating that CH_4 concentrations differed significantly among sites and between treatment periods. Seasonality was not a significant main effect ($F(1, 41) = 1.78$, $p = 0.189$). However, the treatment × season interaction was highly significant ($F(1, 41) = 91.74$, $p < 0.001$), suggesting that the treatment effect varied across seasons. Lastly, a significant site × treatment interaction ($F(2, 41) = 7.25$, $p = 0.002$) and a three-way interaction among site, treatment, and season ($F(2, 41) = 4.55$, $p = 0.016$) indicate that the treatment effect differed across locations and was further modulated by time of sampling. No significant interaction was found between site and season ($F(2, 41) = 0.20$, $p = 0.823$).

DISCUSSION

CH_4 & CO_2 Production Following Oxygenation

Pre-Growing Season Soil. In the pre-growing season incubations, the CO_2 concentrations increased in all three sites following the O_2 pulse (**Fig. 4**). However, this was not the case

regarding CH_4. Compared to Site 1, there was a plateau in CH_4 concentrations in Site 2 and 3 observed early in the anoxic phase of the incubation that could indicate (1) a lack of usable substrates for methanogenesis (methanogenesis slows) and/or (2) CH_4 is oxidized under anaerobic conditions (i.e., anaerobic CH_4 oxidation). The slight increase in CH_4 concentrations following the O_2 pulse in Sites 2 and 3, may be due to aerobic methanotrophy co-occurring with methanogenesis (**Fig. 5).** The dramatic increase in CH_4 following oxygenation in Site 1, relative to 2 and 3, may be due to Site 1 samples existing in a more inundated field condition; C here would likely be less bioavailable (larger, more reduced organic molecules) compared to soil collected from other transect locations (Angle et al., 2017; Wilmoth et al., 2021) (**Fig. 5**).

Growing-Season Soil. For soils collected during the growing season, Sites 2 and 3 had increasing concentrations of CH_4, which then reached a plateau by the second week **(Fig. 7)**. For the anoxic control group, this plateau was maintained throughout the remainder of the incubation. The oxygenated treatment did decrease in concentration in incubated soils from all three sites; however, by the end of week 6, the rate of CH_4 production was greater than that of the anoxic control. The steady decline of CH_4 concentration could be explained by its oxidation into CO_2 and be representative of a 'lag phase'. During this phase, perhaps aerobic microorganisms break down larger C compounds into C-1 compounds, and fermenters provide hydrogen and acetate, leading to the substrates for methanogenesis. These substrates could have contributed to the increase in the CH_4 production rate observed during the last week of incubation.

Influence of Growing Season & Transect Location

In the pre-growing season incubations, CH_4 concentrations varied by site throughout the incubation. Sites 2 and 3 reached a plateau by day 11, indicating a lack of CH_4 generating C compounds; however, Site 1 behaved differently, having CH_4 concentrations near the detection limit of the instrument until the O_2 pulses were administered. In the field, Site 1 would likely have the *most* anaerobic conditions with the lack of plant and tidal-mediated redox oscillations, because of the timing of the sampling in the pre-growing season and consistent inundation being the most interior position along the transect respectively. The amount of smaller, previously broken-down C compounds would be significantly less, following the observation of CH_4 generation only after the O_2 pulse (**Fig. 5)** (Wilmoth et al., 2021).

In the incubations of soil and water collected from the growing season, differences in CO_2 and CH_4 concentrations were also observed by position along the transect. Site 1 had minimal variation between the anoxic control and oxygenated group (Week 6) compared to that of Sites 2 and 3. The decrease in CH_4 concentrations from Site 1, in both the treatment and anoxic control, could be due to aerobic CH_4 oxidation and anaerobic CH_4 oxidation, respectively. The similarities in the observations of these groups could be due to inundation levels. With Site 1 being most interior and subsequently the most consistently saturated, it would be expected for the Phragmites to have more active pressurized gas flow to the subsurface, meaning more ROL (Afreen et al., 2007). Site 1's lack of difference in CH_4 concentrations between the treatment and control groups could be an indication of the priming effect already occurring, given that in the pre-growing season samples the plant-mediated diurnal pulsing of O_2, it would require an artificial oxygenation event to free up previously preserved C that would lead to the generation

of greenhouse gasses **(Fig. 7)**. This would also be supported by Site 1 having the lowest concentration of CO_2 after the pulse, potentially from the lack of CH_4 oxidation or the lack of usable C compounds **(Fig. 6)**. Site 1 is closest to the larger tidal creek that feeds from the surrounding landscapes, some of which are agricultural fields. Therefore, there could be more nutrient input in the soil water that was present during sampling. These substrates, as well as sulfates in the brackish water, could have competitively inhibited CH_4 generation. Even though the oxygenated treatment had lower CH_4 concentrations than that of the anoxic control, the rate of CH_4 production in week 6 (steepness of the line) was greater than that of the anoxic control in Sites 2 and 3.

These differences observed for CH_4 between Sites were also observed in terms of CO_2 concentrations but amongst different sites. Site 3 had little change in concentrations between the anoxic and oxygenation treatment groups compared to Sites 1 and 2 **(Fig. 6)**. The oxygenated treatment groups show higher CO_2 concentrations in both Sites 1 and 2, consistent with the idea of CH_4 oxidation via methanotrophy.

When comparing the gas dynamics of these incubations from a seasonal lens, differences between the oxygenated treatments of the pre- and active growing season sampling campaigns were observed. The slightly higher CO_2 concentrations observed in all sites from the growing season compared to the pre-growing season were expected and attributed to the increase in microbial activity from higher temperatures as well as root exudate inputs. After the O_2 pulse, the limited change in CO_2 concentrations from the growing season site indicates the previous priming that had taken place, potentially contributing to the greater increase seen in the pre-growing season samples in Sites 1 and 2.

CONCLUSIONS

The differences in C emissions between sites both seasonally and throughout the incubation indicate that pulsed oxygenation plays a stimulatory role in wetland C dynamics. Our data support the importance of transient oxygenation, analogous to that mediated by vegetation in the field, as a priming agent and subsequent integral catalyst of greenhouse gas production in wetland soils. In the field, this effect might require equivalent or longer time scales compared to our study conditions. However, considering the spatiotemporal complexity within these systems, in situ studies would help confirm that transient oxygenation facilitates increased C emissions in the field, aiding in the identification/quantification of *hot spots* and *hot moments* of C cycling.

Our emerging conceptual framework is that these transient dynamics influence wetland soil chemistry and have the potential to explain the often-observed large-scale variability in wetland C emissions. In Chapter III, we will investigate the chemical nature of SOM in this wetland soil to help explain the linkages between C emissions and broad-spectrum organic transformations. Through this work, we seek to understand how the dissolved organic profile changed before and after the pulse, as well as the influence of seasonality and wetland position on C chemistry. Future work should investigate the microbial community composition and how they shift by site, throughout the incubation period, and field conditions after oxygenation events to help shed light on additional drivers of wetland C cycling.

FIGURES

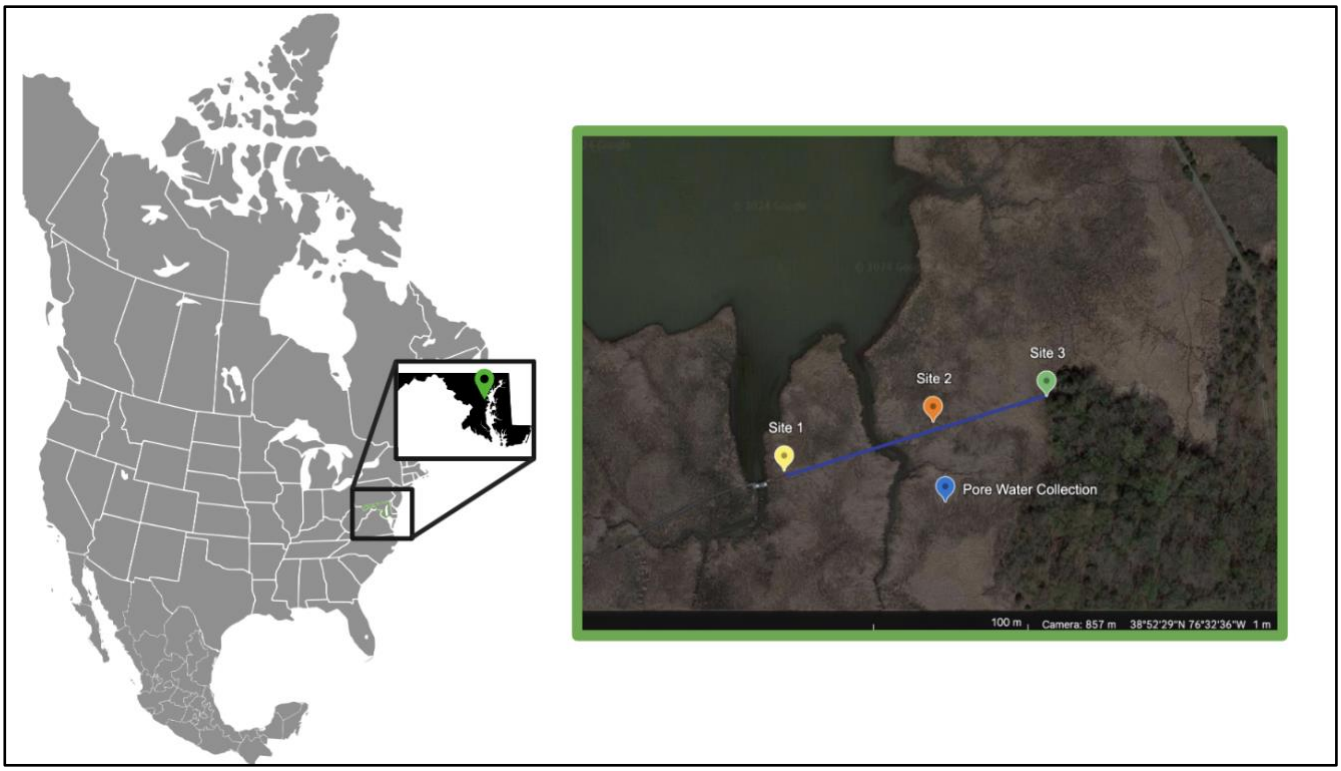

Figure 1.

Above shows North America, specifically highlighting the sampling location on the Rhode river. On the right, the field transect used to collect soils for the laboratory incubation experiments. Each plot is denoted as, "Site 1, 2, and 3" in yellow, orange, and green, respectively, with the area that the bulk site water was denoted as "Bulk Water Collection" in blue. The entire area is dominated by *Phragmites*. Site 1 has two creeks on either side, followed by Site 2 with a creek to the west. Site 3 is close to the forest edge, with a more developed, mineral-rich, soil profile.

Figure 2.

Shown above from left to right are three soil cores from Site 1, 2, and 3, respectively. Sites 1 and 2 have more similar profiles with an upper and lower layer. The top being more organic and mucky, followed by a lower layer that is significantly more peaty with a dense layer of rhizomes separating the two. The third core from Site 3 has much more development with three distinct layers, the top still organic and mucky but with a darker color compared to the first two sites, a darker grey and sandier middle layer, followed by a redox feature-rich bottom layer with an apparent increase in sand and clay content.

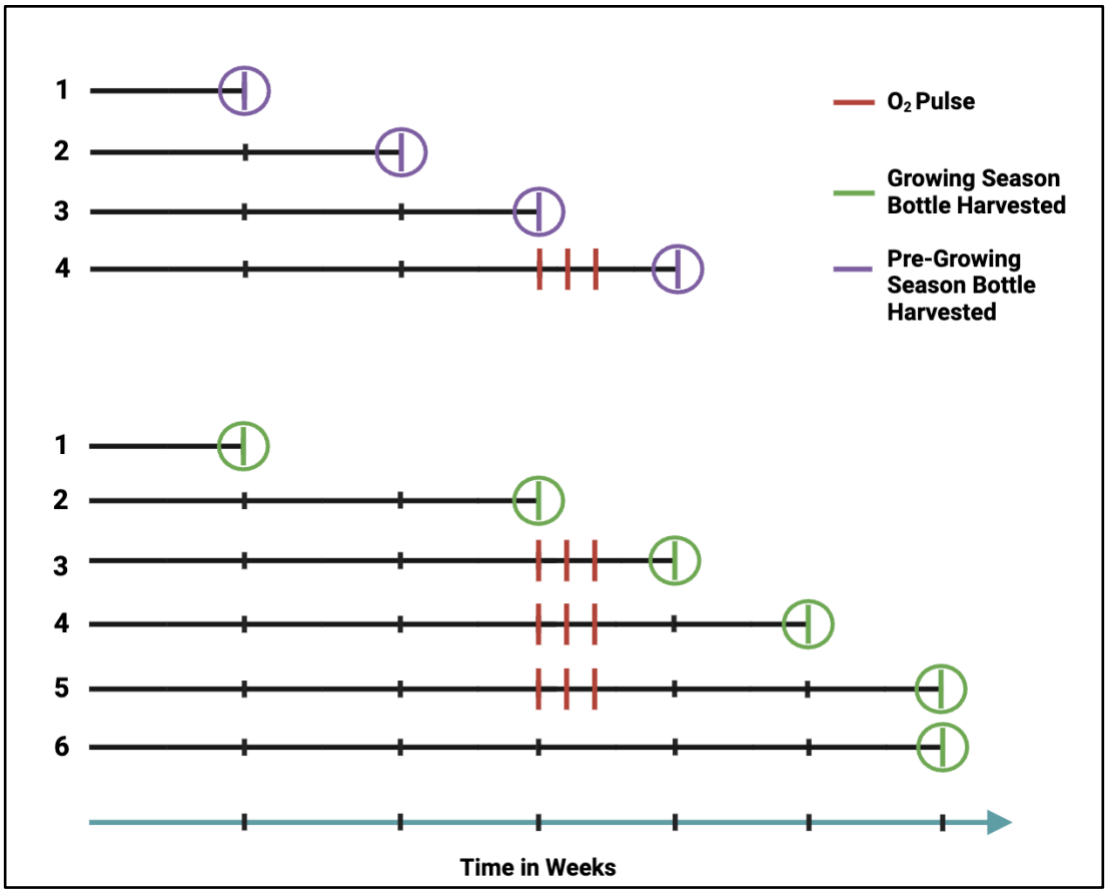

Figure 3.

Above is a schematic describing the experimental setup for the incubations. Each numbered set was triplicated, the purple lines and circles indicate when the set was destructively harvested for the pre-growing season (March sampling) set of incubations, and the green lines with circles indicate the incubations constructed with soil from the active growing season (July sampling). The red lines indicate the 10 ml pulse of ambient air to oxygenate the bottles.

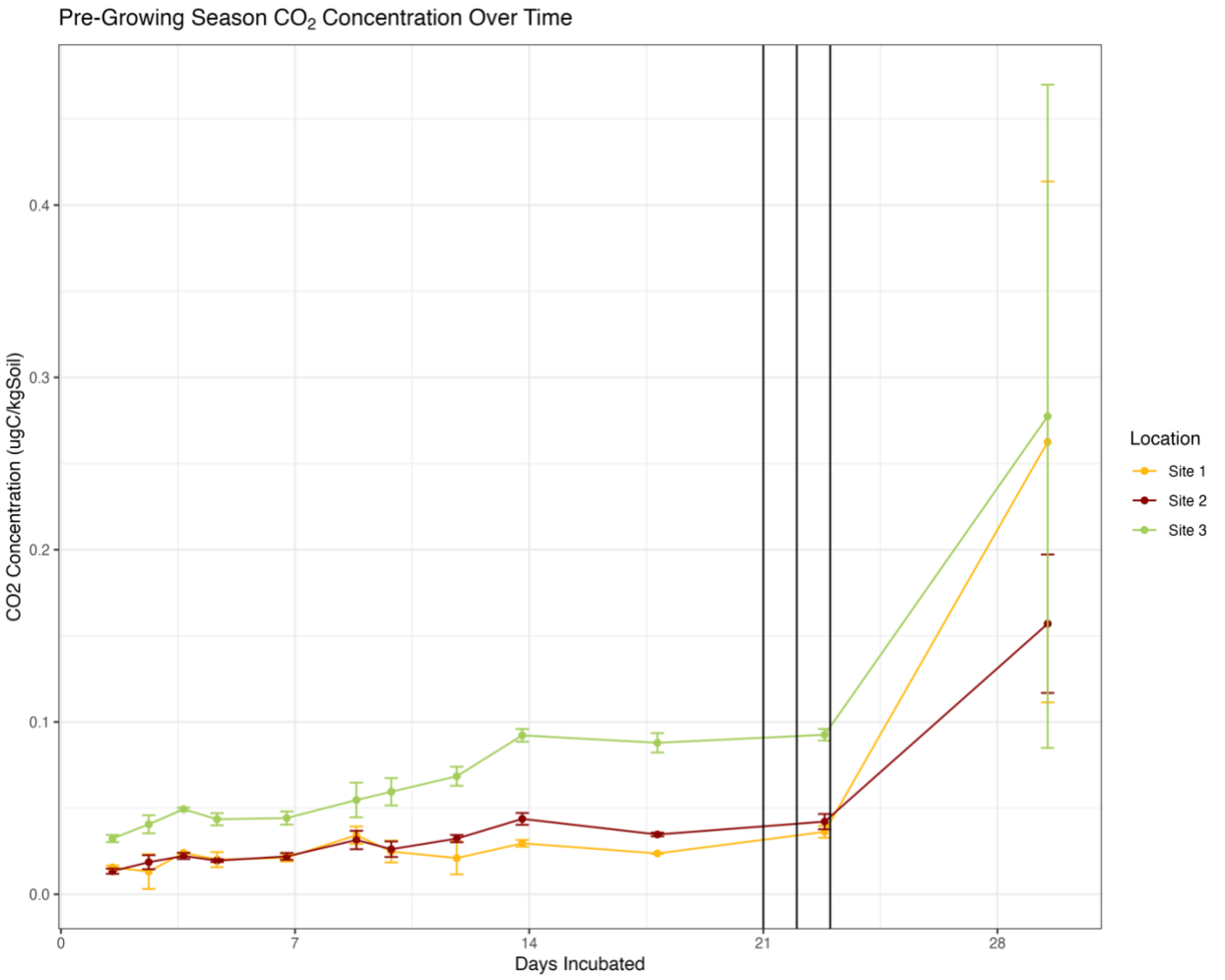

Figure 4.

The concentration of CO_2 in the headspace gas in µg C/kg soil is plotted against the days incubated for each of the sites along the transect for the incubations assembled with materials collected before the growing season had begun. Green indicates Site 3, closest to the forest edge, red for Site 2 between the forest and the most interior point on the transect, Site 1, in yellow. The three black vertical lines on days 21, 22, and 23 indicate the O_2 pulse administered, with the third line being offset to the right so as not to overlap with the measurement. Even though a destructive sampling scheme was used, n = 3 throughout the entire incubation.

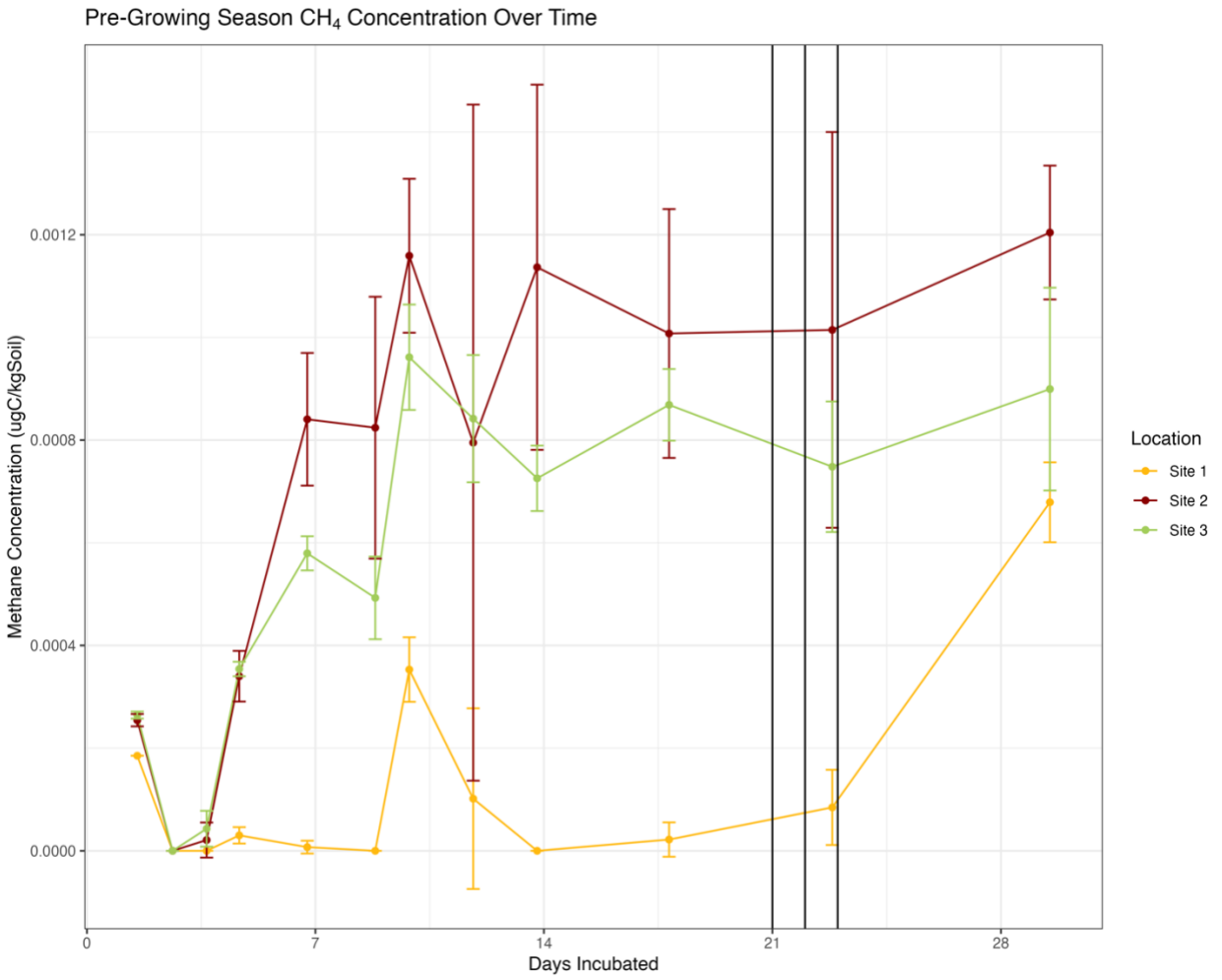

Figure 5.

The concentration of CH_4 in the headspace gas in µg C/kg soil is plotted against the days incubated for each of the sites along the transect for the incubations assembled with materials collected before the growing season had begun. Green indicates Site 3, closest to the forest edge, red for Site 2 between the forest and the most interior point on the transect, Site 1, in yellow. The three black vertical lines on days 21, 22, and 23 indicate the O_2 pulse administered, with the third line being offset to the right so as not to overlap with the measurement. Even though a destructive sampling scheme was used, n = 3 throughout the entire incubation.

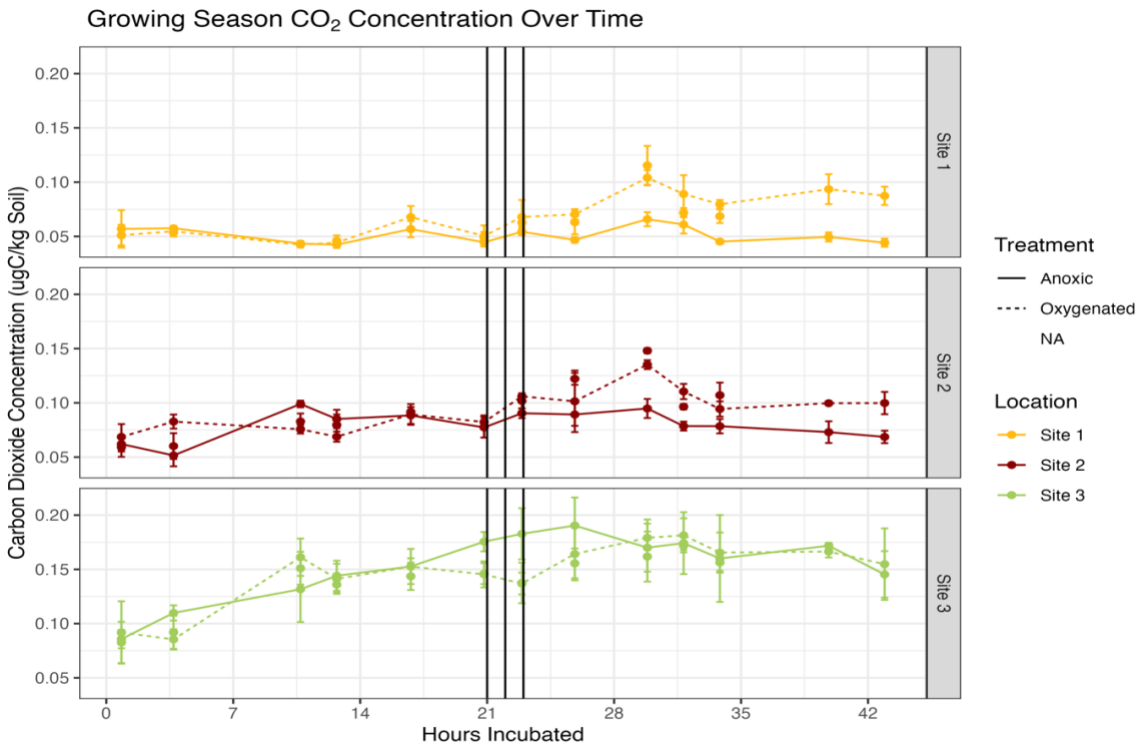

Figure 6.

The average CO_2 concentration was plotted in µg of C/kg of soil against the days incubated for the incubations constructed with soils collected in March, before the growing season. The three black vertical lines on days 21, 22, and 23 indicate the O_2 pulse administered, with the third line being offset to the right so as not to overlap with the measurement. Even though a destructive sampling scheme was used, n = 3 throughout the entire incubation.

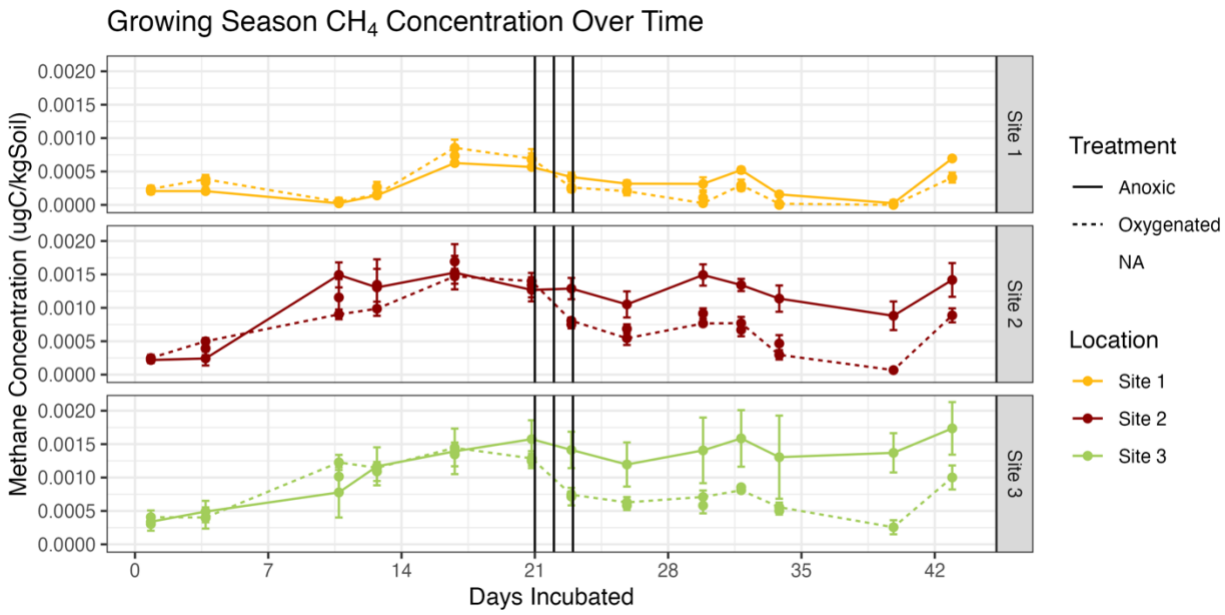

Figure 7.

The average CH_4 concentration was plotted in µg of C/kg of soil against the days incubated for the incubations constructed with soils collected in March, before the growing season. The three black vertical lines on days 21, 22, and 23 indicate the O_2 pulse administered, with the third line being offset to the right so as not to overlap with the measurement. Even though a destructive sampling scheme was used, n = 3 throughout the entire incubation.

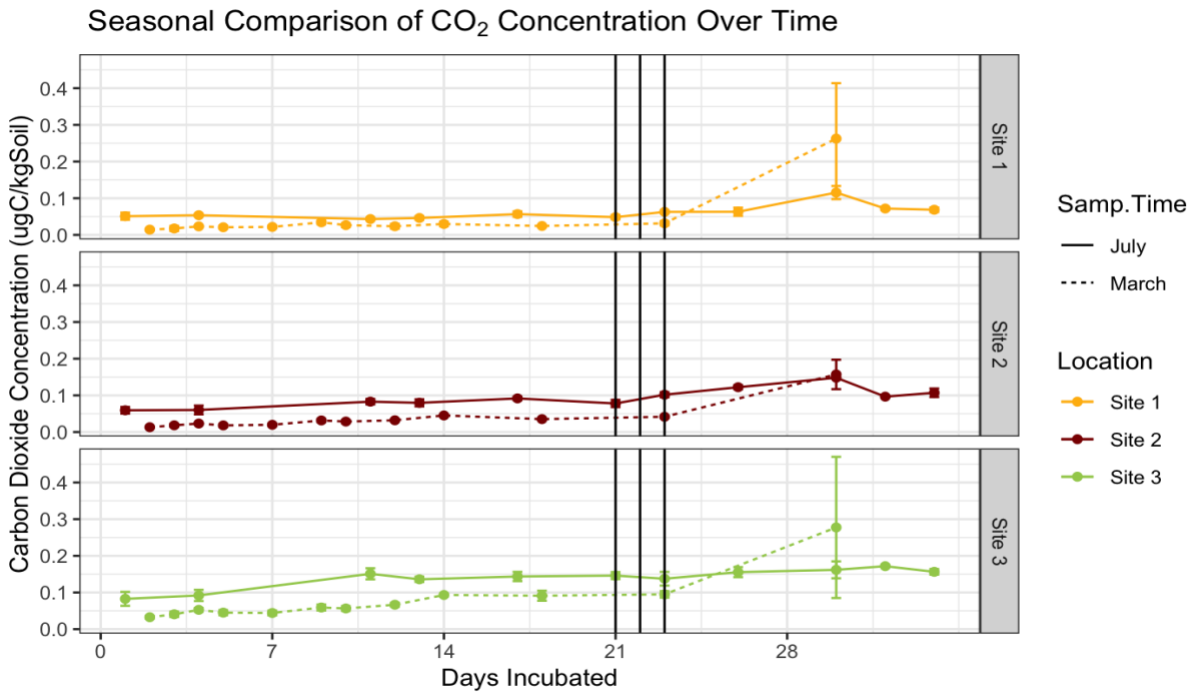

Figure 8.

The concentration of CO_2 in the headspace gas in µg C/kg soil is plotted against the days incubated for each of the sites along the transect for the incubations assembled with materials collected both before the growing season had begun in March, indicated by the dashed line, and during the growing season in July, indicated by the solid line. Green indicates Site 3, closest to the forest edge, red for Site 2 in between the forest and the most interior point on the transect, Site 1, in yellow. The three black vertical lines on days 21, 22, and 23 indicate the O_2 pulse administered, with the third line being offset to the right so as not to overlap with the measurement. Even though a destructive sampling scheme was used, n = 3 throughout the entire incubation.

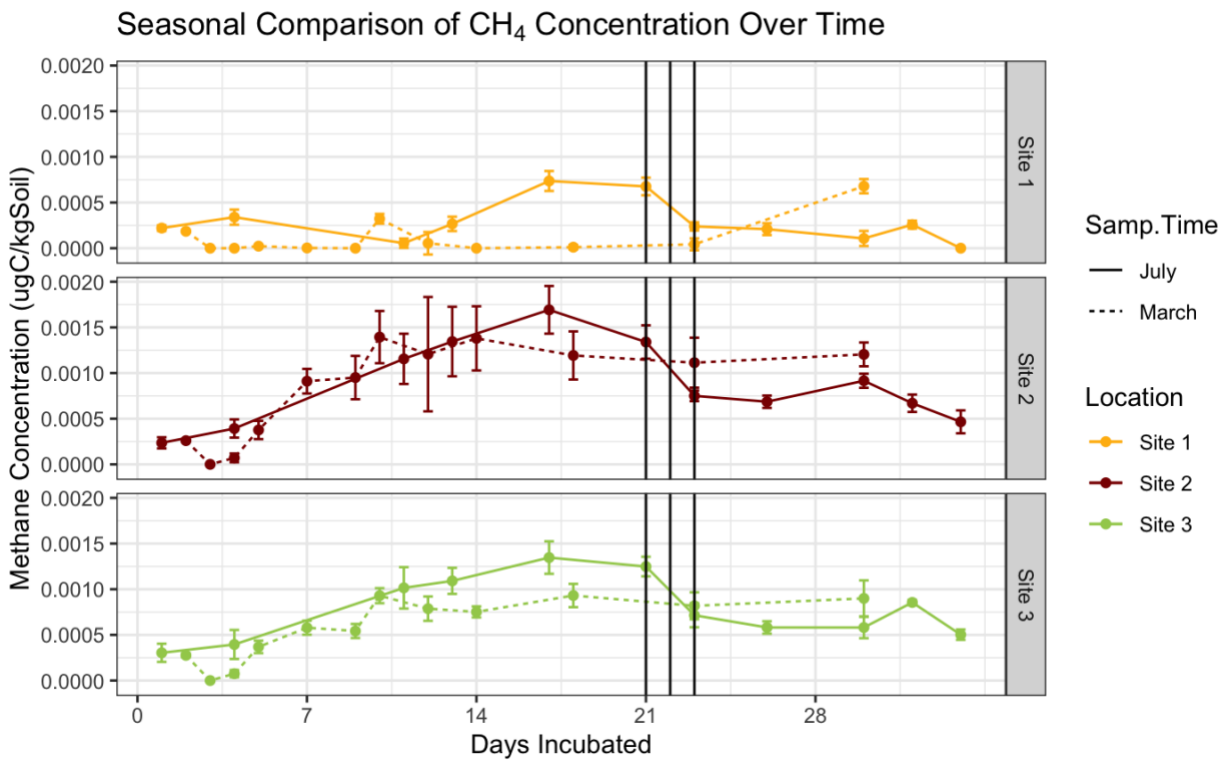

Figure 9.

The concentration of CH_4 in the headspace gas in µg C/kg soil is plotted against the days incubated for each of the sites along the transect for the incubations assembled with materials collected both before the growing season had begun in March, indicated by the dashed line, and during the growing season in July, shown by the solid line. Green indicates Site 3, closest to the forest edge, red for Site 2 between the forest and the most interior point on the transect shown in yellow, Site 1. The three black vertical lines on days 21, 22, and 23 indicate the O_2 pulse administered, with the third line being offset to the right so as not to overlap with the measurement. Even though a destructive sampling scheme was used, n = 3 throughout the entire incubation.

WORKS CITED

Afreen, F., Zobayed, S. M. A., Armstrong, J., & Armstrong, W. (2007). Pressure gradients along whole culms and leaf sheaths, and other aspects of humidity-induced gas transport in Phragmites australis [Article]. *Journal of Experimental Botany*, *58*(7), 1651-1662. https://doi.org/10.1093/jxb/erm017

Angle, J. C., Morin, T. H., Solden, L. M., Narrowe, A. B., Smith, G. J., Borton, M. A., Rey-Sanchez, C., Daly, R. A., Mirfenderesgi, G., Hoyt, D. W., Riley, W. J., Miller, C. S., Bohrer, G., & Wrighton, K. C. (2017). Methanogenesis in oxygenated soils is a substantial fraction of wetland methane emissions. *Nature Communications*, *8*, Article 1567. https://doi.org/10.1038/s41467-017-01753-4

Armstrong, J., & Armstrong, W. (1988). PHRAGMITES-AUSTRALIS - A PRELIMINARY-STUDY OF SOIL-OXIDIZING SITES AND INTERNAL GAS-TRANSPORT PATHWAYS [Article]. *New Phytologist*, *108*(4), 373-382. https://doi.org/10.1111/j.1469-8137.1988.tb04177.x

Canadell, J. G., P.M.S. Monteiro, M.H. Costa, L. Cotrim da Cunha, P.M. Cox, A.V. Eliseev, S. Henson, M. Ishii, S. Jaccard, C. Koven, A. Lohila, P.K. Patra, S. Piao, J. Rogelj, S. Syampungani, S. Zaehle, and K. Zickfeld. (2021). Global Carbon and other Biogeochemical Cycles and Feedbacks. *Sixth Assessment Report of the Intergovernmental Panel on Climate Change*(Climate Change 2021: The Physical Science Basis).

Craft, M. J. V. a. C. B. (2016). *Wetland Soils: Genesis, Hydrology, Landscapes, and Classification* (Second Edition ed.). CRC Press.

Ge, M. Y., Korrensalo, A., Laiho, R., Lohila, A., Makiranta, P., Pihlatie, M., Tuittila, E. S., Kohl, L., Putkinen, A., & Koskinen, M. (2023). Plant phenology and species-specific traits control plant CH₄ emissions in a northern boreal fen. *New Phytologist*, *238*(3), 1019-1032. https://doi.org/10.1111/nph.18798

Hu, S. W., He, R. J., Wang, W. J., Zhao, D. Y., Zeng, J., Huang, R., Duan, M., & Yu, Z. B. (2021). Composition and co-occurrence patterns of Phragmites australis rhizosphere bacterial community. *Aquatic Ecology*, *55*(2), 695-710. https://doi.org/10.1007/s10452-021-09855-4

Justin, S., & Armstrong, W. (1987). THE ANATOMICAL CHARACTERISTICS OF ROOTS AND PLANT-RESPONSE TO SOIL FLOODING. *New Phytologist*, *106*(3), 465-495. https://doi.org/10.1111/j.1469-8137.1987.tb00153.x

Kirwan, M. L., & Gedan, K. B. (2019). Sea-level driven land conversion and the formation of ghost forests. *Nature Climate Change*, *9*(6), 450-457. https://doi.org/10.1038/s41558-019-0488-7

Korrensalo, A., Mammarella, I., Alekseychik, P., Vesala, T., & Tuittila, E. S. (2022). Plant mediated methane efflux from a boreal peatland complex. *Plant and Soil*, *471*(1-2), 375-392. https://doi.org/10.1007/s11104-021-05180-9

Lacroix, E. M., Aeppli, M., Boye, K., Brodie, E., Fendorf, S., Keiluweit, M., Naughton, H. R., Noël, V., & Sihi, D. (2023). Consider the Anoxic Microsite: Acknowledging and Appreciating Spatiotemporal Redox Heterogeneity in Soils and Sediments. *Acs Earth and Space Chemistry*, *7*(9), 1592-1609. https://doi.org/10.1021/acsearthspacechem.3c00032

Lacroix, E. M., Rossi, R. J., Bossio, D., & Fendorf, S. (2021). Effects of moisture and physical disturbance on pore-scale oxygen content and anaerobic metabolisms in upland soils. *Science of the Total Environment*, *780*, Article 146572. https://doi.org/10.1016/j.scitotenv.2021.146572

Lenzewski, N., Mueller, P., Meier, R. J., Liebsch, G., Jensen, K., & Koop-Jakobsen, K. (2018). Dynamics of oxygen and carbon dioxide in rhizospheres of Lobelia dortmanna - a planar optode study of belowground gas exchange between plants and sediment [Article]. *New Phytologist*, *218*(1), 131-141. https://doi.org/10.1111/nph.14973

Li, C., Ding, S. M., Chen, M. S., Sun, Q., Zhang, Y., Ma, X., Zhong, Z. L., Tsang, D. C. W., & Wang, Y. (2022). O2 distribution and dynamics in the rhizosphere of Phragmites australis, and implications for nutrient removal in sediments [Article]. *Environmental Pollution*, *806*, 10, Article 150735. https://doi.org/10.1016/j.scitotenv.2021.150735

Martins, P. D., Hoyt, D. W., Bansal, S., Mills, C. T., Tfaily, M., Tangen, B. A., Finocchiaro, R. G., Johnston, M. D., McAdams, B. C., Solensky, M. J., Smith, G. J., Chin, Y. P., & Wilkins, M. J. (2017). Abundant carbon substrates drive extremely high sulfate reduction rates and methane fluxes in Prairie Pothole Wetlands. *Global Change Biology*, *23*(8), 3107-3120. https://doi.org/10.1111/gcb.13633

Megonigal, J. P. (2019). Biogeochemistry of Tidal Freshwater Wetlands. In *Coastal Wetlands: An Integrated Ecosystem Approach* (pp. Pages 641-683). https://doi.org/https://doi.org/10.1016/B978-0-444-63893-9.00019-8

Mitsch, W. J. a. G. J. G. (2007). *Wetlands* (Fourth Edition ed.). John Wiley & Sons, Inc.

Mueller, P., Hager, R. N., Meschter, J. E., Mozdzer, T. J., Langley, J. A., Jensen, K., & Megonigal, J. P. (2016). Complex invader-ecosystem interactions and seasonality mediate the impact of non-native Phragmites on CH₄ emissions. *Biological Invasions*, *18*(9), 2635-2647. https://doi.org/10.1007/s10530-016-1093-6

Nahlik, A. M., & Fennessy, M. S. (2016). Carbon storage in US wetlands. *Nature Communications*, *7*, Article 13835. https://doi.org/10.1038/ncomms13835

Noyce, G. L., & Megonigal, J. P. (2021). Biogeochemical and plant trait mechanisms drive enhanced methane emissions in response to whole-ecosystem warming. *Biogeosciences*, *18*(8), 2449-2463. https://doi.org/10.5194/bg-18-2449-2021

Noyce, G. L., Smith, A. J., Kirwan, M. L., Rich, R. L., & Megonigal, J. P. (2023). Oxygen priming induced by elevated CO₂ reduces carbon accumulation and methane emissions in coastal wetlands. *Nature Geoscience*, *16*(1), 63-+. https://doi.org/10.1038/s41561-022-01070-6

O'Connell, C. S., Ruan, L., & Silver, W. L. (2018). Drought drives rapid shifts in tropical rainforest soil biogeochemistry and greenhouse gas emissions. *Nature Communications*, *9*, Article 1348. https://doi.org/10.1038/s41467-018-03352-3

Raivonen, M., Smolander, S., Backman, L., Susiluoto, J., Aalto, T., Markkanen, T., Mäkelä, J., Rinne, J., Peltola, O., Aurela, M., Lohila, A., Tomasic, M., Li, X. F., Larmola, T., Juutinen, S., Tuittila, E. S., Heimann, M., Sevanto, S., Kleinen, T., . . . Vesala, T. (2017). HIMMELI v1.0: HelsinkI Model of MEthane buiLd-up and emIssion for peatlands. *Geoscientific Model Development*, *10*(12), 4665-4691. https://doi.org/10.5194/gmd-10-4665-2017

Sowers, K. R. (2019). Methanogenesis. In *Encyclopedia of Microbiology, 4th Ediition - Reference Module in Biomedical Sciences*. Ellsevier Inc. https://doi.org/10.1016/b978-0-12-801238-3.02447-8

Srivastava, J., Kalra, S. J. S., & Naraian, R. (2014). Environmental perspectives of Phragmites australis (Cav.) Trin. Ex. Steudel. *Applied Water Science*, *4*(3), 193-202. https://doi.org/10.1007/s13201-013-0142-x

Stagg, C. L., Schoolmaster, D. R., Krauss, K. W., Cormier, N., & Conner, W. H. (2017). Causal mechanisms of soil organic matter decomposition: deconstructing salinity and flooding impacts in coastal wetlands. *Ecology*, *98*(8), 2003-2018. https://doi.org/10.1002/ecy.1890

van den Berg, M., van den Elzen, E., Ingwersen, J., Kosten, S., Lamers, L. P. M., & Streck, T. (2020). Contribution of plant-induced pressurized flow to CH4 emission from a Phragmites fen. *Scientific Reports*, *10*(1), Article 12304. https://doi.org/10.1038/s41598-020-69034-7

Wang, X. L., Yao, B., & Su, X. Y. (2018). Linking Enzymatic Oxidative Degradation of Lignin to Organics Detoxification. *International Journal of Molecular Sciences*, *19*(11), Article 3373. https://doi.org/10.3390/ijms19113373

Wania, R., Ross, I., & Prentice, I. C. (2010). Implementation and evaluation of a new methane model within a dynamic global vegetation model: LPJ-WHyMe v1.3.1. *Geoscientific Model Development*, *3*(2), 565-584. https://doi.org/10.5194/gmd-3-565-2010

Wilmoth, J. L., Moran, M. A., & Thompson, A. (2018). Transient O₂ pulses direct Fe crystallinity and Fe(III)-reducer gene expression within a soil microbiome. *Microbiome*, *6*, Article 189. https://doi.org/10.1186/s40168-018-0574-5

Wilmoth, J. L., Schaefer, J. K., Schlesinger, D. R., Roth, S. W., Hatcher, P. G., Shoemaker, J. K., & Zhang, X. N. (2021). The role of oxygen in stimulating methane production in wetlands. *Global Change Biology*, *27*(22), 5831-5847. https://doi.org/10.1111/gcb.15831

Xu, Z. Y., Peng, B., Kitata, R. B., Nicora, C. D., Weitz, K. K., Pu, Y. Q., Shi, T. J., Cort, J. R., Ragauskas, A. J., & Yang, B. (2022). Understanding of bacterial lignin extracellular degradation mechanisms by Pseudomonas putida KT2440 via secretomic analysis. *Biotechnology for Biofuels and Bioproducts*, *15*(1), Article 117. https://doi.org/10.1186/s13068-022-02214-x

Yang, W. H., McNicol, G., Teh, Y. A., Estera-Molina, K., Wood, T. E., & Silver, W. L. (2017). Evaluating the Classical Versus an Emerging Conceptual Model of Peatland Methane Dynamics. *Global Biogeochemical Cycles*, *31*(9), 1435-1453. https://doi.org/10.1002/2017gb005622

Zhang, L. H., Shao, H. B., Wang, B. C., Zhang, L. W., & Qin, X. C. (2019). Effects of nitrogen and phosphorus on the production of carbon dioxide and nitrous oxide in salt-affected soils under different vegetation communities. *Atmospheric Environment*, *204*, 78-88. https://doi.org/10.1016/j.atmosenv.2019.02.024

Zhao, J. F., Peng, S. S., Chen, M. P., Wang, G. Z., Cui, Y. B., Liao, L. G., Feng, J. G., Zhu, B., Liu, W. J., Yang, L. Y., & Tan, Z. H. (2019). Tropical forest soils serve as substantial and persistent methane sinks. *Scientific Reports*, *9*, Article 16799. https://doi.org/10.1038/s41598-019-51515-z

Zhuang, Q., Melillo, J. M., Kicklighter, D. W., Prinn, R. G., McGuire, A. D., Steudler, P. A., Felzer, B. S., & Hu, S. (2004). Methane fluxes between terrestrial ecosystems and the atmosphere at northern high latitudes during the past century: A retrospective analysis with a process-based biogeochemistry model. *Global Biogeochemical Cycles*, *18*(3), Article Gb3010. https://doi.org/10.1029/2004gb002239

CHAPTER III

Soil Organic Profiles Corresponding to Variation in Wetland Carbon Emissions

ABSTRACT

At the interface of land and water, coastal wetlands store massive reservoirs of soil carbon (C) that are disproportionately impacted by sea level rise. As we seek the development of more accurate models to predict changes in wetland C cycling, there remain critical knowledge gaps due to the oversimplification of widely diverse C transformations in the wetland rhizosphere and how they influence C emissions. A major challenge in measuring these broad-scale transformations is that they occur over different spatiotemporal scales in a heterogeneous environment, which are uniquely complicated by redox perturbations mediated by wetland plants. In this study, we focus on broad changes in soil organic matter (SOM) affected by changes in transect position/elevation (relevant to sea level and wetland migration) and transient redox status (analogous to radial oxygen loss (ROL) by wetland plants) by investigating soil collected from across a tidal marsh to assess the correspondence between these factors and C emissions. We characterized changes in SOM during a time-series incubation of soil using high-resolution (15 T) Fourier transform mass spectrometry (FTICR-MS) and compared the results to corresponding methane (CH_4) and carbon dioxide (CO_2) emissions. Important differences were observed in the molecular fingerprint (i.e., broad SOM profile and associated chemical metrics) depending on the combination of transect position and transient oxygenation, particularly in the carboxylic-rich alicyclic molecules (CRAM) and the more oxidized lignin-like compounds of

high molecular weight. Over daily to weekly time scales, we find that shifts in these two pools signal rapid changes in CH_4 levels, helping to account for dynamic variation, while higher lignin oxidation state more generally accounts for higher CO_2 levels. Although SOM chemical metrics like mass, nominal oxidation state of carbon (NOSC), aromaticity, and double bond equivalents help explain long-term potential for C emissions in our study, our work provides novel evidence that the dynamic presence/absence of CRAM is a more unique indicator (signal) for CH_4 production, and potentially for anaerobic/aerobic CH_4 consumption in systems where both production and consumption occur simultaneously. These results warrant further investigations of CRAM chemistry in the C cycle of redox-fluctuating environments. This will help to characterize transient changes in SOM profiles in the field, improve models of C cycling to better account for variation, and ideally lead to more effective climate mitigation policies.

GRAPHICAL ABSTRACT

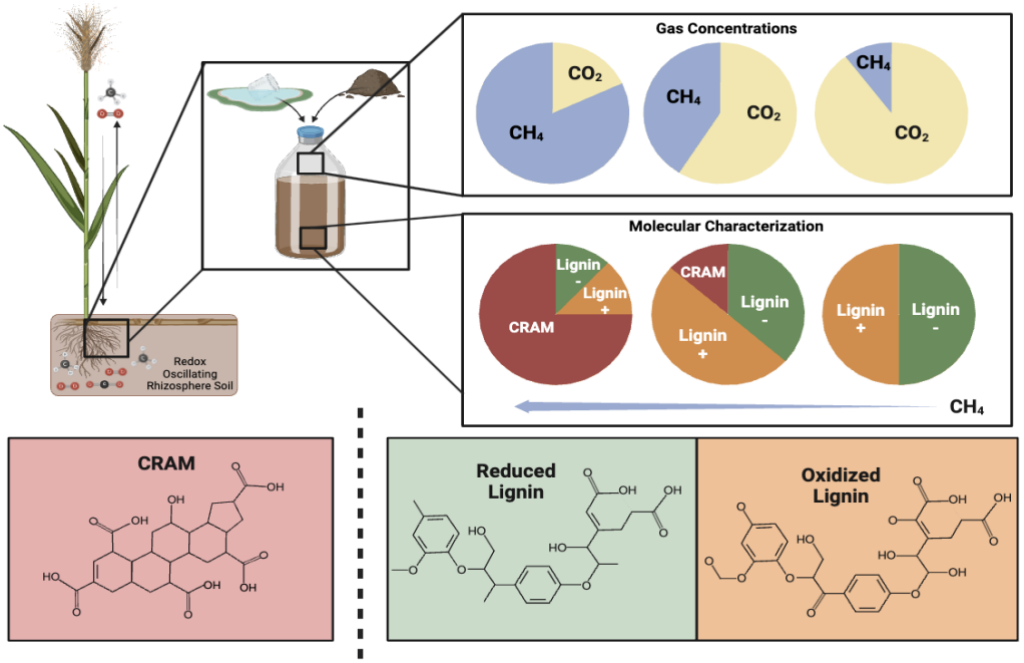

HIGHLIGHTS

- The carboxylic-rich alicyclic molecule (CRAM) pool of SOM is a unique, sensitive, *signal* for predicting/indicating CH4 production.
- The presence of large, *more oxidized*, lignin-like molecules corresponds to higher C emissions over time compared to large, *more reduced*, lignin-like molecules.
- Plant-mediated ROL has the potential to oxidize large (high molecular weight) lignin-like molecules, increasing their bioavailability and degradation toward increased C emissions.
- High-resolution FTICR-MS accurately identifies and groups soil based on its original field location regardless of incubation conditions; soils from neighboring locations that are separated by small distances across the wetland interior to forest ecotone retain site-specific SOM *fingerprints* during environmentally relevant perturbations.
- **Practical Application**: Knowledge of CRAM and large-oxidized-lignin composition could be used to finetune methods to assess SOM for CH_4 potential.

INTRODUCTION

Wetlands store massive amounts of carbon, accounting for 20-30% of Earth's soil C pool. Understanding their biogeochemical dynamics is ever more crucial under environmental change (Craft, 2016; Mitsch, 2007; Nahlik & Fennessy, 2016). Coastal wetlands of the US Mid-Atlantic are experiencing some of the highest rates of sea level rise compared to other areas. Understanding how this impacts their ability to store carbon is critical. At the land-water interface, there is a particularly high risk of accelerated soil carbon degradation through complex

biogeochemical transformations and greenhouse gas emissions driven by changes in sea level and redox perturbations (Noyce & Megonigal, 2021). Being able to predict these transformations and understand their link to greenhouse gas emissions requires a detailed characterization of soil organic chemistry in the wetland rhizosphere (Canadell, 2021; Stagg et al., 2017). The potential of transient environmental drivers to induce dynamic effects on soil organic C chemistry in coastal wetlands across different spatiotemporal scales has not been comprehensively assessed (Noyce et al., 2023).

Wetland vegetation can be used as a model to study the impact of transient redox perturbations on SOM chemistry in the rhizosphere. Specifically, *Phragmites australis* has been shown to be one of the more potent oxygenating species that is globally distributed. It can easily invade new areas and establish itself as a vast monoculture. This is due in part to its dense network of roots and rhizomes, salinity tolerance, and its ability to survive in a variety of saturation conditions (Srivastava et al., 2014). The aerenchyma tissues of *Phragmites* allow survival in extremely wet conditions, especially in transitional systems like coastal wetlands. *Phragmites* is ultimately an indicator of coastal climate change as salinity and saturation levels shift (Canadell, 2021; Kirwan & Gedan, 2019; Srivastava et al., 2014). Over smaller spatiotemporal scales, *Phragmites* can act as an indicator of redox oscillations within the soil rhizosphere (Afreen et al., 2007; Armstrong & Armstrong, 1988).

With the use of 2D planar optode imaging technologies, the *Phragmites* root/rhizome interface has been shown to have a diel pattern of ROL and microbial respiration (CO_2 production) (Lenzewski et al., 2018; Li et al., 2022; van den Berg et al., 2020). *Phragmites* efficiently transport gas, making it an aggressive oxygenator of the soil but also an efficient

transport system for other gasses between soils and the atmosphere (Afreen et al., 2007; Justin & Armstrong, 1987; van den Berg et al., 2020). Because of its global distribution, *Phragmites* provides a unique and important set of conditions to be observed while investigating the role of oxygenation on soil carbon stability (Srivastava et al., 2014; Vroom et al., 2022).

Momentary environmental oscillations are known to strongly impact carbon cycling, as well as that of nitrogen (N), iron (Fe), phosphorus (P), and sulfur (S) (Noyce et al., 2023; Zhang et al., 2019). With the intrinsic entangling of oxygen presence and the regulation of these biogeochemical cycles, looking closely at the intermittent distribution of oxygen pulses in soils is critical (Wilmoth et al., 2021). Historically, methane (CH_4) production has been considered to be inhibited by O_2, however, recent studies have shown that upward of 90% (or more) of CH4 emitted from some wetlands may originate in the uppermost layers of the soil where O2 is intermittently present (Angle et al., 2017). It is now recognized that pulsed oxygenation of otherwise anoxic soils has the potential to prime organic C toward degradation and substrate generation, increasing CH_4 emissions. This observation has been referred to as the soil "methane paradox" (Angle et al., 2017; Sowers, 2019; Wilmoth, 2021; Yang et al., 2017). Additionally, CO_2 production has been observed to be stimulated in redox-oscillating soils with high amounts of organic inputs and Fe^{III} minerals under redox-oscillating conditions (Wilmoth et al., 2018). Some tropical soils rich in Fe^{III} minerals have been shown to release more CO_2 under anaerobic vs aerobic conditions when organic inputs are high (O'Connell et al., 2018; Wilmoth et al., 2018; Zhao et al., 2019). Similar observations have been made in the Prairie Pothole wetlands of North America, where SO_4^{2-} and CH_4 can be produced at high levels simultaneously without competition due to high levels of DOC driving both pathways (Martins et al., 2017). Clearly,

traditional conceptual frameworks that are rooted in redox hierarchy and thermodynamic favorability begin to break down as SOM chemistry shifts in redox dynamic environments. This point alone gives insight into the failures of numerical and conceptual models attempting to predict the extreme variability often displayed by C emissions in different wetland environments.

The mechanism behind the stimulation of C emissions from periodic O_2 exposure is still not fully understood (Angle et al., 2017; Lacroix et al., 2023; Wilmoth et al., 2021; Yang et al., 2017). With numerous environmental drivers influencing O_2 in coastal soils (e.g., tidal fluctuations, wetting/drying, precipitation, etc.), wetland plants in particular, are known to regulate O_2 levels more locally in the rhizosphere and potentially on a diurnal cycle. In such cases, any spatiotemporal variation (e.g., gradient, transition, oscillation) in rhizosphere oxygenation could influence CH_4 and CO_2 fluxes. Oxygen has the potential to stimulate heterotrophic microbial respiration and replenish terminal electron acceptors. This could stimulate CH_4 generation by increasing the bioavailability of C compounds through the degradation of larger molecules into smaller, more oxidized ones (e.g., acetate, CO_2, H_2, and C-1 compounds); stimulating a trophic-driven cascade of substrates toward methanogenesis. Theoretically, terminal electron acceptors are used in order of decreasing thermodynamic yield; however, in a dynamic soil system, these substrates and terminal electron acceptors are simultaneously present and utilized (Megonigal, 2019), where their thermodynamic potential is controlled by the abundance of bioavailable organics. The broad biotic and abiotic transformations of OC due to exudate input and rhizosphere oxygenation have the potential to increase the vulnerability of wetland carbon stocks. In addition to oxygen inputs, plant exudate inputs also can stimulate a multitude of biochemical pathways leading to terminal electron

acceptor competition and an increase in the bioavailability of these substrates; however, the characterization of these exudates is limited (Määttä & Malhotra, 2024; Philippot et al., 2009; Seyfferth et al., 2020; Stanley & Ward, 2010).

In coastal regions, sea level rise and the resulting migration of wetlands are expected to further complicate C transformations between the wetland interior and the adjacent upland soils. Tidal marshes bordered by forest are of unique concern due to marked differences in SOM chemistry along the wetland-to-forest transect. To better understand the variability of C emissions in such a dynamic system, a multifaceted approach is necessary. The correspondence between transient changes in soil organic chemistry and transient oxygenation of the wetland rhizosphere of a *Phragmites*-dominated tidal marsh was investigated utilizing ultra-high resolution mass spectrometry coupled with CO_2 and CH_4 measurements. Early works utilizing FTICR-MS within the Chesapeake Bay left one unanswered question regarding how this data is interpreted. Given the lack of structural information associated with mass spec data, structural isomers of the same molecular formula could plot in similar regions but have different reactivities within the system, notably CRAM and lignin.

In this study, we investigated the correspondence between transient changes in soil organic chemistry and transient oxygenation of the wetland rhizosphere of a *Phragmites*-dominated tidal marsh. Our hypothesis, based on the prevailing thermodynamic theory (i.e., Gibbs energy vs nominal oxidation state (NOSC) relationship for SOM), was that transient oxygenation of an otherwise anoxic wetland soil system would cause a positive correlation between the presence of small, highly oxidized, organics and higher C emissions (LaRowe & Van Cappellen, 2011). We characterized SOM transformations by measuring changes in the DOC

pool with FTICR-MS, and compared this to the corresponding CH_4 and CO_2 emissions. To test and mimic the oxygenation levels known to occur via *Phragmites* ROL on this process, laboratory oxygenation was initiated after three weeks of anoxic incubation of soils collected from the field (in March, before the growing season) to examine the effect that natural diurnal oxygenation might have on SOM transformations and C emissions. A broader objective of our study was to test the extent to which our experimental design could help constrain interpretations of variation often encountered with wetland C emissions in the field. Our work will allow for new conceptual and numerical approaches to be developed that explicitly use diagnostic SOM chemical metrics to understand changes in wetland C cycling, perhaps allowing similar improvements for other soil environments.

MATERIALS & METHODS

Field Sampling & Site Description

Soil samples were collected within the Smithsonian Environmental Research Center's Global Change Research Wetlands (G-CREW) in Edgewater, Maryland, land previously occupied by the Piscataway People (38.87516782°, –76.54525616°). The transect runs for approximately 180 m from the center of Kirkpatrick Marsh, crossing a small land-fed creek, and ends at the forest edge shown in **Figure 1**. *Phragmites australis* dominates the entire transect, however, the soil characteristics and inundation levels varied from site to site. The salinity of the site is about 8.45 ppt, which changes slightly with the tides and has a pH of approximately 6.0.

In early March of 2024, six soil cores were collected perpendicular to the transect using a McCauley Auger at each location from 0 cm to 20 cm below the surface where rhizomes were abundant. Similar profiles were observed at both Sites 1 and 2 with a more extensive organic layer from 0 to 5 cm followed by a layer of peat, likely from a prior population of *Spartina alterniflora*. Although the profiles were rich in rhizomes, many that were active were not observed below the dense bottom layer of peat. The profiles of Site 3, closest to the forest, had much more development with more distinct horizonation. In short, there was a much darker silty top layer, followed by a redox feature-rich bottom layer with an apparent increase in sand and clay content Figure 2. Pore water was collected from the "Pore Water Collection Site" indicated by the blue marker in **Figure 1.** Two cores were augered to a depth of 20 cm to allow for the collection of porewater via core recharge with Falcon sample tubes. Both soil and water were kept in coolers to maintain their temperature and transferred to the lab for immediate assembly into incubations.

Incubation Setup

To test the effect of transient oxygenation on dissolved organic chemistry and greenhouse gas emissions, benchtop incubations were constructed using soil and porewater collected from the field site. Once brought into the lab, the six cores from each transect site were homogenized by hand in ambient conditions, large plant material was picked out by hand, and fine roots were removed with forceps. Porewater from the bulk collection site shown in **Figure 1** was portioned into falcon tubes and spun down at 10G for 15 minutes to remove suspended solids. Soil slurries were constructed using a soil-to-water ratio of 1:10 in 120 ml amber serum bottles with a total volume of 60 ml, leaving 60 ml of headspace. They were then sealed with thick butyl stoppers

and aluminum crimp caps, flushing the headspace with pure N_2 gas while stirring to maintain anaerobic conditions for around 5 minutes. Serum bottles were gently shaken end-over-end and kept in the lab at 22 to 25°C throughout the incubation. Each week, one set of triplicate samples was placed in the freezer to halt the incubation to measure liquid and solid phase changes over time. At the beginning of the third week, a pulse of 10 ml of ambient air was injected into the bottles, making the headspace O_2 concentration 3.5% by total gas composition under ambient conditions. It is important to note that *Phragmites* has been shown to elevate rhizosphere O_2 concentrations up to, and even above, 20% of total gas composition. Our experimental oxygenation was carried out every 24 hours for 72 hours. At the conclusion of the fourth week, the last set of bottles was destructively harvested, as shown in **Figure 3**, to assess the impact of transient O_2 pulsing on the system dynamics.

Gas Concentrations of CH_4 and CO_2

Throughout the incubation, headspace gas samples were taken and measured on an SRI-8610C gas chromatograph fitted with a flame ionization detector to measure CH_4 and CO_2 concentrations within the headspace. Before each measurement, calibration curves were run using 0.5 ml of 3-4 standard gases. N_2 at 0.5 ml was injected into the bottles, swirled, and 0.5 ml of mixed headspace gas was sampled during GC measurements.

High-Resolution Mass Spectrometry

The benchtop incubation bottles were stored at -20° C until sampled for mass spectrometry analysis. The bottles were thawed in room temperature water; once the slurry had liquified, it was removed via needle and syringe and aliquoted into microcentrifuge tubes. They

were spun at 10,000 G for 15 minutes to collect the suspended solids. The supernatant was removed and filtered through a 0.22 ul Polyethersulfone filter and stored in small amber glass serum vials at -20° C until further processing.

Electrospray ionization (ESI) Fourier transform ion cyclotron mass spectrometry (FT-ICR MS) analysis was used to characterize the molecular composition of SOM in the DOC fraction in soil incubations from all three sites on one of the replicate bottles chosen randomly at 5 different time points throughout the incubation as follows: 24 hours after the construction of the incubations (T_0), 1 week (T_1), 2 weeks (T_2), right before the oxygen pulses at 3 weeks (T_3), and one week after the initial oxygen pulse (T_4). The samples were desalted through Agilent PPL solid-phase extraction cartridges and diluted with methanol. The prepared samples were injected at an infusion rate of 120 µl h−1 by a syringe pump to the ESI source of a Bruker 15 T FTICR-MS in negative ion mode with electrospray voltages optimized for each sample to maintain stable and consistent ion currents (Sleighter & Hatcher, 2008). Ions between 200 and 1200 m/z were transferred to the ICR cell after accumulating at a hexapole for 1.0 s.

Fourier transformation and initial magnitude calculations and assignments were made using the Bruker Daltonics Data Analysis software. A custom script in TEnvR was used to assign molecular formulas in a logical heuristic approach based on the following criterion: 12C2–50, 1H5–100, 14N0–6, 16O1–30, 32S0–2, and 31P0–2 within an error of 1 ppm (DiDonato et al., 2016). The resulting chemical assignments were used to calculate and report changes in the aromaticity index, the nominal oxidation state of carbon (NOSC), exact mass, H/C and O/C ratios (for van Krevelen diagrams), and double bond equivalency per C (DBE/C). For general

interpretation of van Krevelen diagrams, refer to (Goranov et al., 2022; Sleighter & Hatcher, 2008; Valle et al., 2018)

Data Representation

The program suite TEnvR (Goranov et al., 2023) was used to generate chemical metrics, PCA, correlations, and Spearman ranked correlations. This open-source software is based in MATLAB and serves as a highly comprehensive toolkit for processing biogeochemical data from various analytical techniques. Its primary function is to analyze complex MS data and compare them against other chemical data types (e.g., NMR). R and R Studio were also used to custom process the TEnvR results as needed.

RESULTS

Groupings within PCA: Variation Explained by Transect Location

The PCA of the FTICR-MS data captured 45% of total variation, where 30% (on PC1) of the total variation could be attributed to field site location. Site 2 (transition zone) and 3 (forest boundary) samples were anticorrelated on PC 1. Site 1 (most interior zone in the wetland) samples grouped on PC2 along with the Pore Water sample. We note that P0, the initial time point for Site 1 was mostly negatively correlated on PC1, while still retaining some similarity with the other Site 1 samples. The F4 sample (Site 3, forest boundary; week 4 of incubation), one week following the laboratory oxygenation treatment, was correlated more along PC2 compared to the other Site 3 samples.

PCA Loadings: Correlations Due to Molecular Fingerprint

The largest separation in PC1 was between soils collected from Sites 2 and 3. Based on the van Krevelen diagrams constructed using the loadings from the PCA analysis, Site 2 DOC was more enriched in carboxyl-rich alicyclic (and/or aliphatic) molecules CRAM (0.0–0.4 O/C; 1.0–2.0 H/C), as represented by the orange points shown in **Figure 5** (Goranov et al., 2023; Valle et al., 2018).Site 1 samples were mostly grouped along on PC2, which correlated positively with large (high molecular weight), more reduced, lignin-like molecules (those between x on the O/C axis and H/C axis) compared to those positively correlated with Site 3 samples. Although Site 1 and Site 3 samples are enriched in large (500-800 amu) lignin-like molecules (those between x on the O/C axis and H/C axis). However, these sites differ by their oxidation with Site 3 having a higher O/C ratio as well as a more positive NOSC (**Fig. 6)**. By the end of the experiment, Site 3 samples showed depleted lignin-like distribution and more enriched CRAM distribution, as well as an average decrease in molecular mass (**Fig. 5)**.

Changes in SOM Using Time-Resolved van Krevelen Data

The van Krevlin plots serve as a tool for tracking *molecular fingerprints* during the experiment, providing information on broad changes in various types of molecules. After subtracting out molecules common across all time points per site (i.e., subtraction of molecules that never changed from their original assignment; i.e., removal of un-unique molecules over time), changes in unique molecular composition were observed across all samples. Site 1 chemistry showed a very sparse distribution of unique molecules 24 hours after the incubation was initiated (T_0). Molecules in the CRAM region (O/C 0.0-0.4; H/C 1.0-2.0) appeared in T_1 and did not return until T_4, one week post oxygenation (**Fig. 8)**. Site 2 samples showed variable

molecular composition throughout the incubation but a consistently large distribution of CRAM (**Fig. 9**). Despite the variation in unique molecules detected and plotted for the Site 2 incubation over time (**Fig. 9)**, van Krevelen diagrams using all molecules detected (i.e., no subtraction of molecules) showed a consistently enriched CRAM pool for Site 2 samples over time (**Figs. 11-15**), which was also supported by our PCA results (**Fig. 4 and 5**). By the end of the experiment, Site 3 incubations showed a large drop in the molecular mass of compounds, most notably following oxygenation (**Fig. 7**)

Pre-Growing Season Gas Trends

The CO_2 concentrations increased in all three sites after the oxygen pulse, with the third site being higher throughout the incubation both before and after the pulse (**Fig. 16**). Less CO_2 was observed in Site 1 during the anoxic portion of the experiment, but after oxygenation, there was an increase in CO_2 concentrations (from 0.03-0.1 ugC/kg Soil to 0.16-0.275). However, CH_4 concentrations decreased within the first 3 days, where Sites 2 and 3 quickly surpassed their initial values by the end of week one, with Site 2 being slightly higher. Around day 10 in Sites 2 and 3, CH_4 began to plateau and remain relatively constant even after the oxygenation treatments. Site 1 remained near the detection limit of the instrument for CH_4, which showed a sharp increase following the oxygen pulse (**Fig. 17)**.

DISCUSSION

SOM Fingerprints Over Time

Site 1. Both Site 1 and Porewater samples were positively correlated along PC2, which captured 15% of the variability in the dataset **(Fig. 4)**. This water was collected from an adjacent site, one much closer and having similar soil depth profiles (in the field) to that of Site 2. However, Site 1, being the most interior location and most frequently inundated, is also located close to a tidal creek, which most likely has a similar composition to that of the Porewater we collected in the field (**Fig. 1**). Taken together, this indicates that tidal waters entering the wetland are enriched in large, reduced, lignin molecules that are likely deposited at Site 1 over time from the tidal creek at the marsh interior (**Fig. 1**). We note that the Site 1 T0 sample was not as strongly correlated with other Site 1 samples, being captured negatively on PC2 (**Fig. 4**). The time-series van Krevelen diagrams of Site 1 showed a small number of unique molecules at T0. (**Figs. 8 & 11**). After these soils incubated for 1 week, the number of unique molecules and overall mass of molecules increased (37-60 Cs; 575 amu), likely due to dissolution kinetics, where smaller molecules enter solution faster than the larger lignin-like pool found in the Porewater. Overall, Site 1 samples showed the greatest variation in CH_4 levels during the incubation, which corresponded with dynamic shifts in the CRAM pool over time. Early in the incubation, the disappearance of CRAM at day 14 seemed to track with a decrease in CH_4 concentrations. The reappearance of CRAM corresponded to the burst in CH_4 production following oxygenation (**Figs. 8 & 17**).

Site 2. Site 2 soil samples were negatively correlated along PC1 (**Fig. 4**), indicating enrichment of CRAM, as shown by the van Krevelen diagram based on the PCA results (**Fig. 5**). When looking at the time resolved van Krevelen of Site 2 samples, there appears to be a sporadic change in the spread of molecules and a general lack of CRAM over all time points (**Fig. 9**). In fact, this only indicates that *unique* CRAM was not present throughout different timepoints for Site 2 samples. In fact, the PCA results (**Fig. 5**), as well as the complete van Krevelen results (**Figs. 11-15**), show that CRAM was always present in Site 2 samples, which corresponds to higher CH_4 emissions compared to other sites.

Site 3. Site 3 samples were positively correlated on PC1, indicating the enrichment of more oxidized, large, lignin-like molecules. These samples collected from the wetland-forest boundary had the highest diversity of lignin-like molecules as well as the most unique lignin-like molecules over time compared to other sites (**Table 1)**. When looking at the PCA results for Site 3 samples (**Fig. 4**), the sample incubated for 4 weeks (1 week after oxygenation), while positively correlated on PC1, was also negatively correlated along PC2. Here, the plot of H/C ratio compared to the molecular weight revealed that this sample contained lighter molecules, indicating that over the course of the incubation, Site 3 soils began to degrade into smaller molecules, especially following oxygenation (**Fig. 5**). This is confirmed by the average mass decreasing throughout the incubation (**Fig. 7**).

The double bond equivalence (DBE) of soils incubated from Site 3 decreased and the aromaticity index (AI) increased over the course of the incubation (**Figs. 18 & 19**). This could be explained by aromatic ring cleavage in lignin-like structures, (potentially from peroxidase enzymes), leaving conjugated carbon side chains, still contributing to the high aromaticity index.

Other aromatic rings could carboxylate and hydrogenate, becoming alicyclic rings, losing their double bonds and contributing to the decrease in DBE. In conjunction, these processes could help explain the changes in AI and DBE as well as the shift from lignin-like molecules, both into CRAM or more oxidized forms of these lignin-like molecules. The van Krevelen plot of the molecules encapsulated by the PCA show that the soils of Site 3 during the anerobic portion of the incubation, (predominantly correlated positively on PC1) and the soil from the semi aerobic portion of the incubation, (predominantly correlated negatively on PC2) indicate a shift with an increase in CRAM molecules and a decrease and diffuse distribution of lignin like molecules.

CH_4 Emissions Signaled by CRAM and Large Oxidized Lignin

Along the transect, shifts in the molecular fingerprint of SOM profiles were observed, which coincided with shifts in CH_4 emissions. Although consistently higher from soils collected from Site 2, Sites 2 and 3 soils displayed similar trends in CH_4 emissions, with steady increases during the anoxic phase of the incubation, up until around day 10, when concentrations began to plateau (**Fig. 17**). Site 2 soils were consistently enriched in CRAM and had the highest CH_4 concentrations throughout the incubation; indicating the CRAM pool signals CH_4 production (**Fig. 8**).

As Sites 2 and 3 samples CH_4 concentrations began to plateau around day 10, their CRAM pools also had the smallest number of molecules relative to other points in the incubation, however, this pool repopulated within one week (**Figs. 13 & 14)**. Even though less enriched in CRAM compared to soils of Site 2, soils collected from Site 3 were still capable of CH_4 generation, potentially due to the relationship of CRAM and lignin-like molecules. Even with a smaller fraction of CRAM, if within the pool of lignin-like molecules, there is a greater

abundance of smaller, more oxidized C (higher NOSC), as indicated by the mass vs. H/C ratio and van Krevelen plots of molecules positively correlated by PC1 (predominantly those of soils incubated from Site 3) (**Fig. 5**). Contrarily, incubated soils of Site 1 (predominantly correlated positively by PC2) were unable to produce CH_4 during the anoxic phase of the incubation because the lignin-like molecules were more reduced and heavier (**Fig. 5**). An increase of CH_4 was observed from soils collected from Site 1 between the second and third weeks of the incubation period (**Fig. 17**). At the start of the second week of the incubation, soils of Site 1 did present with a CRAM pool, however this disappeared by the third week (**Fig. 8**).

The Site 1 samples were able to produce CH_4 after oxygenation at concentrations comparable to that of Sites 2 and 3, which is also when the largest CRAM pool was observed for Site (**Figs. 8 & 17**). Given that the collection of these soils was prior to the growing season of *Phragmites*, the redox conditions would most likely be predominantly driven by the transect location rather than mediated by the plant. With soils of Site 1 most likely experiencing the most reducing field conditions due to inundation as the most interior position along the wetland transect, these soils could require the laboratory-induced oxygenation events to oxidize the lignin-like molecules into an accessible form, allowing these now oxidized lignin-like molecules to be further transformed into CRAM. Unlike soils of Site 3 that experienced a decrease in DBE and increase in AI during the anoxic phase of the incubation, soils of Site 1 decreased in DBE and AI, potentially indicating the cleaving of aromatic constituents to lignin-like molecules as well as the hydrogenation and carboxylation of the newly formed side chains (**Figs. 18 & 19**).

CONCLUSIONS

Molecular fingerprinting of the SOM using FTICR-MS allowed us to characterize broad SOM profiles and chemical metrics depending on the transect position relative to inundation and transient oxygenation analogous to *Phragmites*. In particular, the CRAM region of van Krevlin diagrams, in addition to the oxidation state of the lignin-like molecules, corresponded to changes in CH_4 emissions. Over daily to weekly time scales, we found that shifts in these two pools signal rapid changes in CH_4 levels, helping to account for dynamic variation. These results indicate a need for further investigations of CRAM chemistry in the C cycle of redox-fluctuating environments.

Incubation studies using soils collected at varying times of the year could help gain an understanding of the role of plant-mediated oxygenation in wetland rhizosphere C chemistry. Additionally, isotope-labeled lignin amendments coupled with microbial community characterization could provide insight into the fractionation of C in the gas, liquid, and solid phases and potentially shed light on some of the biological processes at play in these systems. Ultimately, a multifaceted approach is required to gain mechanistic understanding of an increasingly complex system, necessary to improve C cycle models and to create better-informed, effective climate mitigation strategies.

FIGURES

Figure 1:

The above figure shows North America, specifically highlighting the sampling location on the Rhode River. On the right, the field transect used to collect soils for the laboratory incubation experiments. Each plot is denoted as "Site 1, 2, and 3" in yellow, orange, and green, respectively, with the area that the bulk site water was denoted as "Bulk Water Collection" in blue. The entire area is dominated by *Phragmites*. Site 1 has two creeks on either side, followed by Site 2 with a creek to the west. Site 3 is close to the forest edge, with a more developed, mineral-rich soil profile.

Figure 2: Shown above from left to right are three soil cores from Site 1, 2, and 3, respectively. Sites 1 and 2 have more similar profiles with an upper and lower layer. The top being more organic and mucky, followed by a lower layer that is significantly more peaty with a dense layer of rhizomes separating the two. The third core from Site 3 has much more development with three distinct layers, the top still organic and mucky but with a darker color compared to the first two sites, a darker grey and sandier middle layer, followed by a redox feature-rich bottom layer with an apparent increase in sand and clay content.

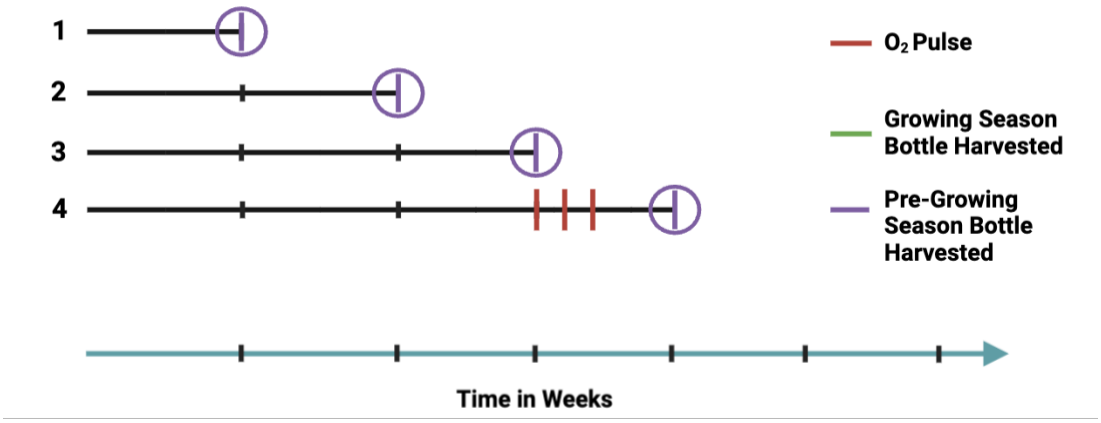

Figure 3:

Above is a schematic describing the experimental setup for the incubations. Each numbered set was triplicated; the purple lines and circles indicate when the set was destructively harvested for the pre-growing season (March sampling) set of incubations. The red lines indicate the 10 ml pulse of ambient air to oxygenate the bottles.

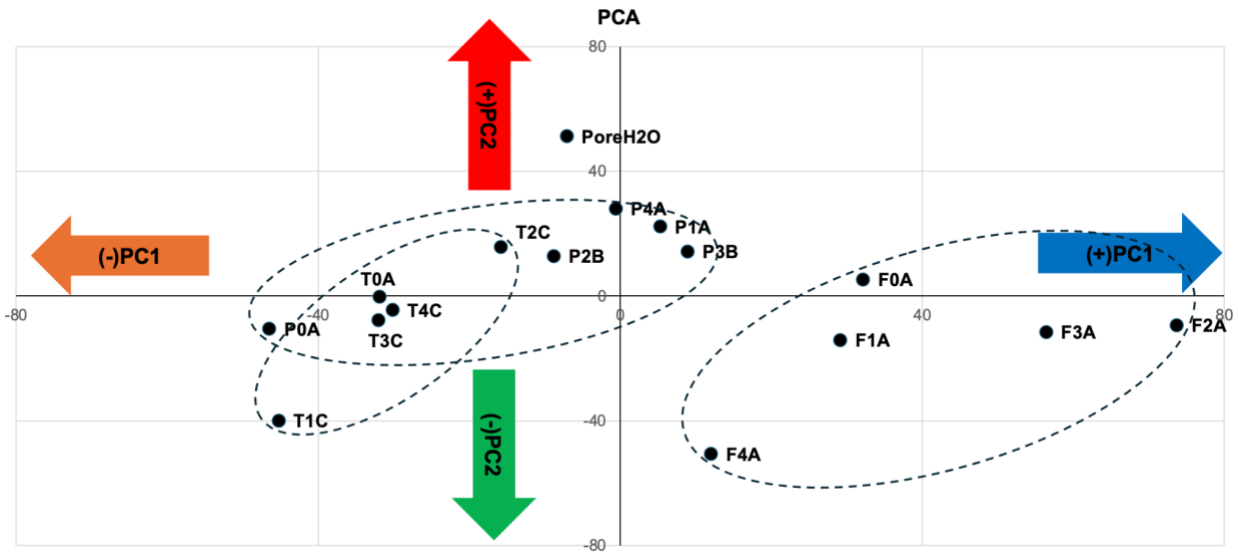

Figure 4:

Above is a PCA of all of the molecules detected from the FTICR-MS across all sample times and locations as well as the pore water, labeled as "PoreH2O". Points that start with "P", "T", and "F" are from Sites 1, 2, and 3, respectively. The numbers correspond to the time point in which the incubation was stopped, "0" for 24 hours, followed by "1", "2", "3", and "4" for 1, 2, 3, and 4 weeks, respectively. The letter is indicative of the replicate, which can be ignored.

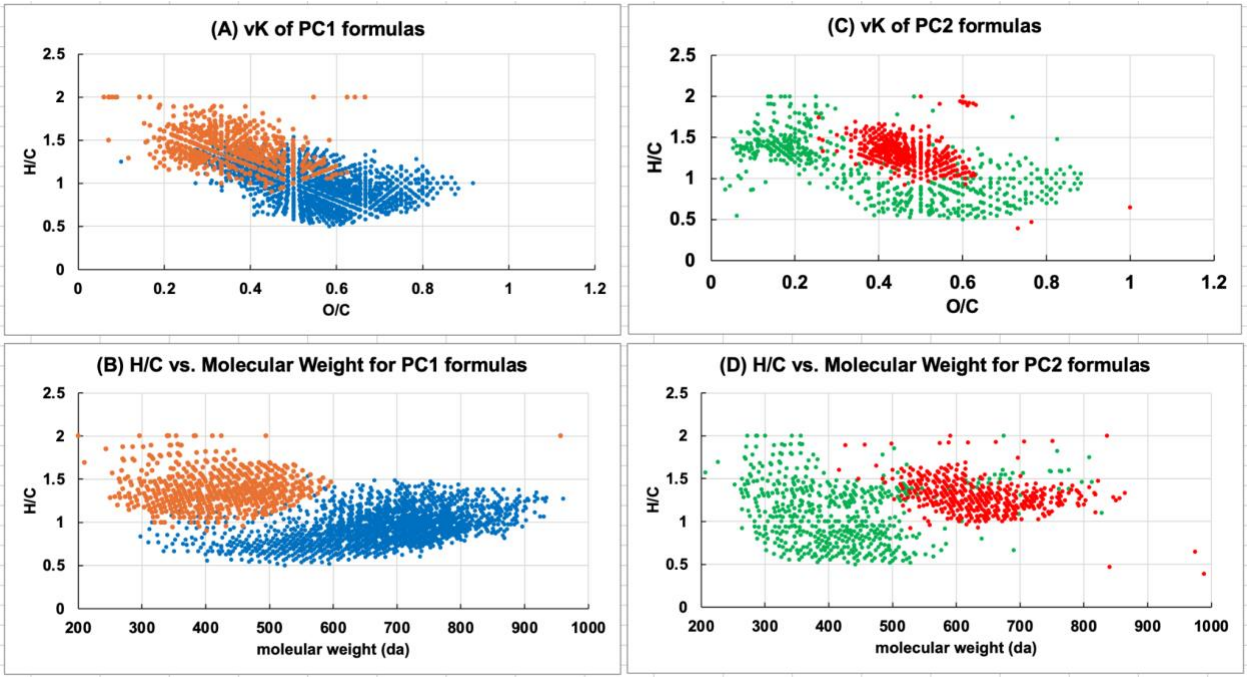

Figure 5:

Panels A and B in the figure above, colored in blue and orange, correspond to the formulas of molecules detected for PC1 in figure 4, representing the positive direction and negative directions, respectively. Panels C and D, colored in red and green, correspond to the formulas of molecules detected for PC 2 in figure 4, representing the positive and negative directions, respectively. Panels A and C are van Krevlen diagrams, showing the O to C ratios plotted against that of H to C. Panels B and D are the molecular weights plotted against the H to C ratios.

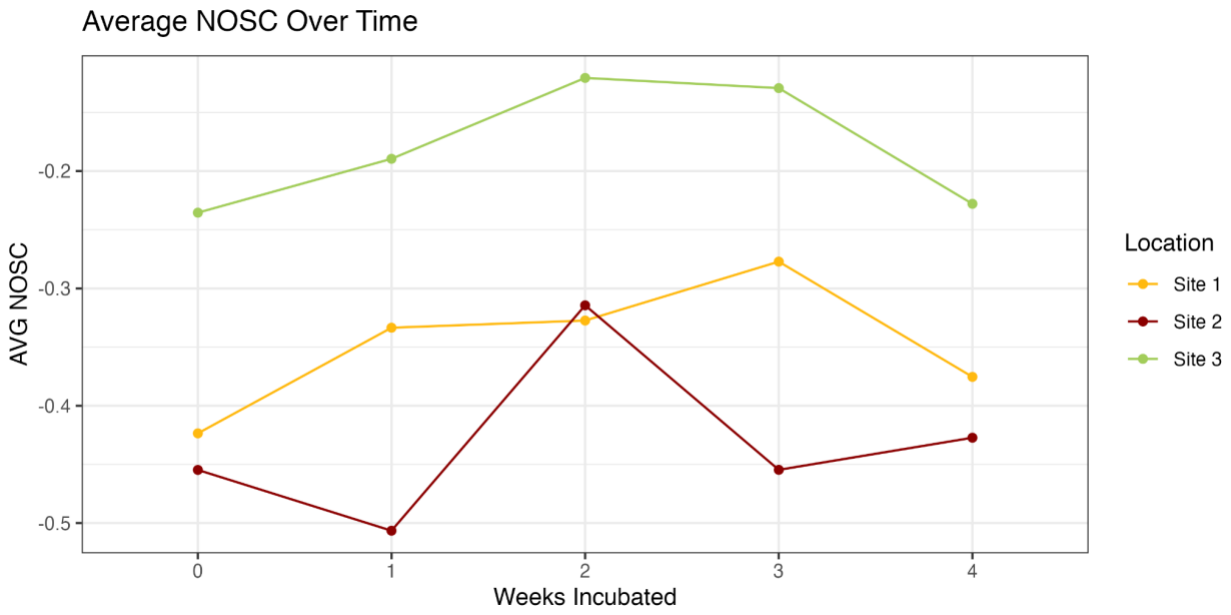

Figure 6:

Above, the average nominal oxidation state of carbon of the molecules detected using FTICR-MS is plotted against the time incubated. Site 3 had the highest average NOSC throughout the incubation, with its biggest decrease being after the oxygenation. Site 1 followed a similar trend, however, with values much more similar to Site 2. Site 2's NOSC varied throughout the incubation with a slight increase after oxygenation.

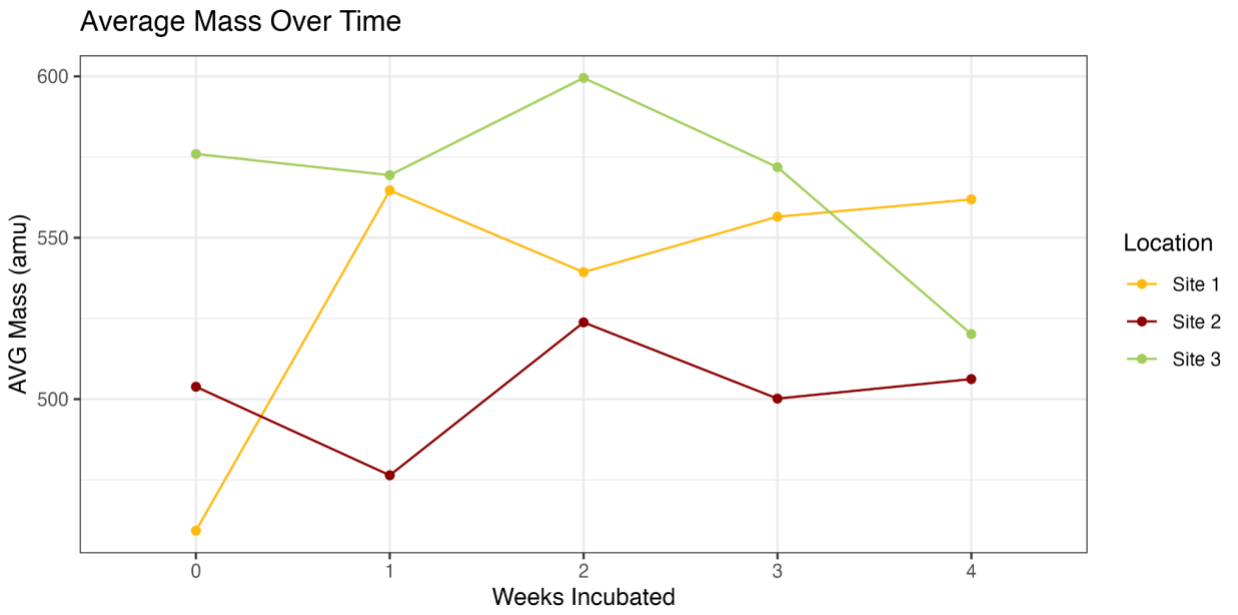

Figure 7

Above the average mass of the molecules detected from FTICR-MS per site and time point was plotted over time. Site 3 had the highest mass during the anoxic portion of the experiment; however, after oxygenation during the third week, there was a decrease. In Site 1, the average mass increased significantly over the course of the first week and plateaued, relatively unaffected by the oxygenation. In Site 2, the average mass oscillated, with the smallest effect being after oxygenation.

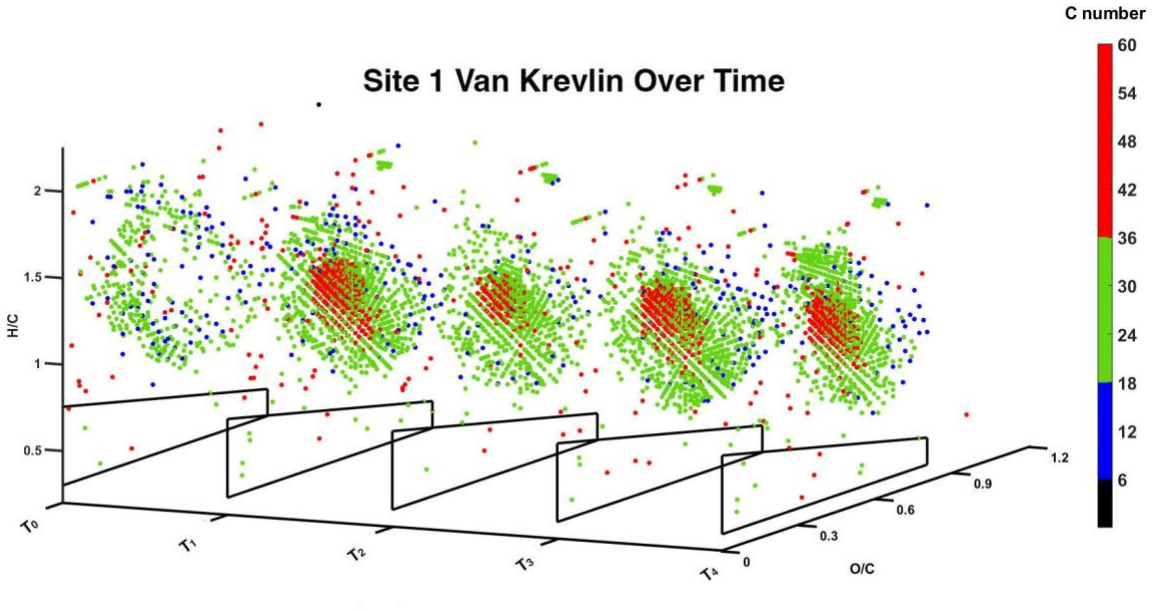

Figure 8:

Above, the O/C ratio (z-axis) was plotted against the H/C ratio (y-axis) over time (x-axis) for the unique H, C, and O-bearing molecules detected at Site 1 using FTICR-MS. The color scale is indicative of how many C atoms are present in the molecule.

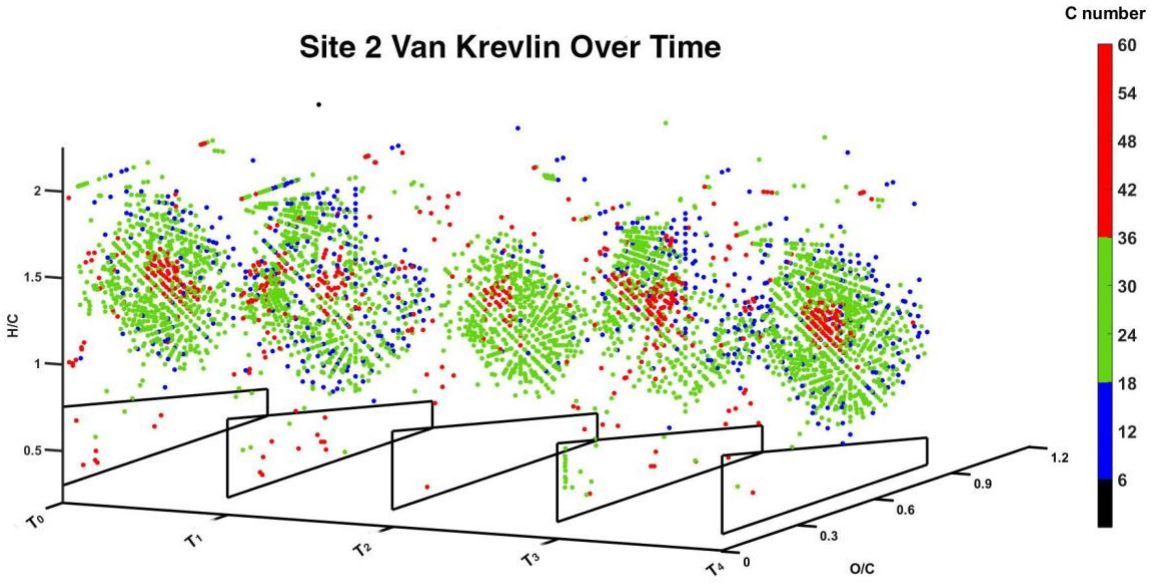

Figure 9:

Above, the O/C ratio (z-axis) was plotted against the H/C ratio (y-axis) over time (x-axis) for the unique H, C, and O-bearing molecules detected at Site 2 using FTICR-MS. The color scale is indicative of how many C atoms are present in the molecule.

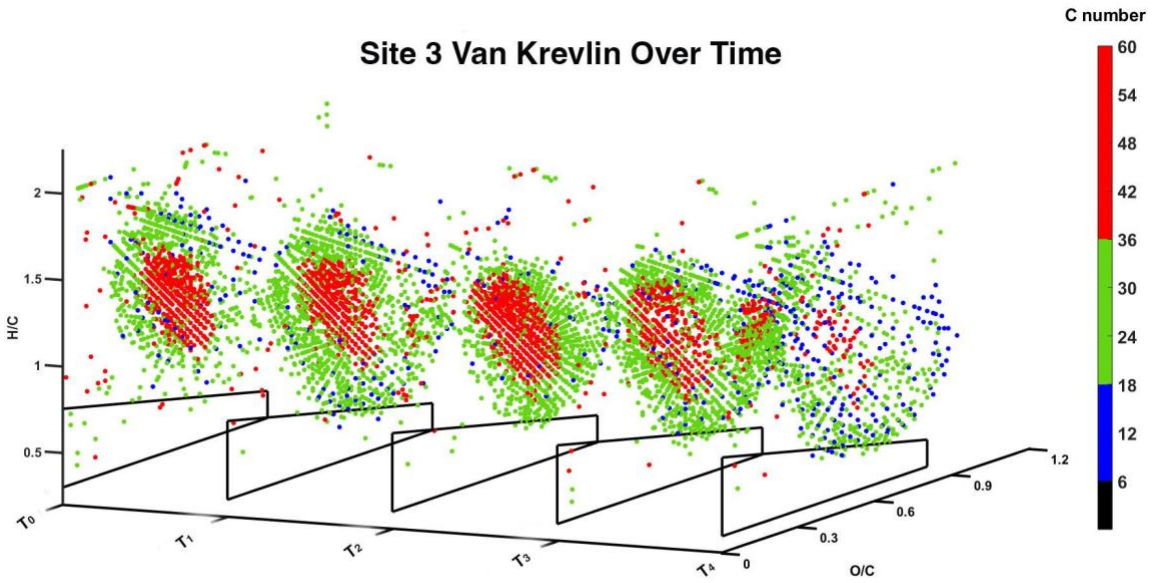

Figure 10:

Above, the O/C ratio (z-axis) was plotted against the H/C ratio (y-axis) over time (x-axis) for the unique H, C, and O-bearing molecules detected at Site 3 using FTICR-MS. The color scale is indicative of how many C atoms are present in the molecule.

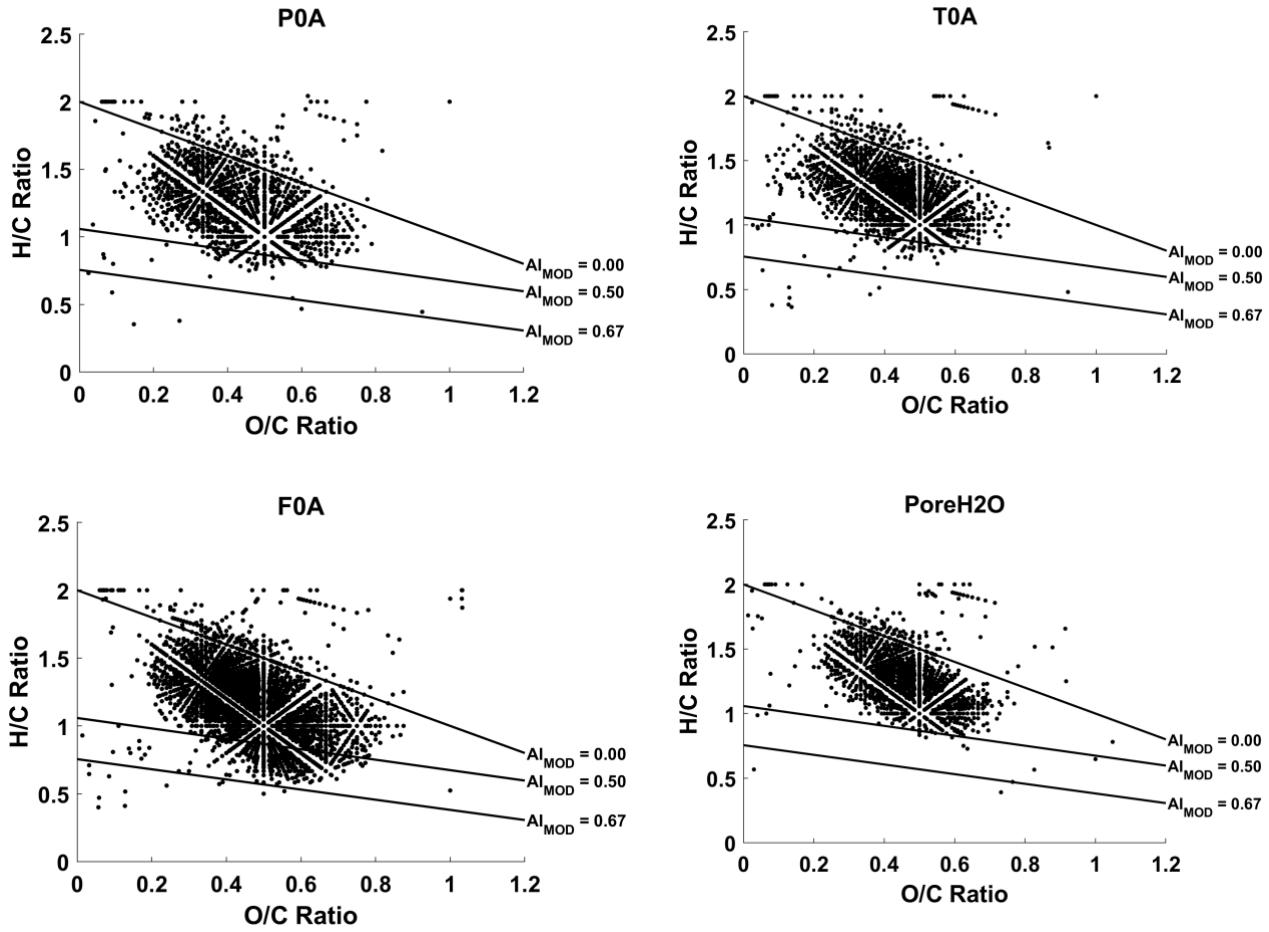

Figure 11:

The van Krevelen diagrams were constructed by plotting the O/C ratio by the H/C ratio, creating a fractal pattern with molecular types corresponding to regions of the plot. Here, Site 1, indicated by the P, after 24 hours of incubation, indicated by the 0, has fewer molecules relative to that of the other two sites and the porewater sample, indicated by "PoreH2O". At the same time point, Site 2, indicated by the T, has a similar configuration to the Pote

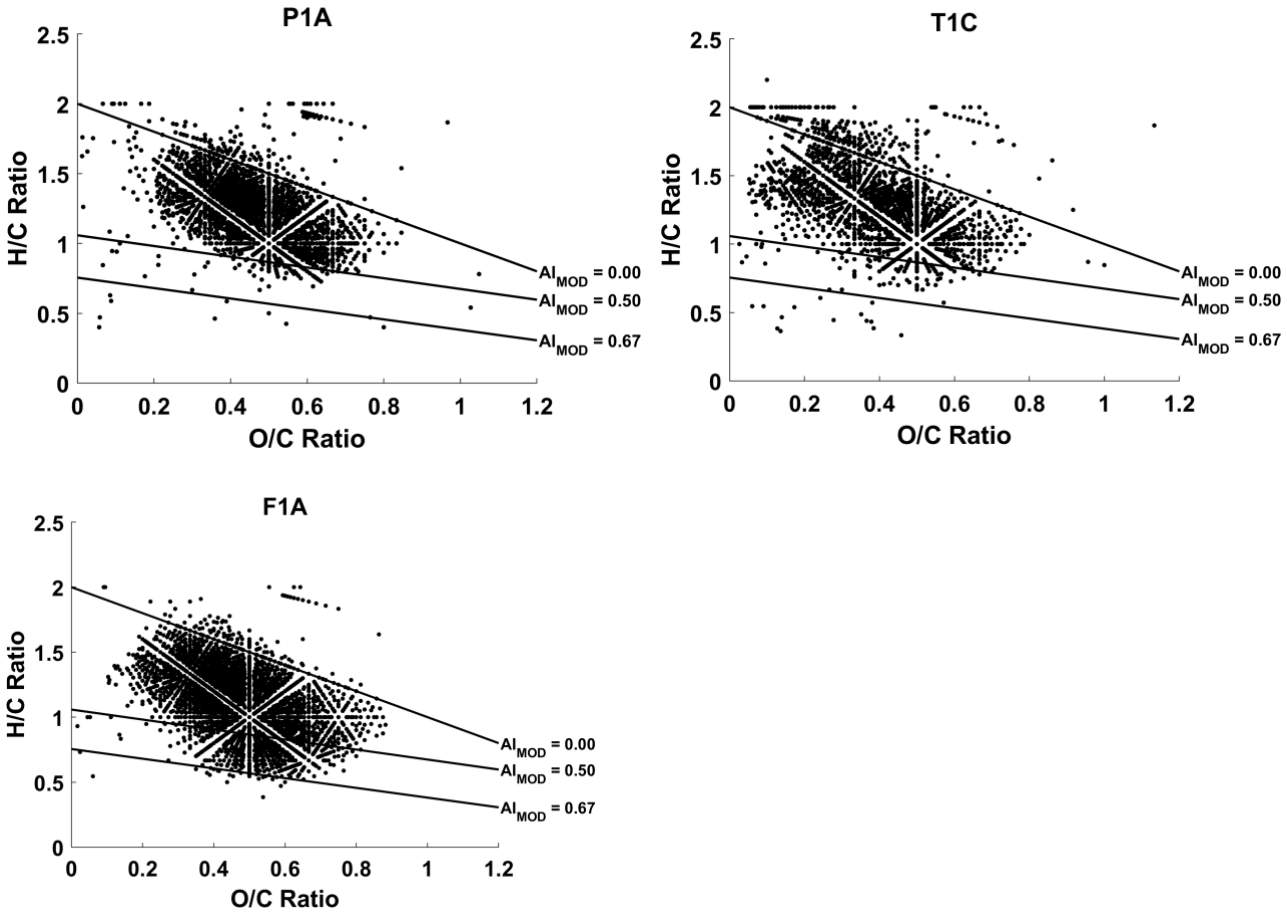

Figure 12:

The van Krevelen diagrams were constructed for all three sites after one week of incubation by plotting the O/C ratio by the H/C ratio. Here, Site 1 is indicated by the P, Site 2 by the T, and Site 3 by the F, after 1 week of incubation, indicated by the 1.

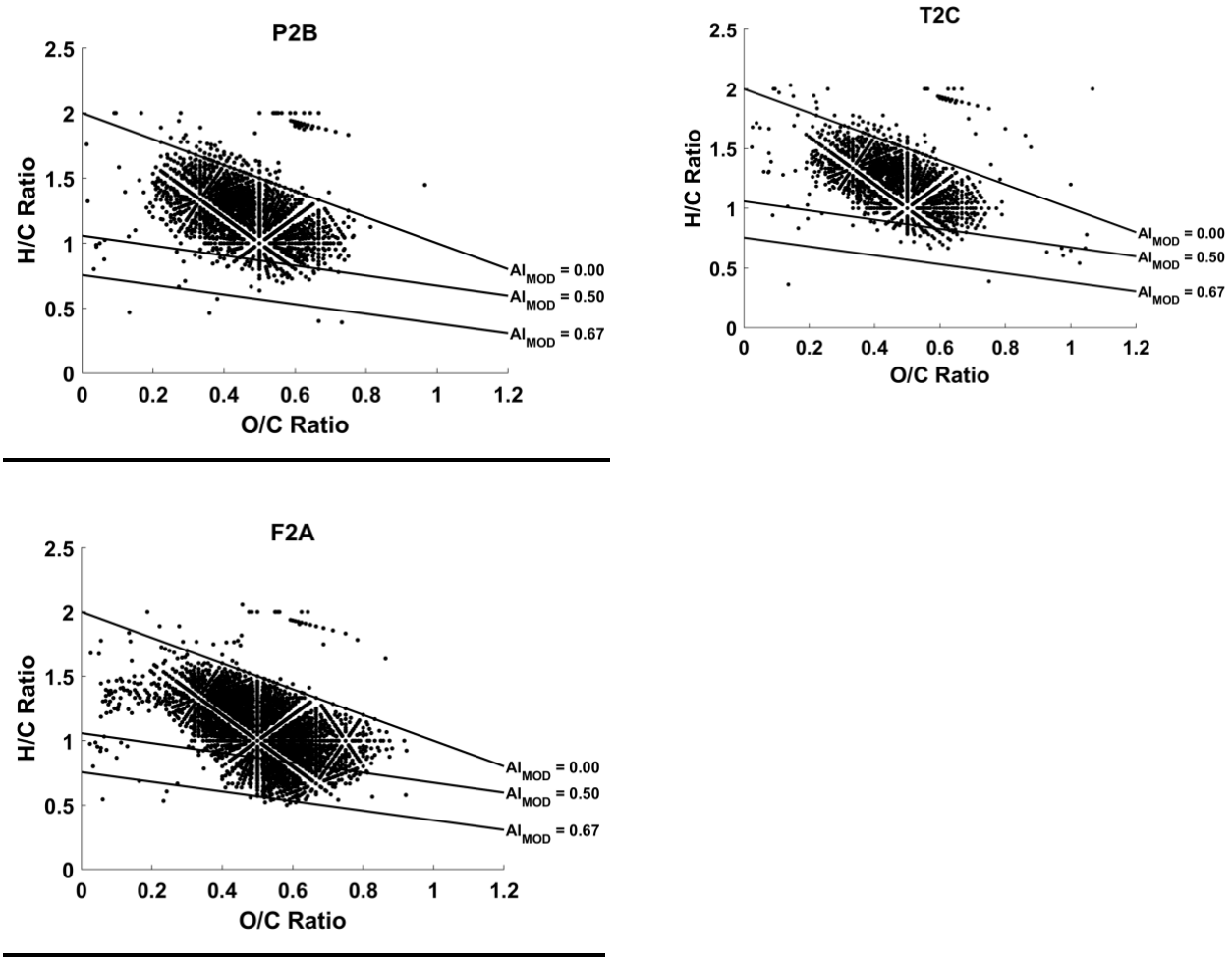

Figure 13:

The van Krevelen diagrams were constructed for all three sites after two weeks of incubation by plotting the O/C ratio by the H/C ratio. Here, Site 1 is indicated by the P, Site 2 by the T, and Site 3 by the F, after 1 week of incubation, indicated by the 2.

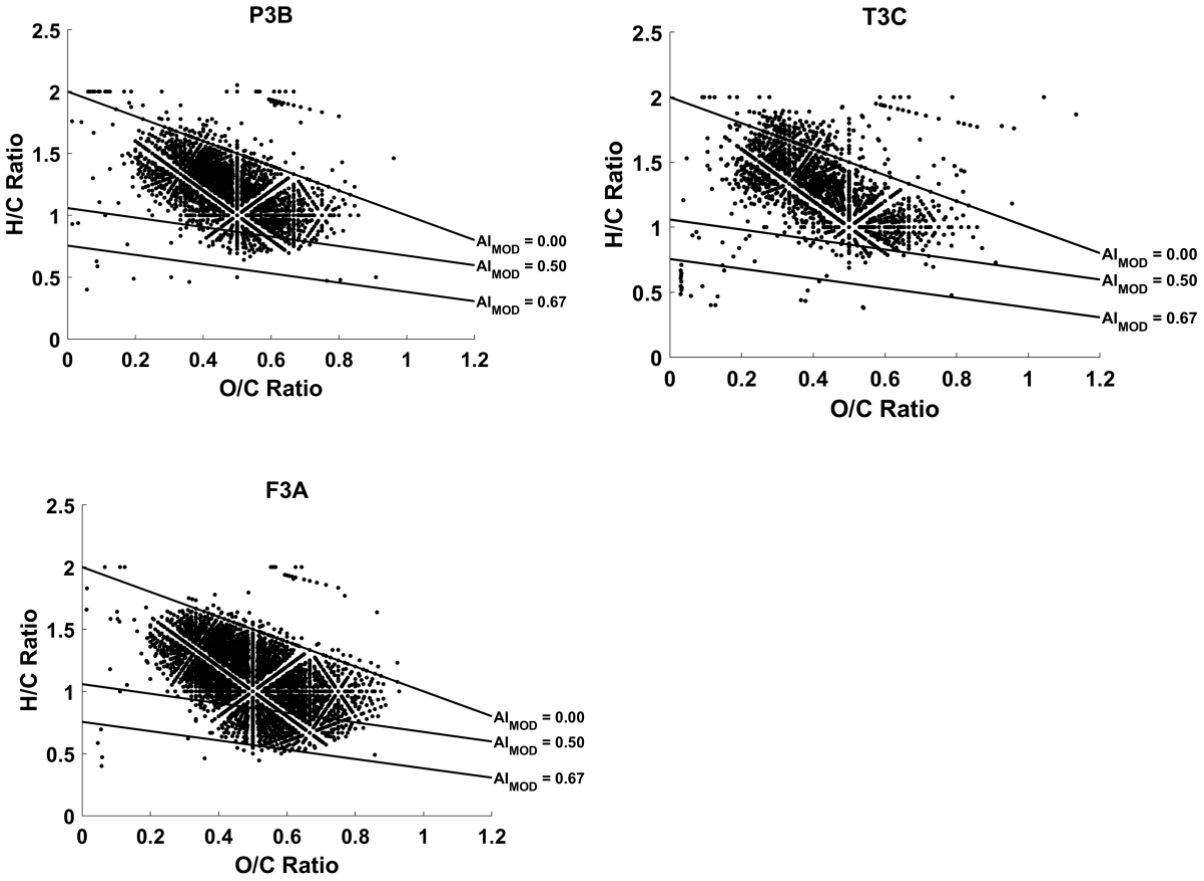

Figure 14:

The van Krevelen diagrams were constructed for all three sites after three weeks of incubation by plotting the O/C ratio by the H/C ratio. Here, Site 1 is indicated by the P, Site 2 by the T, and Site 3 by the F, after 1 week of incubation, indicated by the 3.

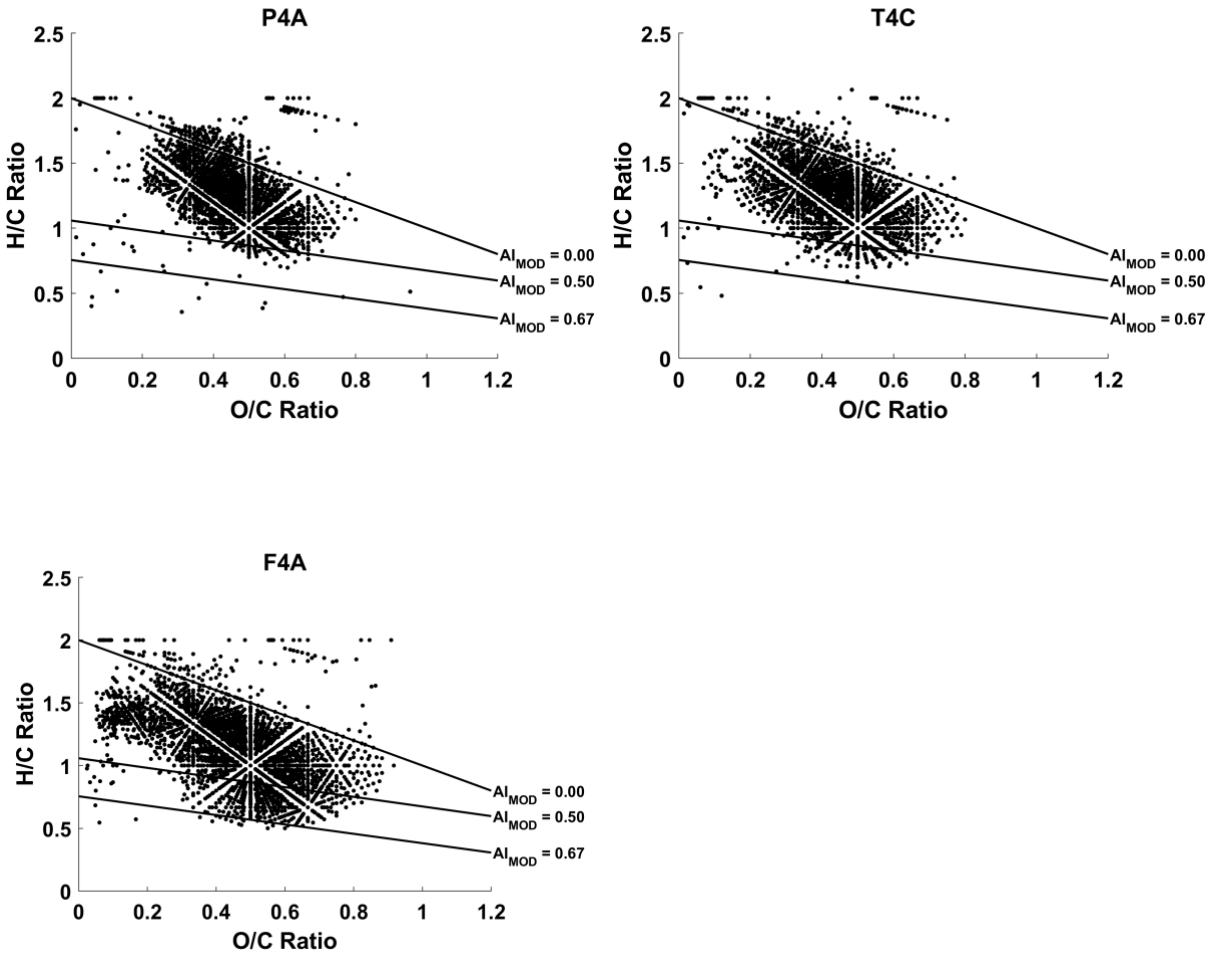

Figure 15:

The van Krevelen diagrams were constructed for all three sites after four weeks of incubation, one week after oxygenation, by plotting the O/C ratio by the H/C ratio. Here, Site 1 is indicated by the P, Site 2 by the T, and Site 3 by the F, after 1 week of incubation, indicated by the 4.

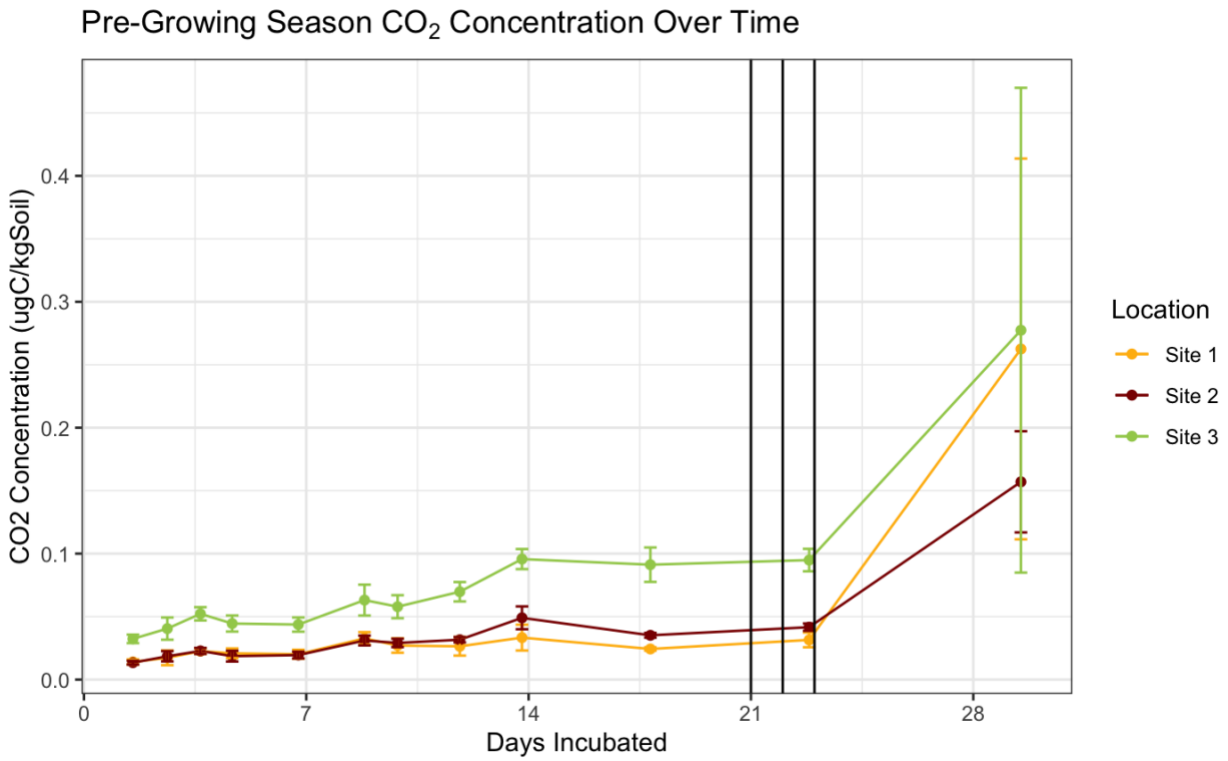

Figure 16:

The concentration of CO_2 in the headspace gas in ug C/kg soil is plotted against the days incubated for each of the sites along the transect for the incubations assembled with materials collected before the growing season had begun. Green indicates Site 3, closest to the forest edge, red for Site 2 in between the forest and the most interior point on the transect, Site 1, in yellow. Given the destructive nature of sampling, the n value changes throughout the graph, from days 0-7 (n = 12), days 7-14 (n = 9), days 14-21 (n = 6), and days 21-29 (n = 3). The three black vertical lines on days 21, 22, and 23 indicate the oxygen pulse administered, with the third line being offset to the right as to not overlap with the measurement.

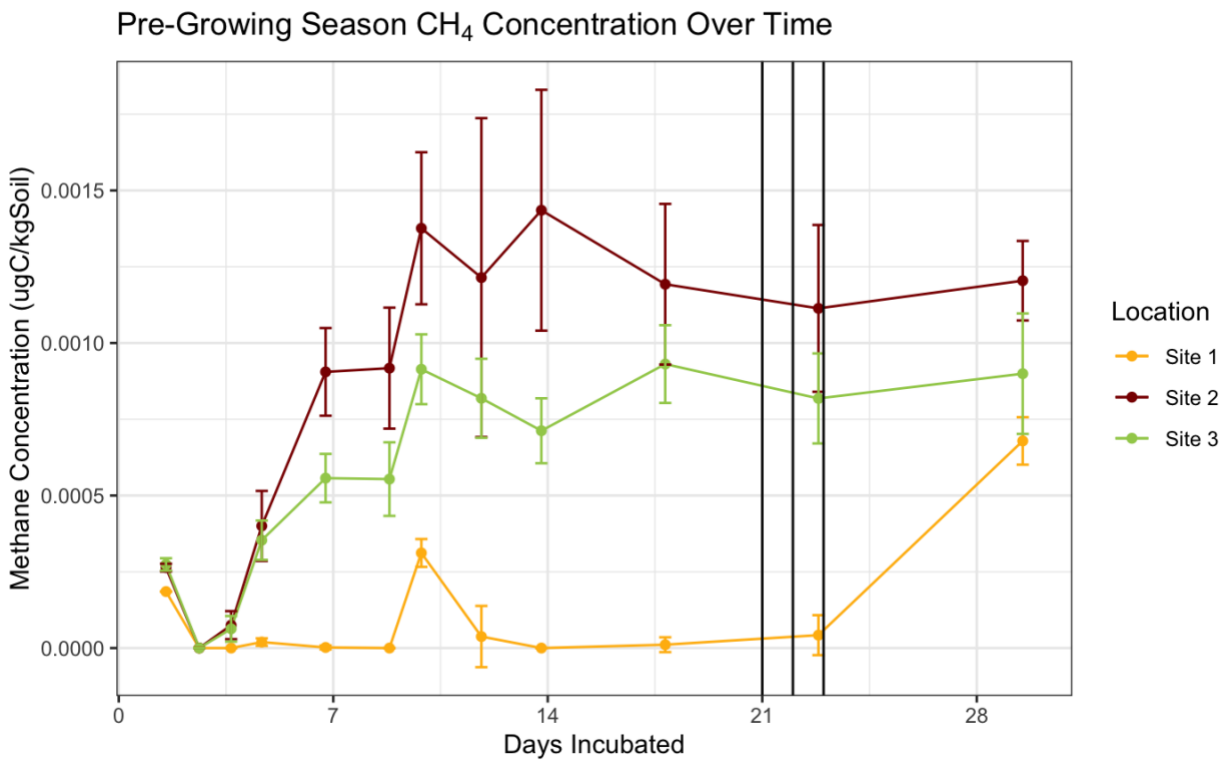

Figure 17:

The concentration of CH_4 in the headspace gas in ug C/kg soil is plotted against the days incubated for each of the sites along the transect for the incubations assembled with materials collected before the growing season had begun. Green indicates Site 3, closest to the forest edge, red for Site 2 in between the forest and the most interior point on the transect, Site 1, in yellow. Given the destructive nature of sampling, the n value changes throughout the graph, from days 0-7 (n = 12), days 7-14 (n = 9), days 14-21 (n = 6), and days 21-29 (n = 3). The three black vertical lines on days 21, 22, and 23 indicate the oxygen pulse administered, with the third line being offset to the right as to not overlap with the measurement.

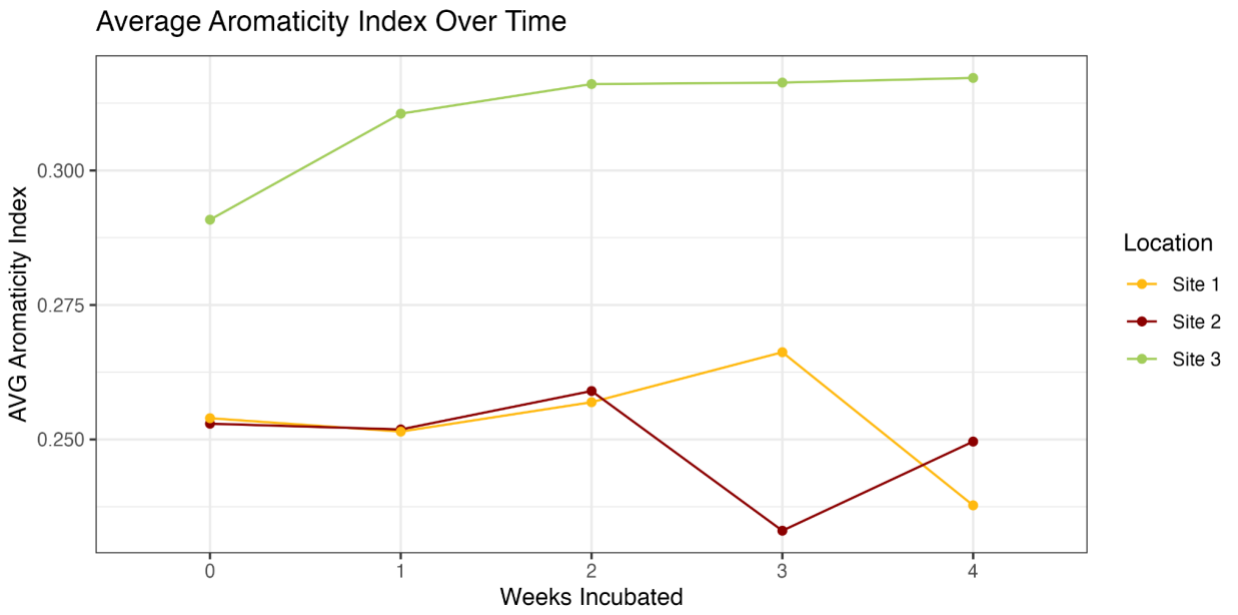

Figure 18:

Plotted above, is the average aromaticity index over the time of the incubation period (4 weeks). Site 3 had the highest average aromaticity index over the course of the incubation period. Sites 1 and 2 had relatively similar average aromaticity indexes until the third week when they diverged; Site 1 trending upward and Site 2 downward, followed by the inverse post oxygenation.

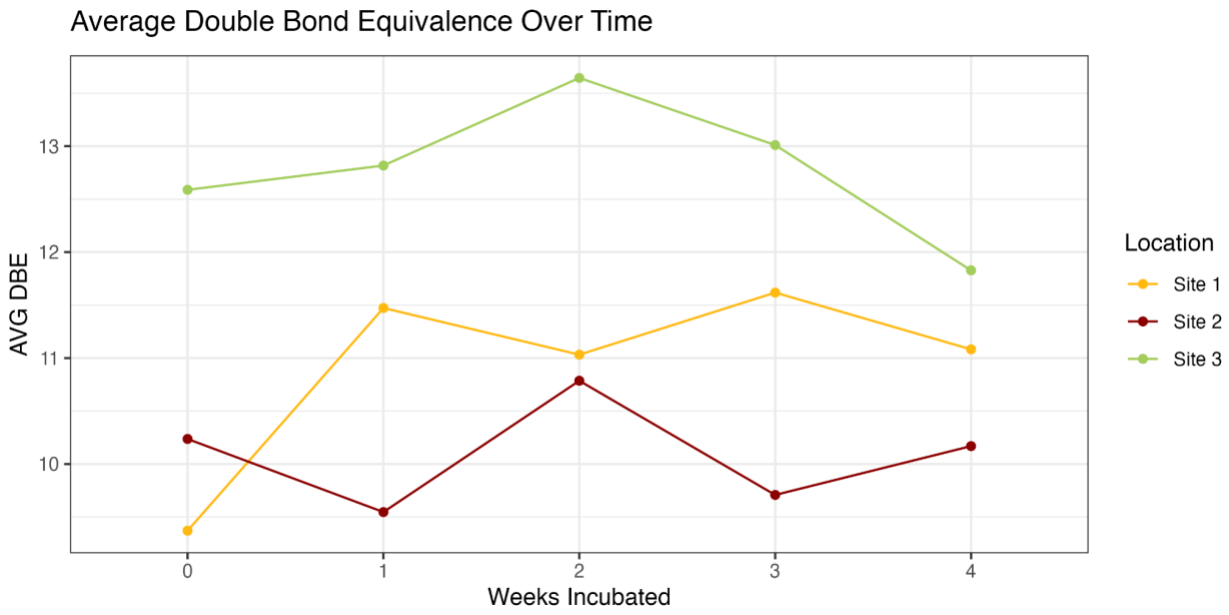

Figure 19:

Above the average double bond equivalence (DBE) for Sites 1, 2, and 3 are plotted against the incubation time. Site 3 had the highest average DBE across the incubation with it's decline beginning between week 2 and 3, further declining post oxygenation. Site 2's DBE oscillated, with the smallest change being between weeks 3 and 4 after oxygenation. Site 1 had a very low DBE initially but increased dramatically within the first week and plateaued relative to the other site behaviors.

WORKS CITED

Afreen, F., Zobayed, S. M. A., Armstrong, J., & Armstrong, W. (2007). Pressure gradients along whole culms and leaf sheaths, and other aspects of humidity-induced gas transport in Phragmites australis [Article]. *Journal of Experimental Botany*, *58*(7), 1651-1662. https://doi.org/10.1093/jxb/erm017

Angle, J. C., Morin, T. H., Solden, L. M., Narrowe, A. B., Smith, G. J., Borton, M. A., Rey-Sanchez, C., Daly, R. A., Mirfenderesgi, G., Hoyt, D. W., Riley, W. J., Miller, C. S., Bohrer, G., & Wrighton, K. C. (2017). Methanogenesis in oxygenated soils is a substantial fraction of wetland methane emissions. *Nature Communications*, *8*, Article 1567. https://doi.org/10.1038/s41467-017-01753-4

Armstrong, J., & Armstrong, W. (1988). PHRAGMITES-AUSTRALIS - A PRELIMINARY-STUDY OF SOIL-OXIDIZING SITES AND INTERNAL GAS-TRANSPORT PATHWAYS [Article]. *New Phytologist*, *108*(4), 373-382. https://doi.org/10.1111/j.1469-8137.1988.tb04177.x

Canadell, J. G., P.M.S. Monteiro, M.H. Costa, L. Cotrim da Cunha, P.M. Cox, A.V. Eliseev, S. Henson, M. Ishii, S. Jaccard, C. Koven, A. Lohila, P.K. Patra, S. Piao, J. Rogelj, S. Syampungani, S. Zaehle, and K. Zickfeld. (2021). Global Carbon and other Biogeochemical Cycles and Feedbacks. *Sixth Assessment Report of the Intergovernmental Panel on Climate Change*(Climate Change 2021: The Physical Science Basis).

Craft, M. J. V. a. C. B. (2016). *Wetland Soils: Genesis, Hydrology, Landscapes, and Classification* (Second Edition ed.). CRC Press.

DiDonato, N., Chen, H. M., Waggoner, D., & Hatcher, P. G. (2016). Potential origin and formation for molecular components of humic acids in soils. *Geochimica Et Cosmochimica Acta*, *178*, 210-222. https://doi.org/10.1016/j.gca.2016.01.013

Goranov, A. I., Sleighter, R. L., Yordanov, D. A., & Hatcher, P. G. (2023). TEnvR: MATLAB-based toolbox for environmental research. *Analytical Methods*, *15*(40), 5390-5400. https://doi.org/10.1039/d3ay00750b

Goranov, A. I., Tadini, A. M., Martin-Neto, L., Bernardi, A. C. C., Oliveira, P. P. A., Pezzopane, J. R. M., Milori, D., Mounier, S., & Hatcher, P. G. (2022). Comparison of Sample Preparation Techniques for the (-)ESI-FT- ICR-MS Analysis of Humic and Fulvic Acids. *Environmental Science & Technology*, *56*(17), 12688-12701. https://doi.org/10.1021/acs.est.2c01125

Justin, S., & Armstrong, W. (1987). THE ANATOMICAL CHARACTERISTICS OF ROOTS AND PLANT-RESPONSE TO SOIL FLOODING. *New Phytologist*, *106*(3), 465-495. https://doi.org/10.1111/j.1469-8137.1987.tb00153.x

Kirwan, M. L., & Gedan, K. B. (2019). Sea-level driven land conversion and the formation of ghost forests. *Nature Climate Change*, *9*(6), 450-457. https://doi.org/10.1038/s41558-019-0488-7

Lacroix, E. M., Aeppli, M., Boye, K., Brodie, E., Fendorf, S., Keiluweit, M., Naughton, H. R., Noël, V., & Sihi, D. (2023). Consider the Anoxic Microsite: Acknowledging and Appreciating Spatiotemporal Redox Heterogeneity in Soils and Sediments. *Acs Earth and Space Chemistry*, *7*(9), 1592-1609. https://doi.org/10.1021/acsearthspacechem.3c00032

LaRowe, D. E., & Van Cappellen, P. (2011). Degradation of natural organic matter: A thermodynamic analysis. *Geochimica Et Cosmochimica Acta*, *75*(8), 2030-2042. https://doi.org/10.1016/j.gca.2011.01.020

Lenzewski, N., Mueller, P., Meier, R. J., Liebsch, G., Jensen, K., & Koop-Jakobsen, K. (2018). Dynamics of oxygen and carbon dioxide in rhizospheres of Lobelia dortmanna - a planar optode study of belowground gas exchange between plants and sediment [Article]. *New Phytologist*, *218*(1), 131-141. https://doi.org/10.1111/nph.14973

Li, C., Ding, S. M., Chen, M. S., Sun, Q., Zhang, Y., Ma, X., Zhong, Z. L., Tsang, D. C. W., & Wang, Y. (2022). O2 distribution and dynamics in the rhizosphere of Phragmites australis, and implications for nutrient removal in sediments [Article]. *Environmental Pollution*, *806*, 10, Article 150735. https://doi.org/10.1016/j.scitotenv.2021.150735

Määttä, T., & Malhotra, A. (2024). The hidden roots of wetland methane emissions. *Global Change Biology*, *30*(2), Article e17127. https://doi.org/10.1111/gcb.17127

Martins, P. D., Hoyt, D. W., Bansal, S., Mills, C. T., Tfaily, M., Tangen, B. A., Finocchiaro, R. G., Johnston, M. D., McAdams, B. C., Solensky, M. J., Smith, G. J., Chin, Y. P., & Wilkins, M. J. (2017). Abundant carbon substrates drive extremely high sulfate reduction rates and methane fluxes in Prairie Pothole Wetlands. *Global Change Biology*, *23*(8), 3107-3120. https://doi.org/10.1111/gcb.13633

Megonigal, J. P. (2019). Biogeochemistry of Tidal Freshwater Wetlands. In *Coastal Wetlands: An Integrated Ecosystem Approach* (pp. Pages 641-683). https://doi.org/https://doi.org/10.1016/B978-0-444-63893-9.00019-8

Mitsch, W. J. a. G. J. G. (2007). *Wetlands* (Fourth Edition ed.). John Wiley & Sons, Inc.

Nahlik, A. M., & Fennessy, M. S. (2016). Carbon storage in US wetlands. *Nature Communications*, *7*, Article 13835. https://doi.org/10.1038/ncomms13835

Noyce, G. L., & Megonigal, J. P. (2021). Biogeochemical and plant trait mechanisms drive enhanced methane emissions in response to whole-ecosystem warming. *Biogeosciences*, *18*(8), 2449-2463. https://doi.org/10.5194/bg-18-2449-2021

Noyce, G. L., Smith, A. J., Kirwan, M. L., Rich, R. L., & Megonigal, J. P. (2023). Oxygen priming induced by elevated CO₂ reduces carbon accumulation and methane emissions in coastal wetlands. *Nature Geoscience*, *16*(1), 63-+. https://doi.org/10.1038/s41561-022-01070-6

O'Connell, C. S., Ruan, L., & Silver, W. L. (2018). Drought drives rapid shifts in tropical rainforest soil biogeochemistry and greenhouse gas emissions. *Nature Communications*, *9*, Article 1348. https://doi.org/10.1038/s41467-018-03352-3

Philippot, L., Hallin, S., Börjesson, G., & Baggs, E. M. (2009). Biochemical cycling in the rhizosphere having an impact on global change. *Plant and Soil*, *321*(1-2), 61-81. https://doi.org/10.1007/s11104-008-9796-9

Seyfferth, A. L., Bothfeld, F., Vargas, R., Stuckey, J. W., Wang, J., Kearns, K., Michael, H. A., Guimond, J., Yu, X., & Sparks, D. L. (2020). Spatial and temporal heterogeneity of geochemical controls on carbon cycling in a tidal salt marsh. *Geochimica Et Cosmochimica Acta*, *282*, 1-18. https://doi.org/10.1016/j.gca.2020.05.013

Sleighter, R. L., & Hatcher, P. G. (2008). Molecular characterization of dissolved organic matter (DOM) along a river to ocean transect of the lower Chesapeake Bay by ultrahigh resolution electrospray ionization Fourier transform ion cyclotron resonance mass spectrometry. *Marine Chemistry*, *110*(3-4), 140-152. https://doi.org/10.1016/j.marchem.2008.04.008

Sowers, K. R. (2019). Methanogenesis. In *Encyclopedia of Microbiology, 4th Ediition - Reference Module in Biomedical Sciences*. Ellsevier Inc. https://doi.org/10.1016/b978-0-12-801238-3.02447-8

Srivastava, J., Kalra, S. J. S., & Naraian, R. (2014). Environmental perspectives of Phragmites australis (Cav.) Trin. Ex. Steudel. *Applied Water Science*, *4*(3), 193-202. https://doi.org/10.1007/s13201-013-0142-x

Stagg, C. L., Schoolmaster, D. R., Krauss, K. W., Cormier, N., & Conner, W. H. (2017). Causal mechanisms of soil organic matter decomposition: deconstructing salinity and flooding impacts in coastal wetlands. *Ecology*, *98*(8), 2003-2018. https://doi.org/10.1002/ecy.1890

Stanley, E. H., & Ward, A. K. (2010). Effects of Vascular Plants on Seasonal Pore Water Carbon Dynamics in a Lotic Wetland. *Wetlands*, *30*(5), 889-900. https://doi.org/10.1007/s13157-010-0087-x

Valle, J., Gonsior, M., Harir, M., Enrich-Prast, A., Schmitt-Kopplin, P., Bastviken, D., Conrad, R., & Hertkorn, N. (2018). Extensive processing of sediment pore water dissolved organic matter during anoxic incubation as observed by high-field mass spectrometry (FTICR-MS). *Water Research*, *129*, 252-263. https://doi.org/10.1016/j.watres.2017.11.015

van den Berg, M., van den Elzen, E., Ingwersen, J., Kosten, S., Lamers, L. P. M., & Streck, T. (2020). Contribution of plant-induced pressurized flow to CH4 emission from a Phragmites fen. *Scientific Reports*, *10*(1), Article 12304. https://doi.org/10.1038/s41598-020-69034-7

Vroom, R. J. E., van den Berg, M., Pangala, S. R., van der Scheer, O. E., & Sorrell, B. K. (2022). Physiological processes affecting methane transport by wetland vegetation - A review. *Aquatic Botany*, *182*, Article 103547. https://doi.org/10.1016/j.aquabot.2022.103547

Wilmoth, J. L. (2021). Redox Heterogeneity Entangles Soil and Climate Interactions [Article]. *Sustainability*, *13*(18), 14, Article 10084. https://doi.org/10.3390/su131810084

Wilmoth, J. L., Moran, M. A., & Thompson, A. (2018). Transient O₂ pulses direct Fe crystallinity and Fe(III)-reducer gene expression within a soil microbiome. *Microbiome*, *6*, Article 189. https://doi.org/10.1186/s40168-018-0574-5

Wilmoth, J. L., Schaefer, J. K., Schlesinger, D. R., Roth, S. W., Hatcher, P. G., Shoemaker, J. K., & Zhang, X. N. (2021). The role of oxygen in stimulating methane production in wetlands. *Global Change Biology*, *27*(22), 5831-5847. https://doi.org/10.1111/gcb.15831

Yang, W. H., McNicol, G., Teh, Y. A., Estera-Molina, K., Wood, T. E., & Silver, W. L. (2017). Evaluating the Classical Versus an Emerging Conceptual Model of Peatland Methane Dynamics. *Global Biogeochemical Cycles*, *31*(9), 1435-1453. https://doi.org/10.1002/2017gb005622

Zhang, L. H., Shao, H. B., Wang, B. C., Zhang, L. W., & Qin, X. C. (2019). Effects of nitrogen and phosphorus on the production of carbon dioxide and nitrous oxide in salt-affected soils under different vegetation communities. *Atmospheric Environment*, *204*, 78-88. https://doi.org/10.1016/j.atmosenv.2019.02.024

Zhao, J. F., Peng, S. S., Chen, M. P., Wang, G. Z., Cui, Y. B., Liao, L. G., Feng, J. G., Zhu, B., Liu, W. J., Yang, L. Y., & Tan, Z. H. (2019). Tropical forest soils serve as substantial and persistent methane sinks. *Scientific Reports*, *9*, Article 16799. https://doi.org/10.1038/s41598-019-51515-z

CONCLUSION

Just shy of 200 incubation bottles later, we are one (small) step closer to understanding the intricate nature of wetland SOM and its role in the C cycle. Given the incredible range in size and scale of products and reactants, it is seemingly impossible to get a clear picture of C cycling. If we were to think of this through the lens of a camera, only so much of the field of view can be in focus; adjusting the focus to gain new insight, in turn, blurs other parts of the image. With the nuanced complexities of the C cycle, we still must remember that the parts of the image that are out of focus will influence those that are and vice versa, not to mention the above-ground processes that are slightly out of the frame. In other words, we must continue using multifaceted analytical approaches to compile the images of different aspects of wetland soils to get a more holistic picture of the mechanisms behind this cryptic cycling.

Time series incubation studies act as a series of pictures with one part of the frame in focus, stripping a dynamic system down to its ingredients in order to maintain some level of experimental control. Investigating the dissolved carbon composition, gas phase, seasonality, position in the wetland, and redox conditions provides new areas of focus within our collage of information. The tension between resolution and scale is a constant; however, it is one we must learn to embrace and adjust as our research scopes and questions change.

Ultra high-resolution mass spectrometry provides detailed information on the presence of molecules, but only of those of particular sizes. Small substrates like CH_4 and acetate are outside of this analytical window but still crucial to understanding these broad scale C transformations. FTICR-MS also lacks in its ability to decipher molecular structure. Lignin, tannin, and CRAM

presence can be interpreted using this data, but other techniques like NMR are required to get an understanding of their reactivity, bioavailability, and subsequent influence on the system.

Given the three-phase system of our natural world, being able to trace these molecules into these different phases, solid, liquid, and gas, would provide a deeper mechanistic layer of understanding. Biologically, a characterization of the microbial community would shed light on the potential biochemical transformations at play. The shifts in these populations and their relationships with each other across the system and through time both impact and are impacted by the system, including gas concentrations, substrate availability, redox conditions, carbon degradation and more.

The C cycle may have been the focus of this study, but biogeochemical cycles do not act in isolation of one another. Given the electron acceptors used in reducing soils, investigations of Fe oxide chemistry may provide insights as to the Fe precipitation seen on the surface soils in the field. The tidal nature of this system cannot leave S out of the equation, amongst others. These cycles operate as a system of interlocking gears, each cycle as a coexisting dimension in constant influence to the system and the system to itself.

The variability in above-ground CH_4 and CO_2 measurements can be explained by the culmination of above and below-ground processes, requiring an integrated analytical approach to investigations. Coupling these analytical techniques with field measurements could allow further connections to be made, specifically amongst the lignin, tannin, and CRAM pools and their signal of CH_4 production. Understanding the intrinsic connection of biogeochemical cycles within our ecosystems is essential for producing accurate global carbon budgets and guiding

evidence-based climate policy to implement effective mitigation and adaptation strategies in this critical era.

“Organic chemistry is the study of carbon compounds.

Biochemistry is the study of carbon compounds that crawl.

[Biogeochemistry is the study of the carbon compounds of our world — those that decompose, dissolve, respire, reduce, circulate, and persist across space and time.]”

SUPPLEMENTAL INFORMATION

Table 1: Tide Conditions

Sampling Event	Date	High Tide	Low Tide	Sampling Time
Pre-Growing Season	03/25/2024	05:37	12:09	10:00 - 13:00
Growing Season	07/19/2024	03:34	10:59	09:00 - 12:30
Post-Growing Season	09/20/2024	06:37	12:53	10:30 - 13:00

Source: NOAA Tides & Currents

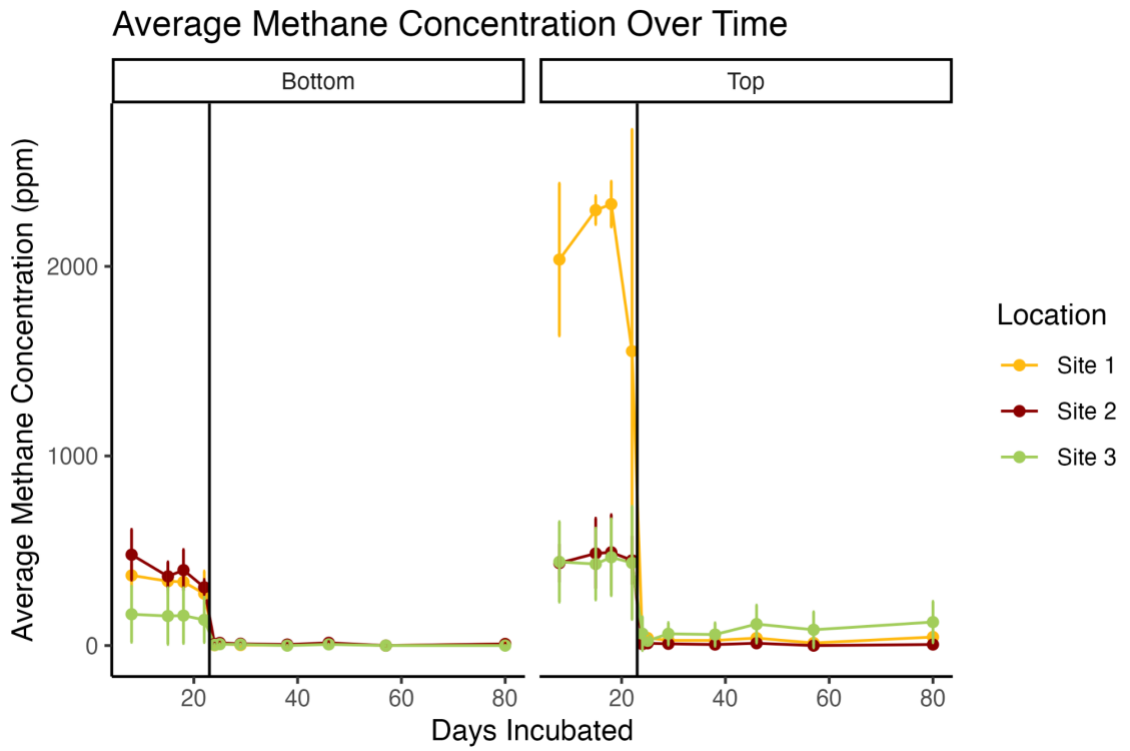

Figure 10: The graph above shows the concentration of CH_4 throughout the incubation assembled using the same protocol as Chapters II and III; however, it used soil that was either collected from 0-28 cm or 28-54 (where horizon distinction occurred). The black lines indicate a complete N2 flush of the headspace, which tested whether the plateau and even slight decrease in gas concentrations was due to over-pressurization.

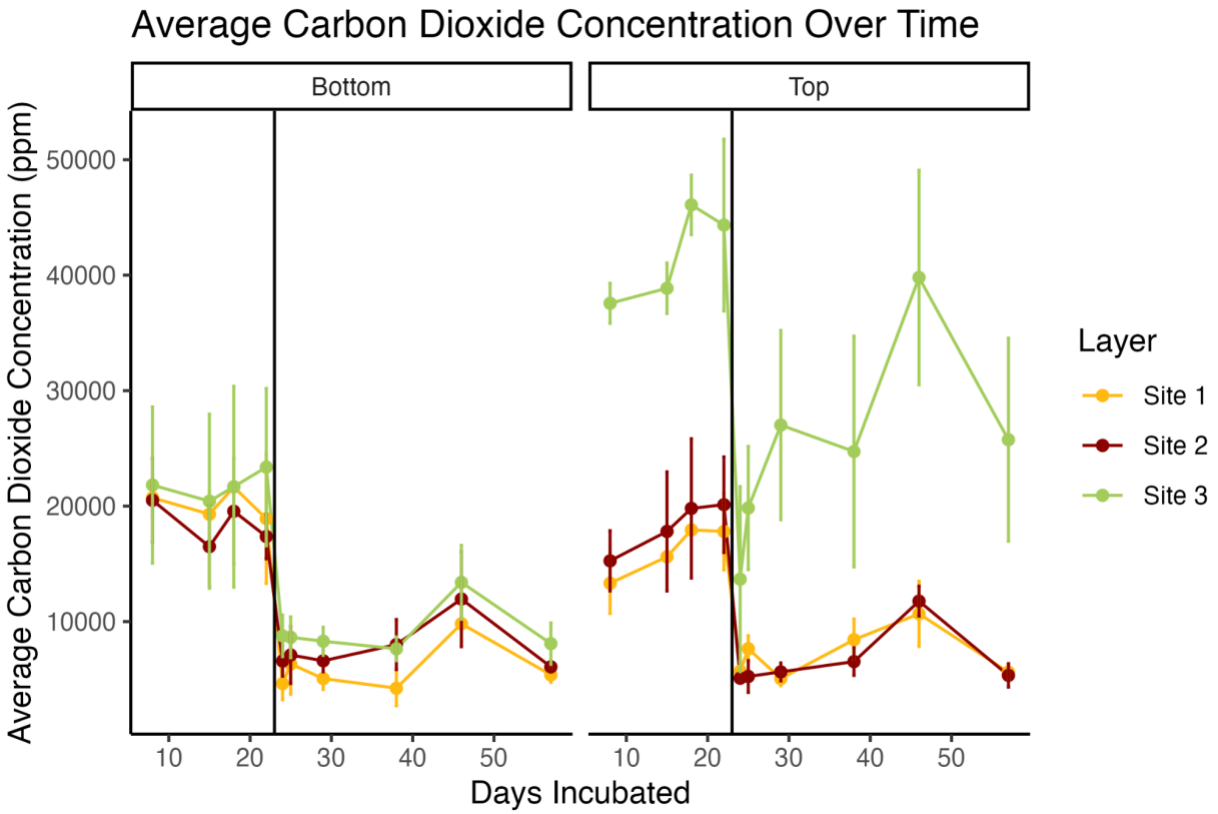

Figure 11: The graph above shows the concentration of CO_2 throughout the incubation assembled using the same protocol of Chapters II and III; however, using soil that was either collected from 0-28 cm or 28-54 (where horizon distinction occurred). The black lines indicate a complete N2 flush of the headspace, which was done to test if the plateau and even slight decrease in gas concentrations was due to over-pressurization.

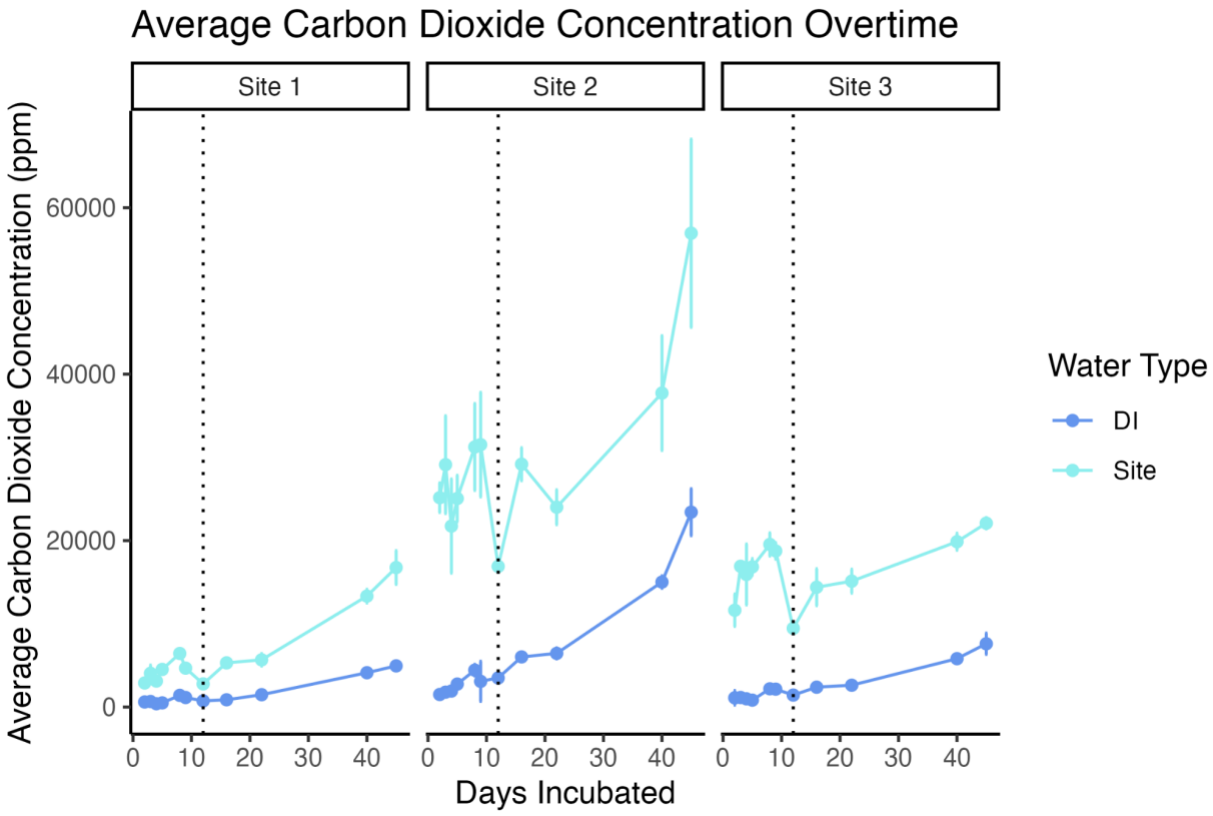

Figure 12: The graph above shows the concentration of CO_2 throughout the incubation assembled using the same protocol of Chapters II and III, however using water that was either collected from the core recharge of the site itself or lab-grade deionized water to see the effect of site water's addition to the slurry. Around day 9 of the incubation, CO_2 began to plateau and decrease slightly. On day 12, an ambient air pulse bringing O_2 concentrations to 3% was administered, and CO_2 concentrations recovered.

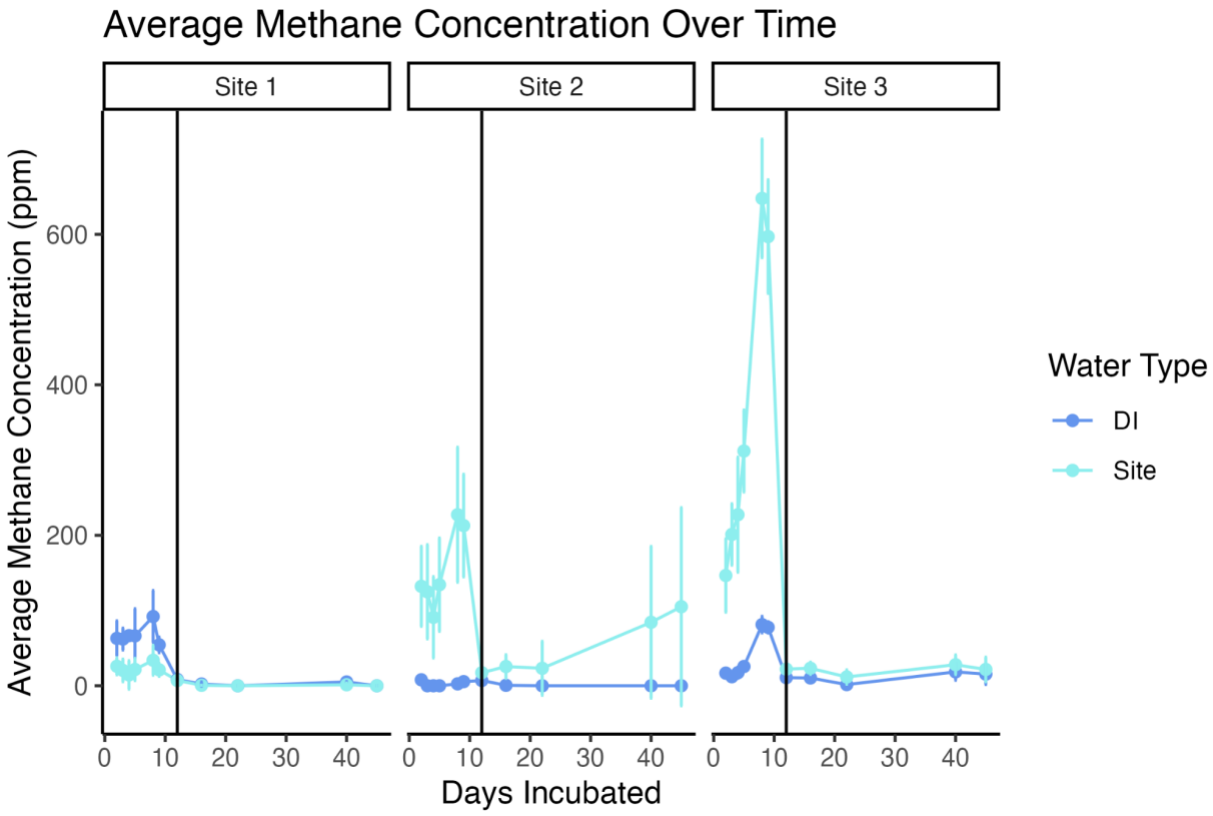

Figure 13: The graph above shows the concentration of CH_4 throughout the incubation assembled using the same protocol of Chapters II and III, however using water that was either collected from the core recharge of the site itself or lab-grade deionized water to see the effect of site water's addition to the slurry. Around day 9 of the incubation, CH_4 began to plateau and decrease slightly. On day 12, an ambient air pulse bringing O_2 concentrations to 3% was administered, and the CH_4 concentrations slightly rose in some of the incubations constructed with the site water.

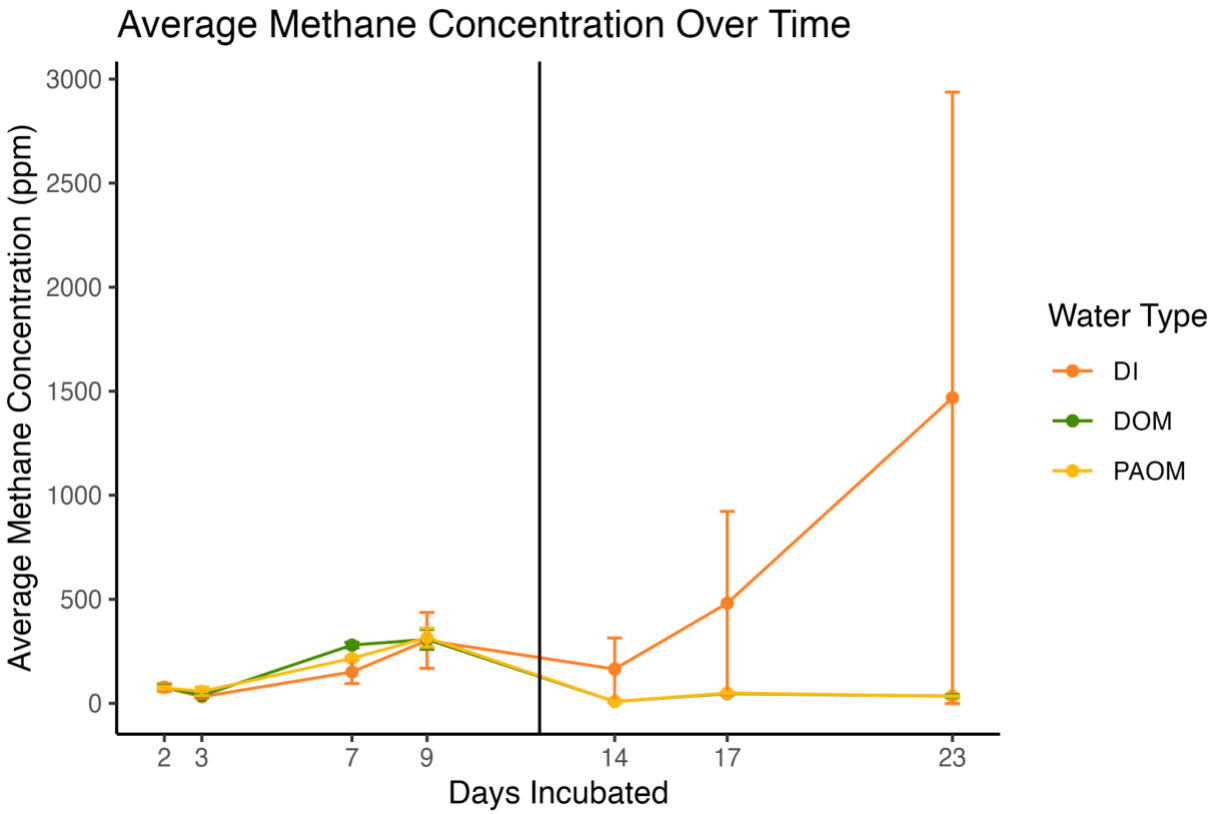

Figure 14: The graph above shows the concentration of CH_4 throughout the incubation assembled using the same protocol of Chapters II and III; however using soil that was from just Site 2 and with water that was either from the site with suspended solids (PAOM), from the site but spun at 10G for 15 minutes to remove suspended solids (DOM), and DI water to see the influence particulates on emissions. The black line indicates the headspace being flushed to test if the plateau in gas concentrations was due to over-pressurization or hydrogen sulfide inhibition.

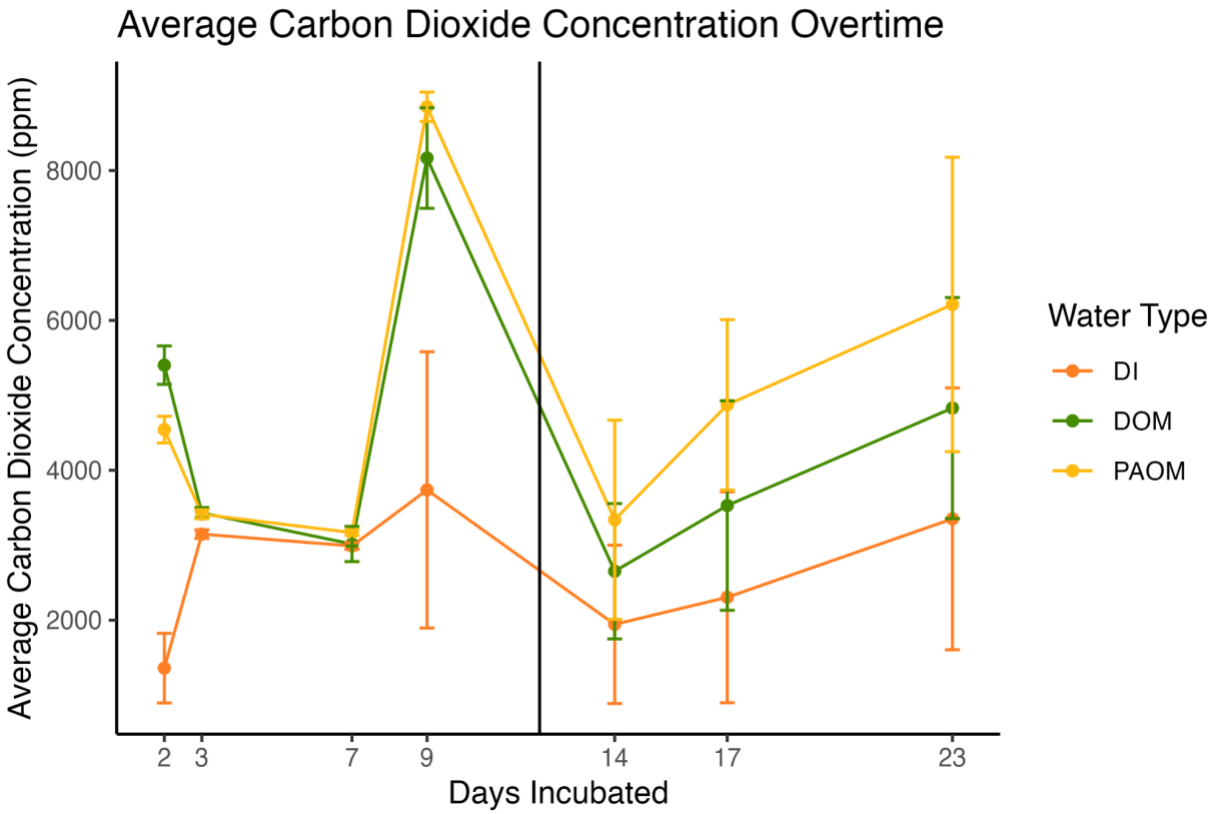

Figure 15: The graph above shows the concentration of CO_2 throughout the incubation assembled using the same protocol of Chapters II and III; however using soil that was from just Site 2 and with water that was either from the site with suspended solids (PAOM), from the site but spun at 10G for 15 minutes to remove suspended solids (DOM), and DI water to see the influence particulates on emissions. The black line indicates the headspace being flushed to test if the plateau in gas concentrations was due to over-pressurization or hydrogen sulfide inhibition.

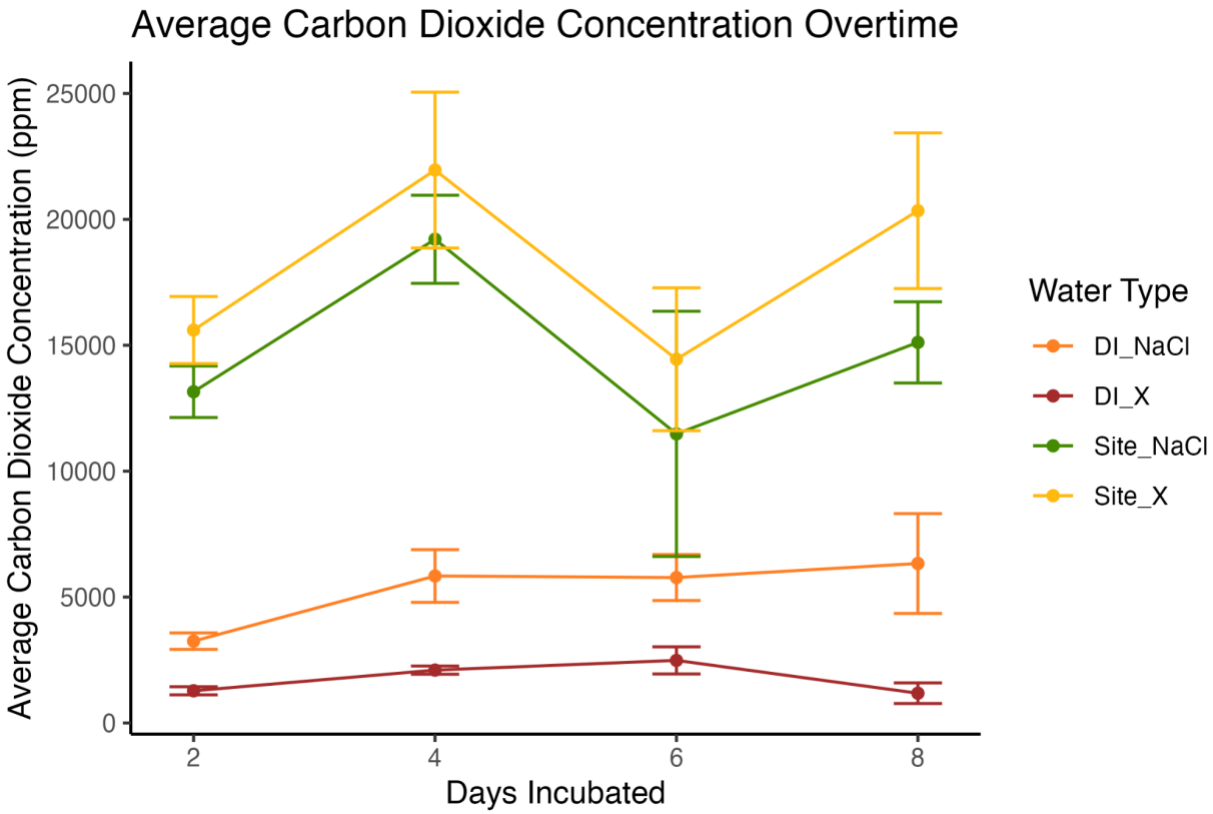

Figure 16: The graph above shows the concentration of CO_2 throughout the incubation assembled using the same protocol of Chapters II and III. However, it uses soil from just Site 2 and water from either the site (~8 ppt), the site with NaCl added (~15 ppt), DI (0 ppt), or DI with NaCl added (~8 ppt) to see the influence of salinity and dissolved organics.

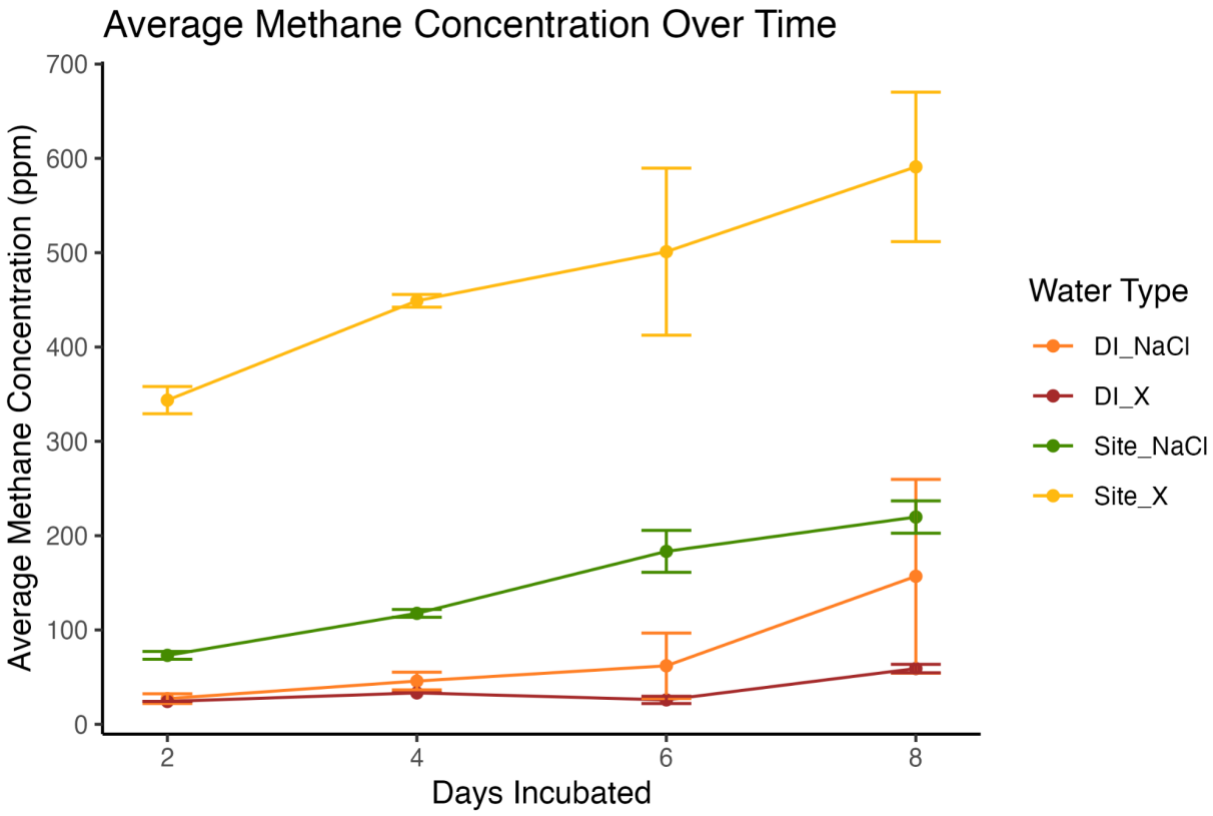

Figure 17: The graph above shows the concentration of CH_4 throughout the incubation assembled using the same protocol of Chapters II and III. However, it uses soil from just Site 2 and water from either the site (~8 ppt), the site with NaCl added (~15 ppt), DI (0 ppt), or DI with NaCl added (~8 ppt) to see the influence of salinity and dissolved organics.

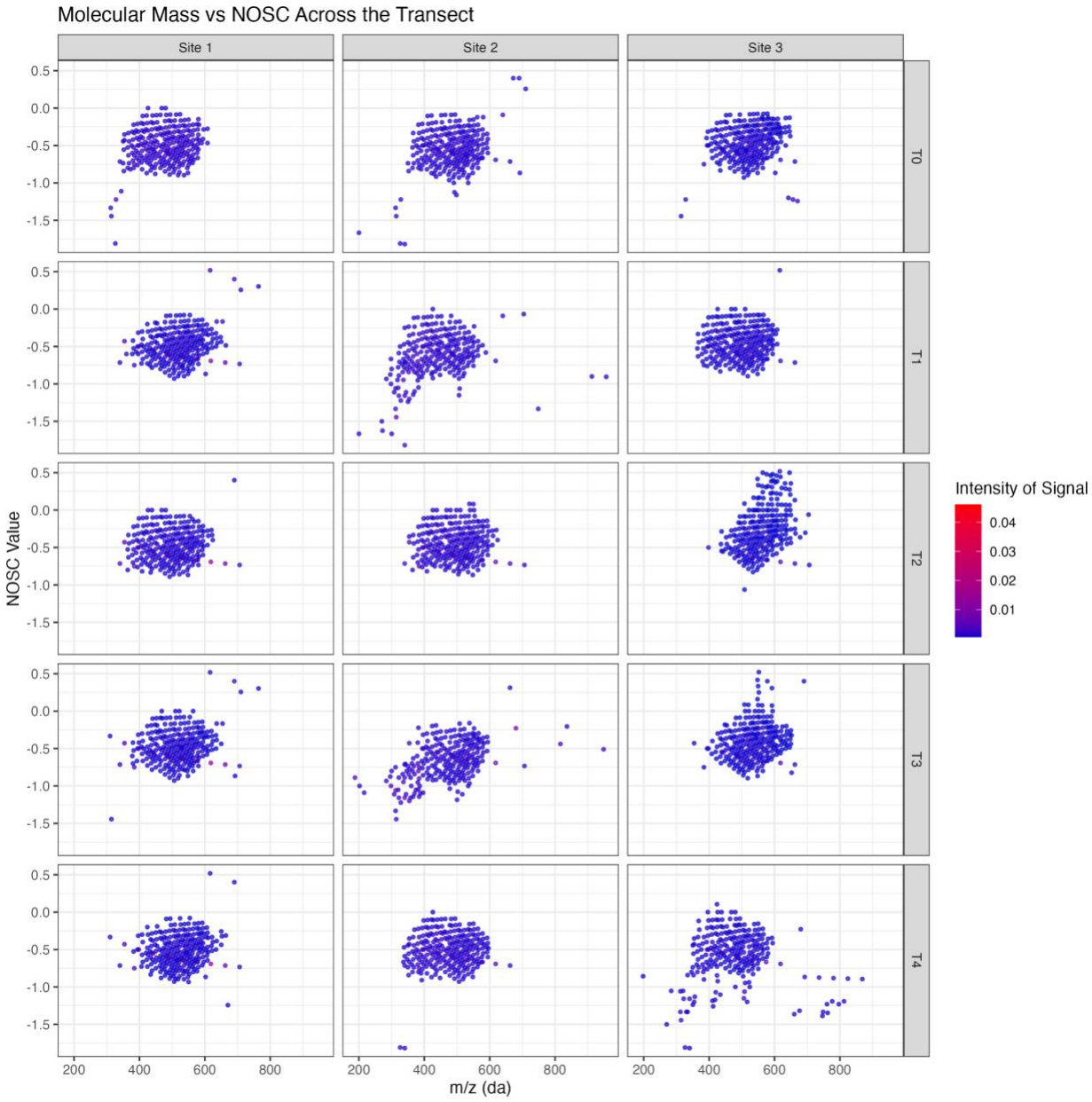

Figure 20:

Above shows mass to charge ratio plotted against the NOSC with the color scale corresponding to the intensity of the signal of the top 250 molecules present in the sample.

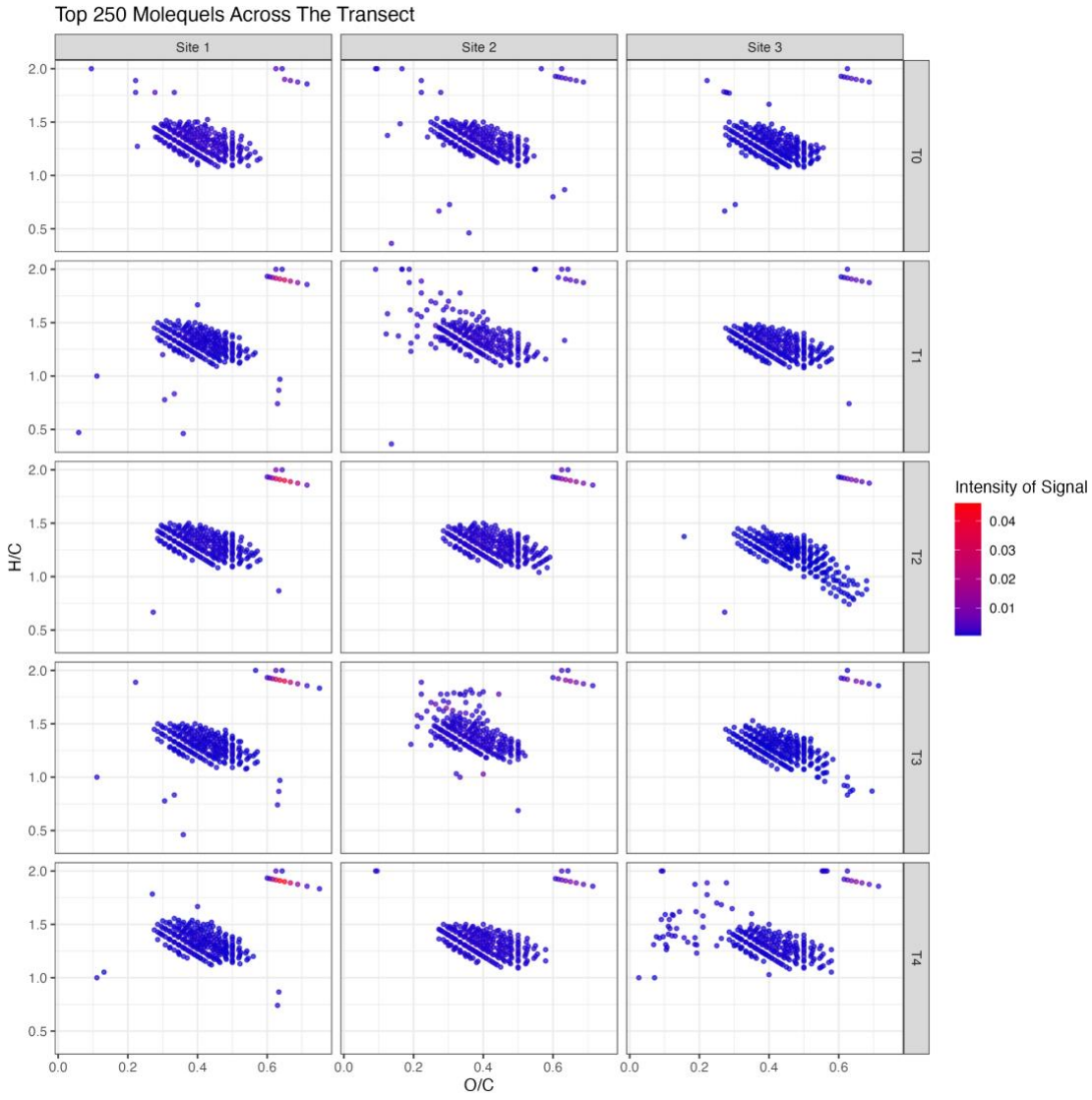

Figure 21:

Above is a Van Krevelen plot of the top 250 molecules the O to C ratios plotted against the H to C ratios with the intensities corresponding to the color.

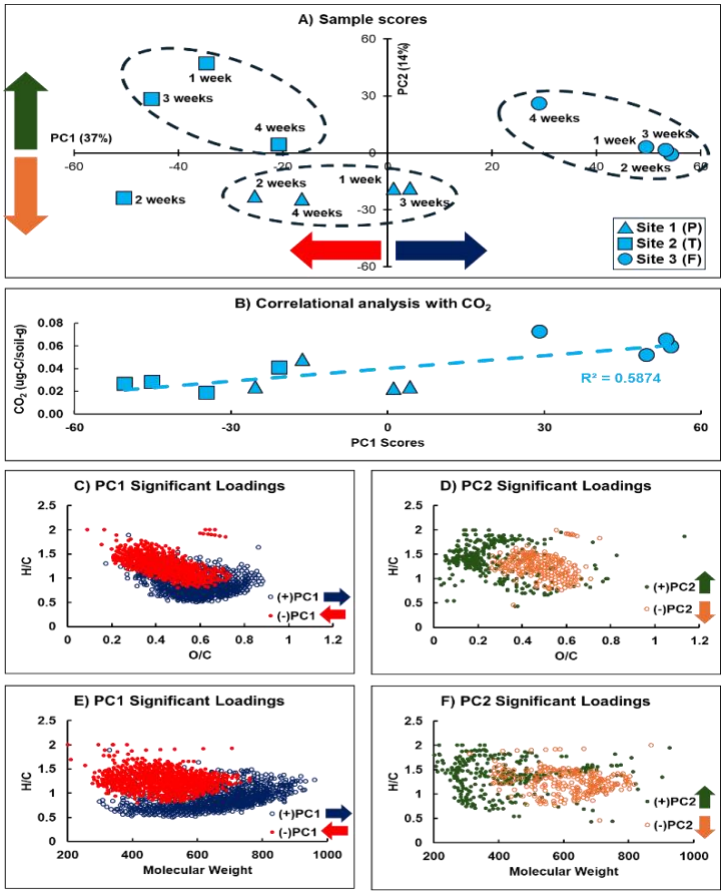

Figure 22:

Principal component analysis of molecular fingerprints determined by ultrahigh resolution mass spectrometry. Panel A shows the sample scores, which separate into three pools as determined by k-means clustering analysis. Panel B shows a correlation ($p < 0.05$) between PC1 scores and CO_2 emissions (correlations between PC2 and CH_4 or between PC2 and CO_2/CH_4 are not shown as they were insignificant, $p > 0.05$). Panels C and D show the van Krevelen diagrams of the formulas of significance ($p < 0.05$), explaining the similarities and differences among samples. Panels E and F show the H/C vs. Molecular weight maps of the same formulas.

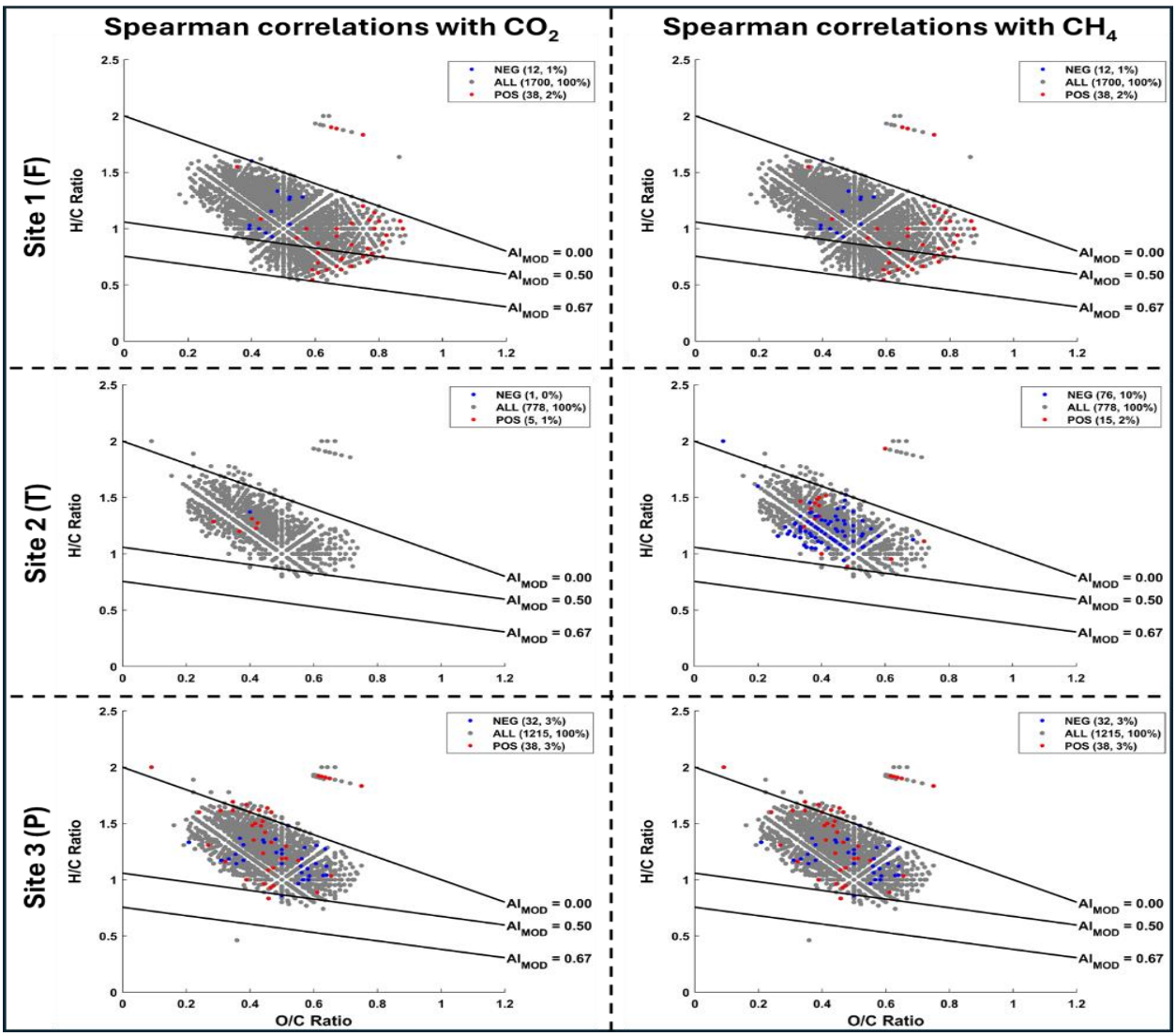

Figure 23:

Spearman correlations between common formulas in Site 1 (top panels), Site 2 (middle panels), or Site 3 (bottom panels) and CO_2 (left panels) or CH_4 emissions (right panels). The intensities of blue formulas covary negatively with CO_2 or CH_4, whereas the intensities of the red formulas covary positively. Grey formulas were not positively correlated ($p > 0.05$).

REFERENCES

Afreen, F., Zobayed, S. M. A., Armstrong, J., & Armstrong, W. (2007). Pressure gradients along whole culms and leaf sheaths, and other aspects of humidity-induced gas transport in Phragmites australis [Article]. *Journal of Experimental Botany*, *58*(7), 1651-1662. https://doi.org/10.1093/jxb/erm017

Angle, J. C., Morin, T. H., Solden, L. M., Narrowe, A. B., Smith, G. J., Borton, M. A., Rey-Sanchez, C., Daly, R. A., Mirfenderesgi, G., Hoyt, D. W., Riley, W. J., Miller, C. S., Bohrer, G., & Wrighton, K. C. (2017). Methanogenesis in oxygenated soils is a substantial fraction of wetland methane emissions. *Nature Communications*, *8*, Article 1567. https://doi.org/10.1038/s41467-017-01753-4

Armstrong, J., & Armstrong, W. (1988). PHRAGMITES-AUSTRALIS - A PRELIMINARY-STUDY OF SOIL-OXIDIZING SITES AND INTERNAL GAS-TRANSPORT PATHWAYS [Article]. *New Phytologist*, *108*(4), 373-382. https://doi.org/10.1111/j.1469-8137.1988.tb04177.x

Armstrong, J., Armstrong, W., Beckett, P. M., Halder, J. E., Lythe, S., Holt, R., & Sinclair, A. (1996). Pathways of aeration and the mechanisms and beneficial effects of humidity- and Venturi-induced convections in Phragmites australis (Cav) Trin ex Steud. *Aquatic Botany*, *54*(2-3), 177-197. https://doi.org/10.1016/0304-3770(96)01044-3

Bastviken, D. (2009). Methane. In G. Likens (Ed.), *Encyclopedia of Inland Waters* (First Edition ed., pp. Pages 783-805). Oxford: Elsevier.

Canadell, J. G., P.M.S. Monteiro, M.H. Costa, L. Cotrim da Cunha, P.M. Cox, A.V. Eliseev, S. Henson, M. Ishii, S. Jaccard, C. Koven, A. Lohila, P.K. Patra, S. Piao, J. Rogelj, S. Syampungani, S. Zaehle, and K. Zickfeld. (2021). Global Carbon and other Biogeochemical Cycles and Feedbacks. *Sixth Assessment Report of the Intergovernmental Panel on Climate Change*(Climate Change 2021: The Physical Science Basis).

Carmichael, M. J., Bernhardt, E. S., Brauer, S. L., & Smith, W. K. (2014). The role of vegetation in methane flux to the atmosphere: should vegetation be included as a distinct category in the global methane budget? *Biogeochemistry*, *119*(1-3), 1-24. https://doi.org/10.1007/s10533-014-9974-1

Cicerone, R. J., & Oremland, R. S. (1988). BIOGEOCHEMICAL ASPECTS OF ATMOSPHERIC METHANE. *Global Biogeochemical Cycles*, *2*(4), 299-327. https://doi.org/10.1029/GB002i004p00299

Craft, M. J. V. a. C. B. (2016). *Wetland Soils: Genesis, Hydrology, Landscapes, and Classification* (Second Edition ed.). CRC Press.

Dean, J. F., Middelburg, J. J., Rockmann, T., Aerts, R., Blauw, L. G., Egger, M., Jetten, M. S. M., de Jong, A. E. E., Meisel, O. H., Rasigraf, O., Slomp, C. P., in't Zandt, M. H., & Dolman, A. J. (2018). Methane Feedbacks to the Global Climate System in a Warmer World [Review]. *Reviews of Geophysics*, *56*(1), 207-250. https://doi.org/10.1002/2017rg000559

DiDonato, N., Chen, H. M., Waggoner, D., & Hatcher, P. G. (2016). Potential origin and formation for molecular components of humic acids in soils. *Geochimica Et Cosmochimica Acta*, *178*, 210-222. https://doi.org/10.1016/j.gca.2016.01.013

Ge, M. Y., Korrensalo, A., Laiho, R., Lohila, A., Makiranta, P., Pihlatie, M., Tuittila, E. S., Kohl, L., Putkinen, A., & Koskinen, M. (2023). Plant phenology and species-specific traits control plant CH₄ emissions in a northern boreal fen. *New Phytologist*, *238*(3), 1019-1032. https://doi.org/10.1111/nph.18798

Goranov, A. I., Sleighter, R. L., Yordanov, D. A., & Hatcher, P. G. (2023). TEnvR: MATLAB-based toolbox for environmental research. *Analytical Methods*, *15*(40), 5390-5400. https://doi.org/10.1039/d3ay00750b

Goranov, A. I., Tadini, A. M., Martin-Neto, L., Bernardi, A. C. C., Oliveira, P. P. A., Pezzopane, J. R. M., Milori, D., Mounier, S., & Hatcher, P. G. (2022). Comparison of Sample Preparation Techniques for the (-)ESI-FT- ICR-MS Analysis of Humic and Fulvic Acids. *Environmental Science & Technology*, *56*(17), 12688-12701. https://doi.org/10.1021/acs.est.2c01125

Hayman, G. D., O'Connor, F. M., Dalvi, M., Clark, D. B., Gedney, N., Huntingford, C., Prigent, C., Buchwitz, M., Schneising, O., Burrows, J. P., Wilson, C., Richards, N., & Chipperfield, M. (2014). Comparison of the HadGEM2 climate-chemistry model against in situ and SCIAMACHY atmospheric methane data. *Atmospheric Chemistry and Physics*, *14*(23), 13257-13280. https://doi.org/10.5194/acp-14-13257-2014

Hu, S. W., He, R. J., Wang, W. J., Zhao, D. Y., Zeng, J., Huang, R., Duan, M., & Yu, Z. B. (2021). Composition and co-occurrence patterns of Phragmites australis rhizosphere bacterial community. *Aquatic Ecology*, *55*(2), 695-710. https://doi.org/10.1007/s10452-021-09855-4

Jackson, R. B., Saunois, M., Bousquet, P., Canadell, J. G., Poulter, B., Stavert, A. R., Bergamaschi, P., Niwa, Y., Segers, A., & Tsuruta, A. (2020). Increasing anthropogenic methane emissions arise equally from agricultural and fossil fuel sources. *Environmental Research Letters*, *15*(7), Article 071002. https://doi.org/10.1088/1748-9326/ab9ed2

Johnson, M. S., Matthews, E., Bastviken, D., Deemer, B., Du, J. Y., & Genovese, V. (2021). Spatiotemporal Methane Emission From Global Reservoirs. *Journal of Geophysical Research-Biogeosciences*, *126*(8), Article e2021JG006305. https://doi.org/10.1029/2021jg006305

Justin, S., & Armstrong, W. (1987). THE ANATOMICAL CHARACTERISTICS OF ROOTS AND PLANT-RESPONSE TO SOIL FLOODING. *New Phytologist*, *106*(3), 465-495. https://doi.org/10.1111/j.1469-8137.1987.tb00153.x

Kirschke, S., Bousquet, P., Ciais, P., Saunois, M., Canadell, J. G., Dlugokencky, E. J., Bergamaschi, P., Bergmann, D., Blake, D. R., Bruhwiler, L., Cameron-Smith, P., Castaldi, S., Chevallier, F., Feng, L., Fraser, A., Heimann, M., Hodson, E. L., Houweling, S., Josse, B., . . . Zeng, G. (2013). Three decades of global methane sources and sinks. *Nature Geoscience*, *6*(10), 813-823. https://doi.org/10.1038/ngeo1955

Kirwan, M. L., & Gedan, K. B. (2019). Sea-level driven land conversion and the formation of ghost forests. *Nature Climate Change*, *9*(6), 450-457. https://doi.org/10.1038/s41558-019-0488-7

Korrensalo, A., Mammarella, I., Alekseychik, P., Vesala, T., & Tuittila, E. S. (2022). Plant mediated methane efflux from a boreal peatland complex. *Plant and Soil*, *471*(1-2), 375-392. https://doi.org/10.1007/s11104-021-05180-9

Lacroix, E. M., Aeppli, M., Boye, K., Brodie, E., Fendorf, S., Keiluweit, M., Naughton, H. R., Noël, V., & Sihi, D. (2023). Consider the Anoxic Microsite: Acknowledging and Appreciating Spatiotemporal Redox Heterogeneity in Soils and Sediments. *Acs Earth and Space Chemistry*, *7*(9), 1592-1609. https://doi.org/10.1021/acsearthspacechem.3c00032

Lacroix, E. M., Rossi, R. J., Bossio, D., & Fendorf, S. (2021). Effects of moisture and physical disturbance on pore-scale oxygen content and anaerobic metabolisms in upland soils. *Science of the Total Environment*, *780*, Article 146572. https://doi.org/10.1016/j.scitotenv.2021.146572

LaRowe, D. E., & Van Cappellen, P. (2011). Degradation of natural organic matter: A thermodynamic analysis. *Geochimica Et Cosmochimica Acta*, *75*(8), 2030-2042. https://doi.org/10.1016/j.gca.2011.01.020

Lenzewski, N., Mueller, P., Meier, R. J., Liebsch, G., Jensen, K., & Koop-Jakobsen, K. (2018). Dynamics of oxygen and carbon dioxide in rhizospheres of Lobelia dortmanna - a planar optode study of belowground gas exchange between plants and sediment [Article]. *New Phytologist*, *218*(1), 131-141. https://doi.org/10.1111/nph.14973

Li, C., Ding, S. M., Chen, M. S., Sun, Q., Zhang, Y., Ma, X., Zhong, Z. L., Tsang, D. C. W., & Wang, Y. (2022). O2 distribution and dynamics in the rhizosphere of Phragmites australis, and implications for nutrient removal in sediments [Article]. *Environmental Pollution*, *806*, 10, Article 150735. https://doi.org/10.1016/j.scitotenv.2021.150735

Määttä, T., & Malhotra, A. (2024). The hidden roots of wetland methane emissions. *Global Change Biology*, *30*(2), Article e17127. https://doi.org/10.1111/gcb.17127

Martins, P. D., Hoyt, D. W., Bansal, S., Mills, C. T., Tfaily, M., Tangen, B. A., Finocchiaro, R. G., Johnston, M. D., McAdams, B. C., Solensky, M. J., Smith, G. J., Chin, Y. P., & Wilkins, M. J. (2017). Abundant carbon substrates drive extremely high sulfate reduction rates and methane fluxes in Prairie Pothole Wetlands. *Global Change Biology*, *23*(8), 3107-3120. https://doi.org/10.1111/gcb.13633

Megonigal, J. P. (2019). Biogeochemistry of Tidal Freshwater Wetlands. In *Coastal Wetlands: An Integrated Ecosystem Approach* (pp. Pages 641-683). https://doi.org/https://doi.org/10.1016/B978-0-444-63893-9.00019-8

Mitsch, W. J. a. G. J. G. (2007). *Wetlands* (Fourth Edition ed.). John Wiley & Sons, Inc.

Mueller, P., Hager, R. N., Meschter, J. E., Mozdzer, T. J., Langley, J. A., Jensen, K., & Megonigal, J. P. (2016). Complex invader-ecosystem interactions and seasonality mediate the impact of non-native Phragmites on CH₄ emissions. *Biological Invasions*, *18*(9), 2635-2647. https://doi.org/10.1007/s10530-016-1093-6

Myhre, G., Nilsen, J. S., Gulstad, L., Shine, K. P., Rognerud, B., & Isaksen, I. S. A. (2007). Radiative forcing due to stratospheric water vapour from CH4 oxidation. *Geophysical Research Letters*, *34*(1), Article L01807. https://doi.org/10.1029/2006gl027472

Nahlik, A. M., & Fennessy, M. S. (2016). Carbon storage in US wetlands. *Nature Communications*, *7*, Article 13835. https://doi.org/10.1038/ncomms13835

Noyce, G. L., & Megonigal, J. P. (2021). Biogeochemical and plant trait mechanisms drive enhanced methane emissions in response to whole-ecosystem warming. *Biogeosciences*, *18*(8), 2449-2463. https://doi.org/10.5194/bg-18-2449-2021

Noyce, G. L., Smith, A. J., Kirwan, M. L., Rich, R. L., & Megonigal, J. P. (2023). Oxygen priming induced by elevated CO₂ reduces carbon accumulation and methane emissions in coastal wetlands. *Nature Geoscience*, *16*(1), 63-+. https://doi.org/10.1038/s41561-022-01070-6

O'Connell, C. S., Ruan, L., & Silver, W. L. (2018). Drought drives rapid shifts in tropical rainforest soil biogeochemistry and greenhouse gas emissions. *Nature Communications*, *9*, Article 1348. https://doi.org/10.1038/s41467-018-03352-3

Philippot, L., Hallin, S., Börjesson, G., & Baggs, E. M. (2009). Biochemical cycling in the rhizosphere having an impact on global change. *Plant and Soil*, *321*(1-2), 61-81. https://doi.org/10.1007/s11104-008-9796-9

Raivonen, M., Smolander, S., Backman, L., Susiluoto, J., Aalto, T., Markkanen, T., Mäkelä, J., Rinne, J., Peltola, O., Aurela, M., Lohila, A., Tomasic, M., Li, X. F., Larmola, T., Juutinen, S., Tuittila, E. S., Heimann, M., Sevanto, S., Kleinen, T., . . . Vesala, T. (2017). HIMMELI v1.0: HelsinkI Model of MEthane buiLd-up and emIssion for peatlands. *Geoscientific Model Development*, *10*(12), 4665-4691. https://doi.org/10.5194/gmd-10-4665-2017

Saunois, M., Stavert, A. R., Poulter, B., Bousquet, P., Canadell, J. G., Jackson, R. B., Raymond, P. A., Dlugokencky, E. J., Houweling, S., Patra, P. K., Ciais, P., Arora, V. K., Bastviken, D., Bergamaschi, P., Blake, D. R., Brailsford, G., Bruhwiler, L., Carlson, K. M., Carrol, M., . . . Zhuang, Q. L. (2020). The Global Methane Budget 2000-2017. *Earth System Science Data*, *12*(3), 1561-1623. https://doi.org/10.5194/essd-12-1561-2020

Seyfferth, A. L., Bothfeld, F., Vargas, R., Stuckey, J. W., Wang, J., Kearns, K., Michael, H. A., Guimond, J., Yu, X., & Sparks, D. L. (2020). Spatial and temporal heterogeneity of geochemical controls on carbon cycling in a tidal salt marsh. *Geochimica Et Cosmochimica Acta*, *282*, 1-18. https://doi.org/10.1016/j.gca.2020.05.013

Sleighter, R. L., & Hatcher, P. G. (2008). Molecular characterization of dissolved organic matter (DOM) along a river to ocean transect of the lower Chesapeake Bay by ultrahigh resolution electrospray ionization Fourier transform ion cyclotron resonance mass spectrometry. *Marine Chemistry*, *110*(3-4), 140-152. https://doi.org/10.1016/j.marchem.2008.04.008

Sorrell, B. K., & Brix, H. (2013). *Gas Transport and Exchange through Wetland Plant Aerenchyma* (Vol. 10). Soil Science Society of America.

Sowers, K. R. (2019). Methanogenesis. In *Encyclopedia of Microbiology, 4th Ediition - Reference Module in Biomedical Sciences*. Ellsevier Inc. https://doi.org/10.1016/b978-0-12-801238-3.02447-8

Srivastava, J., Kalra, S. J. S., & Naraian, R. (2014). Environmental perspectives of Phragmites australis (Cav.) Trin. Ex. Steudel. *Applied Water Science*, *4*(3), 193-202. https://doi.org/10.1007/s13201-013-0142-x

Stagg, C. L., Schoolmaster, D. R., Krauss, K. W., Cormier, N., & Conner, W. H. (2017). Causal mechanisms of soil organic matter decomposition: deconstructing salinity and flooding impacts in coastal wetlands. *Ecology*, *98*(8), 2003-2018. https://doi.org/10.1002/ecy.1890

Stanley, E. H., & Ward, A. K. (2010). Effects of Vascular Plants on Seasonal Pore Water Carbon Dynamics in a Lotic Wetland. *Wetlands*, *30*(5), 889-900. https://doi.org/10.1007/s13157-010-0087-x

Valle, J., Gonsior, M., Harir, M., Enrich-Prast, A., Schmitt-Kopplin, P., Bastviken, D., Conrad, R., & Hertkorn, N. (2018). Extensive processing of sediment pore water dissolved organic matter during anoxic incubation as observed by high-field mass spectrometry (FTICR-MS). *Water Research*, *129*, 252-263. https://doi.org/10.1016/j.watres.2017.11.015

van den Berg, M., van den Elzen, E., Ingwersen, J., Kosten, S., Lamers, L. P. M., & Streck, T. (2020). Contribution of plant-induced pressurized flow to CH4 emission from a Phragmites fen. *Scientific Reports*, *10*(1), Article 12304. https://doi.org/10.1038/s41598-020-69034-7

Vroom, R. J. E., van den Berg, M., Pangala, S. R., van der Scheer, O. E., & Sorrell, B. K. (2022). Physiological processes affecting methane transport by wetland vegetation - A review. *Aquatic Botany*, *182*, Article 103547. https://doi.org/10.1016/j.aquabot.2022.103547

Wang, X. L., Yao, B., & Su, X. Y. (2018). Linking Enzymatic Oxidative Degradation of Lignin to Organics Detoxification. *International Journal of Molecular Sciences*, *19*(11), Article 3373. https://doi.org/10.3390/ijms19113373

Wania, R., Ross, I., & Prentice, I. C. (2010). Implementation and evaluation of a new methane model within a dynamic global vegetation model: LPJ-WHyMe v1.3.1. *Geoscientific Model Development*, *3*(2), 565-584. https://doi.org/10.5194/gmd-3-565-2010

Wilmoth, J. L. (2021). Redox Heterogeneity Entangles Soil and Climate Interactions [Article]. *Sustainability*, *13*(18), 14, Article 10084. https://doi.org/10.3390/su131810084

Wilmoth, J. L., Moran, M. A., & Thompson, A. (2018). Transient O₂ pulses direct Fe crystallinity and Fe(III)-reducer gene expression within a soil microbiome. *Microbiome*, *6*, Article 189. https://doi.org/10.1186/s40168-018-0574-5

Wilmoth, J. L., Schaefer, J. K., Schlesinger, D. R., Roth, S. W., Hatcher, P. G., Shoemaker, J. K., & Zhang, X. N. (2021). The role of oxygen in stimulating methane production in wetlands. *Global Change Biology*, *27*(22), 5831-5847. https://doi.org/10.1111/gcb.15831